

Aus dem Institut für Diabetologie und klinische Stoffwechselforschung des
Universitätsklinikums Schleswig-Holstein, Campus Kiel

Characterization of specific Gut Bacteria and bacterial Metabolites in Human Obesity and Type 2 Diabetes

Dissertation

zur Erlangung des Doktorgrades
der Agrar- und Ernährungswissenschaftlichen Fakultät
der Christian-Albrechts-Universität
zu Kiel

vorgelegt von
M.Sc. Lea Henneke
aus Kiel

Kiel, 2022

Dekan/in: Prof. Dr. Karl H. Mühling

1. Berichterstatter: Prof. Dr. med. Matthias Laudes
2. Berichterstatter: Prof. Dr. Karin Schwarz

Tag der mündlichen Prüfung: 29.06.2022

Veröffentlicht mit Genehmigung der Agrar- und Ernährungswissenschaftlichen
Fakultät der Christian-Albrechts-Universität zu Kiel

Summary

Recent rodent microbiome experiments suggest that besides *Akkermansia*, *Parasutterella* sp. are important in type 2 diabetes and obesity development. Further, bacterial metabolites become one focus in microbiome research. As an example of this, it could be shown, both in animal models and in biostatistical modeling, that the metabolite agmatine has life-prolonging effects.

In the present thesis, firstly we aimed to characterize *Parasutterella* in our cross-sectional FoCus cohort (n=1,544). The major results were then validated in an independent Canadian cohort (n=438). Furthermore, we examined *Parasutterella excrementihominis* abundance in response to a weight loss intervention (n=55). *Parasutterella* was positively associated with BMI (body mass index), fasting insulin and type 2 diabetes independently of low-grade inflammation. Dietary analysis revealed a positive association between *Parasutterella* sp. with the dietary intake of carbohydrates but not with fat or protein consumption. MS-metabolomics analysis appointed L-cysteine as strongly reduced in subjects with high *Parasutterella* abundance. Additionally, metabolic network enrichment analysis identified an association of high *Parasutterella* abundance with the activation of the human fatty acid biosynthesis pathway suggesting a mechanism for body weight gain. This was supported by a reduction of *Parasutterella excrementihominis* abundance during a low-carb diet supplemented with ω 3-linolenic acid within the weight loss intervention. Together, these data indicate a role of *Parasutterella* in human obesity and type 2 diabetes.

Secondly, the present thesis shows by biostatistical modeling that agmatine, measured by MS-metabolomics, was elevated in FoCus subjects with an increased BMI (n=1,704) coupled with reduced microbial α -diversity. Followed by dietary calculations, we were able to show, that maltose was negatively associated with agmatine, and plant protein was positively associated with it. The genus *Bacteroides* was abundant in subjects with measured agmatine, which might indicate an agmatine-producing capacity of this microbe. In addition, cell culture models provided insight into the effect of agmatine on decelerating adipogenesis and activating inflammatory processes in human macrophages. These results suggest that agmatine has effects on metabolic processes and these should be validated in future clinical interventions.

Zusammenfassung

Jüngste Nagetier-Mikrobiom-Experimente legen nahe, dass neben *Akkermansia*, *Parasutterella* sp. in der Entwicklung von Krankheiten wie Typ-2-Diabetes und Adipositas wichtig sind. Darüber hinaus sind bakterielle Metaboliten zu einem Schwerpunkt in der Mikrobiomforschung geworden. Als Beispiel hierfür konnte sowohl im Tiermodell als auch in biostatistischen Modellierungen gezeigt werden, dass der Metabolit Agmatin lebensverlängernde Wirkungen aufweist.

In der vorliegenden Arbeit wurde zunächst *Parasutterella* in unserer Querschnittskohorte FoCus (n=1.544) charakterisiert. Im Anschluss wurden die wichtigsten Ergebnisse in einer unabhängigen kanadischen Kohorte (n=438) validiert. Des Weiteren untersuchten wir die Abundanz von *Parasutterella excrementihominis* in Bezug auf eine Intervention zur Gewichtsreduktion (n=55). *Parasutterella* war unabhängig von einer "low-grade" Entzündung positiv mit dem BMI (Body Mass Index), Nüchterninsulin und Typ-2-Diabetes assoziiert. Ernährungsanalysen ergaben einen positiven Zusammenhang von *Parasutterella* sp. mit der Nahrungsaufnahme von Kohlenhydraten, aber nicht mit dem Fett- oder Proteinkonsum. Eine MS-Metabolomikanalyse konnte zeigen, dass L-Cystein bei Patienten mit hoher *Parasutterella* Abundanz stark reduziert war. Zudem identifizierte eine metabolische Netzwerkanalyse eine Assoziation von erhöhter *Parasutterella* Abundanz mit der Aktivierung des menschlichen Fettsäure-Biosyntheseweges, das wiederum auf einen Mechanismus der Körpergewichtszunahme hindeuten könnte. Dies wurde durch eine Verringerung der Abundanz von *Parasutterella excrementihominis* während einer kohlenhydratarmen, mit ω 3-Linolensäure zugesetzten Ernährung innerhalb der Gewichtsabnahmeintervention unterstützt. Resümierend weisen diese Daten auf eine Rolle von *Parasutterella* bei humaner Adipositas und Typ-2-Diabetes hin.

Zweitens zeigt die vorliegende Arbeit, dass das mittels MS-Metabolomik gemessene Agmatin bei FoCus Probanden mit einem erhöhten BMI anstieg und mit einer verringerten mikrobiellen α -Diversität einherging. Gefolgt von ernährungsassoziierten Berechnungen konnten wir zeigen, dass Maltose negativ und Pflanzenprotein positiv, mit Agmatin assoziiert waren. Die Gattung *Bacteroides* kam in Probanden mit gemessenem Agmatin gehäuft vor, das auf eine Agmatin-produzierende Kapazität dieser Mikrobe hindeuten könnte. Zusätzlich boten Zellkulturmodelle Einblicke in die Wirkung von Agmatin hingehend einer Verlangsamung der Adipogenese und einer Aktivierung von Entzündungsprozessen in humanen Makrophagen. Diese Ergebnisse legen vor, dass Agmatin Einflüsse auf Stoffwechselprozesse hat und diese in zukünftigen klinischen Interventionen validiert werden sollten.

Table of contents

I. List of abbreviations.....	VIII
II. List of figures.....	X
III. List of tables.....	XIII
1 Introduction.....	1
2 Theoretical background	1
2.1 Human gut microbiota – an overview	1
2.2 Human gut bacteria.....	3
2.2.1 Candidate bacterium – <i>Parasutterella</i>	4
2.3 Host metabolites.....	5
2.3.1 Agmatine.....	5
2.4 Metabolic syndrome, systemic metabolic inflammation & lipid metabolism .	8
2.5 Research objective.....	10
3 Material and methods.....	12
3.1 Study population and study design of the FoCus cohort, ATP cohort & Intervention cohort.....	12
3.1.1 16S rRNA gene sequencing.....	13
3.1.2 Metabolomics sample preparation.....	13
3.2 Bioinformatical analysis	14
3.2.1 Univariate analysis.....	15
3.2.2 Multivariate analysis.....	15
3.2.3 Nutritional analysis.....	16
3.2.4 Microbiome analysis.....	18
3.2.5 Metabolomic analysis.....	19
3.2.6 Genomic analysis (GWAS).....	20
3.3 Cell culture.....	22
3.3.1 3T3-L1 (mouse pre-adipocytes)	22
3.3.2 Caco-2 (human colon adenocarcinoma cells).....	22
3.3.3 Hep-G2 cells (human hepatocytes)	22
3.3.4 THP-1 cells (human monocytes)	22
3.3.5 HEK293 cells (human embryonic kidney cells).....	22
3.4 Material.....	22
3.4.1 Technical instruments	22

3.4.2	Chemicals, antibodies and consumables	24
3.4.3	Buffers	26
3.4.4	Composition of SDS-PAGE (30% acrylamide)	27
3.5	Methods	28
3.5.1	Quantitative polymerase chain reaction.....	28
3.5.2	Cell cultivation 3T3-L1.....	29
3.5.3	Cell cultivation Caco-2	29
3.5.4	Cell cultivation Hep-G2	30
3.5.5	Cell cultivation THP-1.....	30
3.5.6	Cell cultivation HEK293.....	30
3.5.7	General cell counting procedure.....	31
3.5.8	Cell culture experiment with 3T3-L1 cells.....	31
3.5.9	Cell culture experiment with Caco-2 cells.....	32
3.5.10	Cell culture experiment with Hep-G2 cells.....	33
3.5.11	Cell culture experiment with THP-1 cells	33
3.5.12	General cell lysis procedure	34
3.5.13	Bradford protein quantification.....	34
3.5.14	Western Blot	34
3.5.15	Viability assay	38
3.5.16	Luciferase assay with HEK293 cells.....	38
4	Results.....	43
4.1	Characterization of the FoCus cohort, ATP cohort and Intervention cohort	43
4.2	<i>Parasutterella</i> – descriptive statistics.....	43
4.2.1	<i>Parasutterella</i> in relation to various phenotypes	44
4.2.2	<i>Parasutterella</i> and gut microbiomics	57
4.2.3	<i>Parasutterella</i> and host metabolomics.....	58
4.2.4	<i>Parasutterella</i> and host genomics	66
4.2.5	<i>Parasutterella</i> and weight loss intervention	67
4.3	Agmatine – descriptive statistics	67
4.3.1	Agmatine regarding phenotypical parameter and diseases	68
4.3.2	Agmatine and dietary intake including medication (metformin)	78
4.3.3	Agmatine and gut microbiomics	84
4.3.4	Agmatine and host genomics	90
4.3.5	Agmatine and host urine metabolomics.....	92
4.3.6	Agmatine and functional effects on mouse adipocytes	95
4.3.7	Agmatine and functional effects on human gut epithelial cells	97

4.3.8	Agmatine and functional effects on human hepatocytes.....	101
4.3.9	Agmatine and functional effects on human macrophages	102
4.3.10	Agmatine and functional effects on human embryonic kidney cells	106
5	Discussion.....	108
5.1	<i>Parasutterella</i>.....	108
5.1.1	Phenotypes.....	108
5.1.2	Gut microbiomics and host metabolomics	109
5.1.3	Genetics.....	111
5.1.4	Translation to a human intervention study.....	111
5.2	Agmatine.....	112
5.2.1	Phenotypes, urine metabolomics and diet.....	113
5.2.2	Gut microbiomics	114
5.2.3	Genetics.....	115
5.2.4	Experimental cell culture models.....	115
5.3	Strengths and limitations.....	118
6	Conclusion and outlook.....	120
7	References	121
8	Appendix	136
9	Danksagung	151

I. List of abbreviations

ADP	Adenosindiphosphat
ASVs	Amplicon sequence variants
ATP	Alberta's Tomorrow Project
BMR	Basal metabolic rate
BMBF	German Ministry of Education and Research
BMI	Body mass index
Ca ²⁺	Calcium
Caco-2	Human colon adenocarcinoma cells
<i>C. elegans</i>	<i>Caenorhabditis elegans</i>
crp	Cyclic AMP receptor protein
CRP	C-reactive protein
<i>E. coli</i>	<i>Escherichia coli</i>
ELISA	Enzyme-linked immunosorbent assay
FABP4	Fatty acid-binding protein 4
FDR	False discovery rate
FFQ	Food frequency questionnaire
FoCus	Food Chain Plus
gDNA	genomic Deoxyribonucleic acid
GJ	Energy intake
GOS	Galacto-oligosaccharides
GWAS	Genome-wide association study
HDL	High-density lipoprotein
HFD	High-fat diet
HOMA	Homeostasis model assessment insulin resistance index
HPLC	High-performance liquid chromatography
IBD	Inflammatory bowel disease
IDF	International Diabetes Federation
IKMB	Institute of Clinical Molecular Biology
IL-1 β	Interleukin-1 β
IL-6	Interleukin-6
K ⁺	Potassium
KNN	K-nearest neighbor
LOD	Limit of detection
MAF	Minor allele frequency
MTBE	Methyl-tert-butyl ether

MRI	Magnetic resonance imaging study
NFκB	Nuclear factor kappa B
NRF2	Nuclear factor erythroid 2-related factor 2
NMDA	glutamateric N-methyl-D-aspartate
NO	Nitric oxide
NOS	Nitric oxide synthase
LDL	Low-density lipoprotein
PERMANOVA	Permutational multivariate analysis of variance
pH	Potentia hydrogenii
p-NFκB	Phosphorylated nuclear factor kappa B
POMC	Pro-opiomelanocortin
PPAR-γ	Peroxisome proliferator-activated factor gamma
PUFA	Polyunsaturated fatty acid
ROS	Reactive oxygen species
RIPA	Radioimmunoprecipitation assay buffer
SCFA	Short-chain fatty acids
SCI	Systemic chronic inflammation
SD	Standard deviation
SMPDB	Small metabolites pathway database
SNPs	Single nucleotide polymorphisms
SREBP1	Sterol regulatory element-binding protein-1
T2D	Type 2 diabetes
TEER	Trans-Epithelial Electrical Resistance
TNF-α	Tumor necrosis factor alpha
QC	Quality control
qPCR	quantitative polymerase chain reaction
ZO-2	Zonula occludens-2

II. List of figures

Figure 1: Agmatine (including arginine) metabolic pathways in humans	7
Figure 2: Causes and consequences of low-grade systemic chronic inflammation (SCI). .	9
Figure 3: Composition of blotting procedure.....	36
Figure 4: Association of <i>Parasutterella</i> sp. with the particular parameter (count model) without BMI as a covariate	48
Figure 5: <i>Parasutterella</i> sp. abundance in relation to BMI and type 2 diabetes (T2D) groups in the FoCus cohort (A) and ATP cohort (B)	49
Figure 6: Association of <i>Parasutterella</i> sp. with the particular dietary parameter (count model) without BMI as a covariate	56
Figure 7: β -diversity displayed through Bray Curtis distance between <i>Parasutterella</i> sp. groups	57
Figure 8: α -diversity displayed through Species Richness, Shannon Index and Chao1 Index between <i>Parasutterella</i> sp. groups	58
Figure 9: Association of <i>Parasutterella</i> sp. with the particular metabolite (count model) without BMI as a covariate	61
Figure 10: Pathway enrichment analysis (SMPDB database) of metabolites associated with <i>Parasutterella</i> sp.....	64
Figure 11: Association of <i>Parasutterella</i> sp. and SNPs (logistic model) of n=1,397 subjects	66
Figure 12: Difference of BMI (A) and abundance of <i>Parasutterella excrementihominis</i> (B) in subjects of intervention at baseline compared with 12 weeks.....	67
Figure 13: Differences in agmatine absence and agmatine presence regarding BMI (A) and waist (B).....	69
Figure 14: (A) Differences in prevalence of agmatine absence and agmatine presence in male or female subjects, (B) Differences in female or male subjects regarding agmatine intensity.....	71
Figure 15: Differences in BMI groups regarding agmatine intensity in female subjects ...	72
Figure 16: Association of agmatine with phenotypical parameter	73
Figure 17: Association of agmatine with the particular phenotypical parameter (count model)	74
Figure 18: Differences in absence or presence of IBD (A), skin disease (B) or diabetes (C) regarding agmatine.....	76
Figure 19: Association of agmatine with the particular disease (count model).....	78
Figure 20: Association of agmatine with the particular dietary parameter (count model) .	83

Figure 21: (A) Differences in prevalence of agmatine absence and agmatine presence in metformin presence and metformin absence, (B) Differences in metformin presence and metformin absence regarding agmatine intensity, (C) Differences in metformin presence and metformin absence regarding agmatine intensity in subjects with BMI > 25 kg/m ² and type 2 diabetes.....	84
Figure 22: Bray Curtis distance of agmatine groups and general microbiome composition without confounders (A) and with confounders (B).....	85
Figure 23: Jaccard index of agmatine groups and general micobiome composition without confounders (A) and with confounders (B).....	86
Figure 24: α -diversity in subjects with absence or presence of agmatine regarding Shannon Index (A), Species Richness (B) and Chao1 (C).	87
Figure 25: Venn diagram shows the distribution of taxa in agmatine absence and agmatine presence of the core measurable microbiome	88
Figure 26: Distribution of bacterial families in groups of agmatine absence and agmatine presence.....	89
Figure 27: Distribution of bacterial genus in groups of agmatine absence and agmatine presence.....	90
Figure 28: Association of agmatine and SNPs (logistic model) of n=1,486 subjects.....	91
Figure 29: Association of agmatine and SNPs (log-transformed, linear model) of n=410 subjects	92
Figure 30: Viability of mouse pre-adipocytes with exposure of agmatine	95
Figure 31: Expression of PPAR- γ in mouse adipocytes	96
Figure 32: Expression of FABP4 in mouse adipocytes.....	97
Figure 33: Expression of ZO-2 (A) and claudin 3 (B) with TNF- α stimulation in human gut epithelial cells	98
Figure 34: Expression of ZO-2 (A) and claudin 3 (B) without TNF- α stimulation in human gut epithelial cells	99
Figure 35: Expression of pNF κ B with TNF- α stimulation in human gut epithelial cells ..	100
Figure 36: Expression of ZO-2 in human gut epithelial cells differentiated for three weeks	101
Figure 37: Expression of SREBP1 in human hepatocytes.....	102
Figure 38: Viability of human macrophages exposed with agmatine	103
Figure 39: Expression of NF κ B (p105/p50) in human macrophages exposed with agmatine for 2h in a dose-response experiment	104
Figure 40: Expression of NF κ B (p105/p50) in human macrophages exposed with agmatine for 4h in a dose-response experiment	105

Figure 41: Expression of NF κ B (p105/p50) in human macrophages exposed with 1mM agmatine in a time-response experiment	106
Figure 42: Relative NF κ B-promoter activation after an incubation period of 1h with TNF- α , agmatine and TNF- α + agmatine	107

III. List of tables

Table 1: Equations for estimating BMR	17
Table 2: Technical instruments	22
Table 3: Chemicals, antibodies and consumables	24
Table 4: Buffers	26
Table 5: Composition of small gels	27
Table 6: Composition of large gels.....	28
Table 7: Running conditions in relation to antibodies	36
Table 8: Blotting conditions in relation to antibodies.....	37
Table 9: Dilutions of first and secondary antibody	37
Table 10: Reporter genes	40
Table 11: Pipetting scheme (12-well plate)	41
Table 12: Overview of three cohorts involved in the study	43
Table 13: Descriptive statistics of the FoCus cohort (<i>Parasutterella</i> sp.)	44
Table 14: Association of <i>Parasutterella</i> sp. with the particular phenotypical parameter (hurdle model)	45
Table 15: Association of <i>Parasutterella</i> sp. with the particular phenotypical parameter (hurdle model) including BMI as a covariate	46
Table 16: Association of <i>Parasutterella</i> sp. with the particular disease (hurdle model)....	49
Table 17: Association of <i>Parasutterella</i> sp. with the particular dietary parameter (hurdle model)	51
Table 18: Association of <i>Parasutterella</i> sp. with the particular dietary parameter (hurdle model) including BMI as a covariate	53
Table 19: Association of <i>Parasutterella</i> sp. with the particular metabolite (hurdle model) displaying the five highest negative estimates	59
Table 20: Association of <i>Parasutterella</i> sp. with the particular metabolite (hurdle model) displaying the five highest positive estimates.....	60
Table 21: Association of <i>Parasutterella</i> sp. with the particular metabolite (hurdle model) including covariates such as BMI and age, displaying the five highest negative estimates	62
Table 22: Association of <i>Parasutterella</i> sp. with the particular metabolite (hurdle model) including covariates such as BMI and age, displaying the two highest positive estimates	63

Table 23: Gut bacteria of the human gut microbiota with the highest relative L-cysteine consumption in human samples.....	65
Table 24: Descriptive statistics of the FoCus cohort (agmatine).....	68
Table 25: Differences in agmatine absence and agmatine presence regarding the particular parameter.....	70
Table 26: Associations of agmatine and phenotypical parameters.....	73
Table 27: Association of agmatine with the particular phenotypical parameter (hurdle model)	75
Table 28: Differences in prevalence of the particular disease between agmatine absence and agmatine presence	76
Table 29: Association of agmatine with the particular disease (hurdle model).....	77
Table 30: Associations of agmatine with the particular parameter.....	78
Table 31: Association of agmatine with the particular nutrient (hurdle model)	79
Table 32: ASVs, which imply the most difference between clustering of the two groups agmatine absence and agmatine presence.....	87
Table 33: Association of agmatine and positively ionized urine metabolites.....	93
Table 34: Association of agmatine absence/agmatine presence and positively ionized urine metabolites	94

Supplementary figures

Supplementary figure 1.....	136
Supplementary figure 2.....	137
Supplementary figure 3.....	138
Supplementary figure 4.....	138
Supplementary figure 5.....	139
Supplementary figure 6.....	140
Supplementary figure 7.....	140
Supplementary figure 8.....	141

Supplementary tables

Supplementary table 1	142
Supplementary table 2.....	149

1 Introduction

Within the last decade, a tremendous amount of scientific findings on the human gut microbiota have been published, which shows the immense interest in causes and consequences of each individual's body habitat microorganisms (1) concerning health and disease. Several factors influence the adult human gut microbiota composition, such as diet, hygiene, antibiotics and host's genetics (2)(3). In relation to this, the focus of this research was put on specific diseases such as obesity (4) and type 2 diabetes (5) as well as systemic metabolic inflammation. In particular, we aimed to characterize a single genus bacterium namely *Parasutterella* and a microbial produced host metabolite agmatine. Both make up potential specific targets in therapeutic development in human diseases named above.

2 Theoretical background

2.1 Human gut microbiota – an overview

The human gut is hosting approximately 100 trillion microorganisms, 10 times the number of human cells (6). The human gut hosts from 10^1 to 10^3 bacteria per gram in the stomach and duodenum, from 10^4 to 10^7 in the jejunum and ileum and lastly, from 10^{11} to 10^{12} in the colon with the most bacterial cells (7). The human gut microbiome is defined as the totality of all genes colonizing the human gut, whereby the human microbiota can be defined as the totality of microorganisms colonizing the human gut (8).

In healthy individuals, most of these microorganisms are symbionts which maintain a commensal relationship with the host through digesting food and supporting the immune system (9). On the contrary, pathogenic microorganisms in individuals can cause infectious diseases (10), and non-communicable diseases such as obesity and obesity-related comorbidities, namely type 2 diabetes as well as cardiovascular diseases, are associated with a dysbiosis of the human gut microbiome (11). Several studies of the last decade imply that environmental factors influence the composition of the gut microbiome (12) and that the gut microbiome plays a crucial role in the regulation of host metabolism via specific host-microbiome interactions (11).

One of the main functions of the human gut microbiota is to maintain several physiological functions such as modulating appetite and food intake (13), absorption and digestion of nutrients from the gut, triglyceride accumulation in adipose tissue, activation and

Theoretical background

prevention of inflammation (14), fatty acid oxidation in skeletal muscle and liver as well as synthesis of vitamins (15). Additionally, the gut microbiota produces short chain fatty acids that have an effect on the maintenance of colonic epithelial cells (7). Moreover, it influences enzymatic transformation of bile acids, regulation of cholesterol synthesis and modulation of energy homeostasis in general (16).

Human gut microbiota related to obesity & type 2 diabetes

The relationship between the gut microbiota and the regulation of energy balance became the focus of obesity research, since there exists a second rationale besides the obesogenic environment that is defined by a lack of physical exercise and overeating (17). It is argued that energy balance is influenced by several mechanisms, for instance, increased production of short chain fatty acids, increased intestinal permeability, decreased angiopoietin-like protein 4, AMP-activated kinase, de novo lipogenesis and maintenance of subclinical inflammatory status (17)(4). Mechanistically, it is thought that a significant elevation in host metabolism-related microbial communities might be associated with an improved capacity to harvest energy from the diet (18). In more detail, in germ-free mice that either got colonized with microbiota of obese mice or microbiota of lean mice, it turned out that mice colonized by microbes derived from the gut of obese mice increase in total body fat mass. Thus, it appears that obese mice have the possibility to degrade complex polysaccharides and store additional energy in adipose tissue and develop low levels of short chain fatty acids reaching the liver and reduce lipogenesis. This phenomenon is known as the storage hypothesis (18). Contrary, mice with lean microbiota were not able to develop obesity even though they were fed with a high-calorie diet. Those mice had increased levels of AMP-activated kinase in skeletal muscle and liver which promoted fatty acid oxidation suggestively protecting them from becoming obese (19).

A second hypothesis linking obesity with gut microbiota is the metabolic endotoxemia and gut barrier dysfunction. Obesity is related to a 'low-grade inflammation' in humans (20). Intestinal mucosa is in charge of preventing bacterial translocation and absorption of nutrients. Furthermore, epithelial membrane receptor proteins should function properly, otherwise they indicate metabolic disorders such as obesity (21). The concept of endotoxemia is based on bacterial lipoprotein lipase regulation that influences systemic inflammatory status (22).

Type 2 diabetes is a comorbidity of obesity and associated with hyperglycemia and insulin resistance as well as insulin secretion disturbance (23). Type 2 diabetes is known to be linked to alterations in the gut microbiota, whereby an increased number of

Enterobacteriaceae was reported in prediabetes (5). Moreover, the abnormal expansion of Proteobacteria in the gut might foster the development of insulin resistance in germ-free mice (24), which was in turn found to be associated with chronic inflammation in the host. Contrary, a low abundance of Proteobacteria is present in healthy humans (25). In a human study, researchers were able to show that transferring gut microbiota of healthy subjects to type 2 diabetes patients could enhance insulin sensitivity (26).

2.2 Human gut bacteria

In recent years, it has become clear that the human adult gut microbiota includes six main phyla such as Firmicutes, Bacteroidetes, Actinobacteria, Proteobacteria, Fusobacteria and Verrucomicrobia (27). 90% of the microbiota is composed by the two phyla of Firmicutes and Bacteroidetes. But there is still a considerable inter-individual diversity in genus/species level that makes the gut microbiota profile unique and person-specific (28). In adulthood, the human gut microbiota differs in elderly and young adults. Bacteroidetes and *Clostridium* genus are predominant in the elderly, whereas Firmicutes mostly colonize young adults (29).

Several studies investigated the relation of gut microbial composition at the phylum level to metabolic parameters and dietary components (30)(31). However, when it comes to the effect of specific species of the gut microbiota affecting human health, several pilot projects have targeted specific microbial species, like *Akkermansia muciniphila* which have been shown to be associated with beneficial health traits in obese subjects (32)(33)(34).

Also, nutrition-related studies showed an influence of long-term diet on human gut microbiota composition. In early childhood, when human milk is replaced by solid food, there is a change in microbial community composition from *Lactobacillus*, *Bifidobacterium* and Enterobacteriaceae to *Clostridium spp.* and *Bacteroides spp.* (35). Breast-fed infants have advantages in comparison to formula-fed infants through receiving various important nutrients which support the growth of *Bifidobacterium* and intestinal barrier function, among others (36). Additionally, in mice that are obese due to diet or genetic manipulation, supplementation with fructo-oligosaccharides affected the number of *Bifidobacterium spp.* in the gut, which was negatively associated with glucose intolerance and obesity (37). Taking a closer look at the diet of adults, authors found that high levels of animal fat and protein were associated with high levels of Bacteroidetes. On the contrary, individuals consuming vegetables, fruits as well as fiber and less meat and dairy products had high levels of Prevotella (38).

Prebiotics and probiotics have been in the focus of research in the last decades. Studies claim that they can favor the human gut microbiota composition and could positively support managing human obesity (39). When mice are treated with prebiotics, levels of lipoprotein lipase, inflammatory cytokines and oxidative stress decreased (40). This is related to a low level of glucagon-like peptide 2 that maintains bowel mass by reducing apoptosis and stimulating proliferation of enterocytes. Therefore, glucagon-like peptide 2 mediated mechanisms are able to improve microbiota composition through dietary changes (41). Moreover, prebiotics, for instance oligofructose, are used to reduce inflammation and increase the level of Bifidobacteria when following a high-fat diet (HFD) (11). Probiotics such as fermented milk, yogurt, powdered infant milk, butter, cheese used as functional food became popular (42). Yogurt, for instance, contains *Lactobacillus rhamnosus* as well as *Lactobacillus reuteri* and appears to have a positive impact on human health since it is a natural carrier of bacteria. More specifically, another study reports that *Lactobacillus rhamnosus* and *Bifidobacterium lactis* BB-12 occurring in yogurt products seem to be effective in reducing antibiotic-associated diarrhea in children (43).

2.2.1 Candidate bacterium – *Parasutterella*

By focusing on this more specific, translational approach to investigate *Parasutterella* sp. at the genus level (and *Parasutterella excrementihominis* at the species level) in human samples, we build on previous findings in various rodent models (44)(45) and a recent magnetic resonance imaging (MRI) study by our group. Kreutzer et al. found *Parasutterella* to be associated with hypothalamic inflammation in obese humans, which is thought to interfere with appetite- and satiety regulation contributing to the development of obesity (30).

Parasutterella sp. and *Parasutterella excrementihominis* belong to the family of Sutterellaceae, the order of Burkholderiales, the class of Betaproteobacteria and the phylum of Proteobacteria (46). In general, the genus of *Parasutterella* sp. consists of only two known species so far, namely *Parasutterella excrementihominis* and *Parasutterella secunda*. Specifically, the bacterial species *Parasutterella excrementihominis* is gram-negative, non-motile, obligate anaerobic, non-spore forming cocci to coccobacilli (47). From a mechanistic point of view, *Parasutterella* is associated to both, inflammatory reactions in the intestinal mucosa (48) and systemic metabolic abnormalities (49) which might suggest a role in the development of systemic low-grade metabolic inflammation due to dysbiosis. This microbe is linked to metabolic abnormalities in rodents (49) and responds to a high fat diet intervention in obesity-prone mice (44).

2.3 Host metabolites

In general, specific clusters of bacteria are able to produce gut microbial metabolites (of which agmatine and L-cysteine are two of many) that cause metabolic reactions. In order to unravel host health and disease, extensive scientific evidence is needed to study the crosstalk mediated by these metabolites in the setting of host-microbiota interactions (50). Gut microbial metabolites can be grouped as the following: short-chain fatty acids (SCFAs), polyphenols, vitamins, tryptophan catabolites and polyamines (51).

SCFAs occur through dietary fiber fermentation. Certain bacteria in the large intestine as well as in the cecum are capable of degrading fibers. This is of importance since the human body lacks enzymes to metabolize polysaccharides. SCFAs can be classified into three molecules namely acetate, butyrate and propionate which can be determined through peroxisome proliferator-activated factor gamma (ppar- γ) in human colon adenocarcinoma cells (52).

Natural polyamines such as L-ornithine, putrescine, spermidine and spermine are integrated in cellular functions including cell development, differentiation, amino acid and protein synthesis (53).

Polyamines are known to have antioxidant effects and inhibit inflammatory processes in the human body (54). The Mediterranean diet is usually rich in polyamines and associated with enhanced longevity (55).

2.3.1 Agmatine

The natural polyamine agmatine is a decarboxylation product of the semi-essential amino acid L-arginine that is absorbed through dietary intake (56). It has been first reported in 1910 in bacteria and plants (57). In mouse tissue agmatine has a half-life of 12h, whereas in serum it is detectable less than 10 minutes (58). Nutritional sources of agmatine can be commonly found in plants (soy beans, fermented vegetables) but also in meat products (59). Arginine decarboxylase activity is described rather low in mammals (60). Another possible production origin of agmatine in the mammalian body is the gut microbiota. In cultivation experiments dietary arginine is converted to agmatine through *E. coli* (*Escherichia coli*) bacteria depending on pH (potentia hydrogenii) value that involve acid resistant mechanisms (61). Investigations on agmatine producing capacity by the gut microbiota in combination with nutrition and a pharmacological treatment of metformin revealed higher agmatine levels in metformin-treated type 2 diabetes patients than obese patients according to Pryor et al. (62). The authors also found that agmatine in

Theoretical background

combination with metformin activates the transcription factor crp (cyclic AMP receptor protein) in bacteria which can improve lipid metabolism and lifespan in *C. elegans* (*Caenorhabditis elegans*).

L-Arginine

Arginine as a precursor of agmatine, is up-regulating nitric oxide (NO) production in M1 macrophages which has pro-inflammatory effects on the organism (63). Also, the role of arginine for the immune system has been investigated in mice which were colonized with specific bacteria. They had lower amounts of arginine in the gut in comparison to germ-free mice, so that authors conclude that the microbial production capacity of arginine from the diet differs and regulates amounts given to the immune system (64). So far it is known that several gut bacteria such as *Enterococcus*, *Streptococcus*, *Clostridium*, *Lactococcus* and *Lactobacillus sp.* have the arginine deiminase pathway as a common function (51).

L-cysteine

L-cysteine is a semi-essential amino acid (65) because it can be synthesized from methionine in humans (66). It acts as a precursor for several molecules such as hydrogen sulphide, taurine and glutathione (67). The amino acid was found to suppress plasma ghrelin in rats and hunger feelings in humans and has therefore an anorectic effect (67). In particular, whey protein is enriched with L-cysteine and supplementation during meals showed a stimulation of insulin release in type 2 diabetes patients (66). Also, L-cysteine-degrading enzymes are present in *E. coli* and these processes are important in synthetic and biotechnological product development (68). L-cysteine is able to regulate nutrient metabolism, oxidative stress and signalling pathways (65). Authors claim that decreased L-cysteine levels in type 2 diabetes might be associated with impaired glucose metabolism.

2.3.1.1 Absorption and metabolism of agmatine

Through the enzyme agmatinase, the metabolite agmatine can be further degraded to putrescine and enters the urea cycle. Metabolic products of putrescine are spermidine and spermine (fig. 1). Secondly, in the liver and other peripheral tissues, it can be oxidized by diamine oxidase to produce guanidinobutyric acid (56) which is a metabolite readily cleared from the body. Furthermore, agmatine inhibits nitric oxide synthase (NOS) and

modulates cytoplasmic targets such as neurotransmitters (56)(69). The precursor L-arginine can be catabolized via two metabolic pathways. Either arginine is converted by arginase to ornithine, which is then metabolized to putrescine, or it is metabolized to NO and citrulline by NOS (fig. 1) (70).

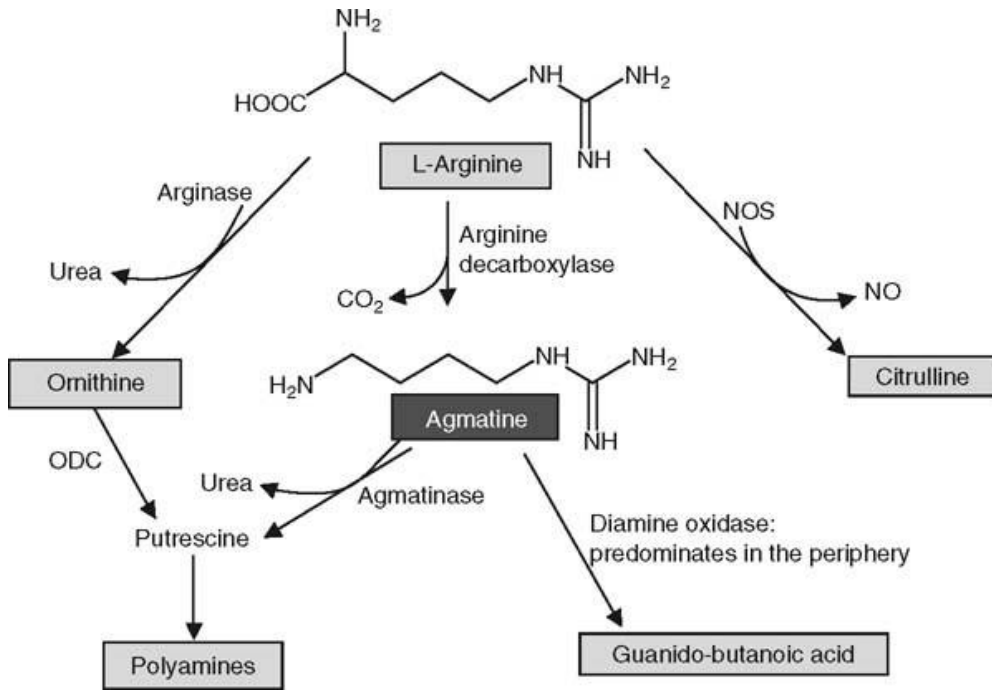


Figure 1: Agmatine (including arginine) metabolic pathways in humans

Abbreviations: NO: nitric oxide; NOS: nitric oxide synthase; ODC: ornithine decarboxylase. Source: Halaris et. al (2007), Agmatine: Metabolic pathway and spectrum of activity in brain, CNS Drugs.

2.3.1.2 Receptors, occurrence and function of agmatine

Agmatine binds on receptors such as α 2-adrenergic, imidazoline I₁-I₃ and glutamateric N-methyl-D-aspartate (NMDA) (69)(70).

The metabolite can be found in most tissues in organs such as kidney and liver (70). Agmatine is an endogenous ligand for the imidazoline receptors which become immensely important in diabetes and obesity research (58). In a rodent model, peripheral I₂-imidazoline receptor activated by agmatine improved insulin activity in type 2 diabetes rats (71) and acts as a target for glucose metabolism research. Further, studies showed that in rats agmatine is able to stimulate pancreatic beta islet cells to secrete insulin (72). Specifically, agmatine inhibits adenosintriphosphat-sensitive potassium channels in a

dose-dependent way. These channels are important regarding insulin secretion. When the ratio of adenosintriphosphat to ADP (adnosindiphosphat) is increasing, channels close due to K^+ (potassium) accumulation. Consequently, this depolarization opens the Ca^{2+} (calcium) channel and Ca^{2+} influx leads to insulin secretion (73). Besides these findings, it was discovered that agmatine is able to decrease inducible NOS (iNOS) in most tissues in response to inflammation or stress systemically (74). Therefore, it might be an interesting target in type 2 diabetes and colitis research (75)(76).

Relatively late in agmatine research, studies proved that mammalian brain tissues contain agmatine (77). That's why the scientific community focused on the neuromodulatory role and synaptic vesicle storage. So far, agmatine is known to function as an antidepressant as well as pain regulating, and a neuroprotective effect in stroke or trauma is postulated (59)(78)(57). Agmatine is defined as an antagonist of NMDA receptor which supports the molecular mechanisms in the antidepressant activity (60). Since agmatine is passing the blood-brain barrier and directly influences the nervous system, it is able to inactivate bioactive amines such as putrescine through the housekeeping enzyme agmatinase (79).

2.4 Metabolic syndrome, systemic metabolic inflammation & lipid metabolism

To end the section on theoretical facts, the metabolic syndrome is worth mentioning. It is defined by the International Diabetes Federation (IDF) as a multifactorial disease that to be diagnosed has to include the following points: increased waist measure (men > 102 cm, women > 88 cm), increased triglycerides, decreased HDL (high-density lipoprotein)-cholesterol, increased blood pressure, increased fasting blood glucose levels or manifestation of diabetes mellitus. At least three of those criteria have to be met (23). These features lead to type 2 diabetes, cardiovascular diseases and non-alcoholic fatty liver disease that often co-occur (80).

In addition, the metabolic syndrome is associated with an increased level of pro-inflammatory adipokines and cytokines. The so called systemic metabolic (or chronic) inflammation is characterized by low-grade inflammatory processes (81). Adipose tissue inflammation might be the reason for this phenomenon which is controlled by deregulation of pro- and anti-inflammatory molecules (82). Therefore, obesity causes systemic metabolic inflammation in most cases. However, systemic metabolic inflammation might also have other sources such as chronic stress or deregulated local immune response concerning infections besides many more (fig. 2) (83).

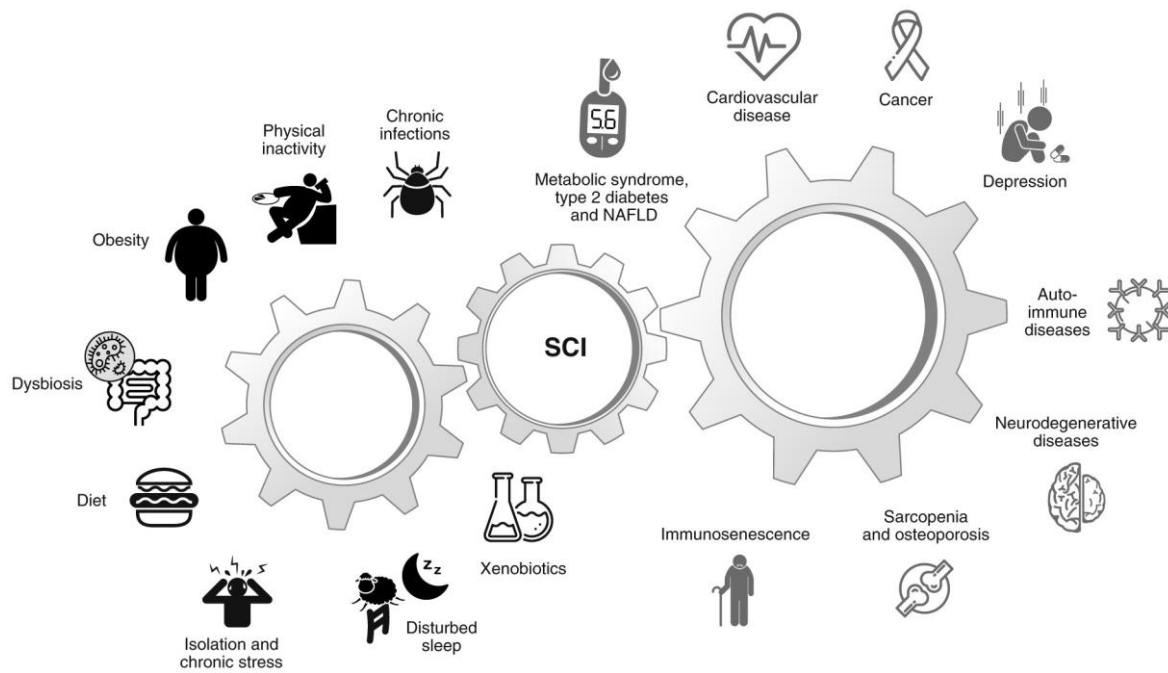


Figure 2: Causes and consequences of low-grade systemic chronic inflammation (SCI).

The causes (left) and consequences (right) of low-grade systemic chronic inflammation have been identified. Source: Furman et al. (2019), Chronic inflammation in the etiology of disease across the life span, Nat. Med.

So far, there are several biomarkers that are used to mirror inflammatory status in humans. Usually, interleukin-6 (IL-6) and C-reactive protein (CRP) are used besides others such as interleukin-1 β (IL-1 β) and tumor necrosis factor alpha (TNF- α) (83). A study investigated the inflammatory state in aging, but authors come to the conclusion that not all biomarker show the same response (84). Therefore, no current standard biomarker for chronic inflammation exists and it is rather a combination of several biomarkers.

The lipid metabolism is an important and central process that fuels the human body. Triglycerides are stored in adipocytes of the adipose tissue and are influenced by constant conversion. Either esterification or lipolysis help to remain constant fat content of the cells (23). Insulin enhances the transport of glucose into adipocytes and activates lipoprotein lipases, which activate the intake of fatty acids and low-density lipoprotein (LDL). In carbohydrate rich diets, insulin is predominant which increases the fat content. If glucagon is predominant (in low insulin levels), the fat content is decreasing and free fatty acids enter the blood to reach organs (23).

2.5 Research objective

Parasutterella

This bacterium seems to be a promising candidate targeting the gut microbiota in relation to obesity and type 2 diabetes since previous published data on rodent models showed metabolic abnormalities (49) and a response to a HFD intervention in obesity-prone mice (44). In addition, recent evidence suggests *Parasutterella* is involved in the mediation of ω 3-fatty acid effects on host physiology (85). From a mechanistic point of view *Parasutterella* is associated to both, inflammatory reactions in the intestinal mucosa (48) and systemic metabolic abnormalities (49), which might suggest a role in the development of systemic low-grade metabolic inflammation due to dysbiosis. Further, a recent magnetic resonance imaging (MRI) study by our group, which has been already mentioned, showed an association of *Parasutterella* with inflammation in obese humans (30). Based on these facts, the aim of this explorative research was to characterize *Parasutterella* (and *Parasutterella excrementihominis*) more deeply with respect to normal human physiology as well as human metabolic and chronic inflammatory diseases and nutrient intake in order to understand the development of obesity and to identify novel therapeutic approaches for future treatments. For this purpose we analyzed 16S rRNA gene sequencing data in 1,544 subjects of our large Food Chain Plus (FoCUS) cohort in Kiel, Germany (86) and in n=438 subjects of Alberta's Tomorrow Project (ATP) cohort (87). In addition, MS-metabolomics and detailed dietary phenotyping were performed (EPIC protocol (88)) and analyzed with regard to *Parasutterella* in the form of metabolic pathway over-representation analysis and microbial metabolic networks. Additionally, genomic analysis was used to associate *Parasutterella* with human single nucleotide polymorphisms (SNPs). To increase reliability and interpretability, we also performed a human intervention study in order to show that *Parasutterella* is not only associated to an obesity phenotype but also responds to a weight loss therapy indicating a potential functional relevance. In addition, in the analysis of the intervention study, we aimed to investigate *Parasutterella* levels by quantitative polymerase chain reaction (qPCR) not to solely rely on 16S rRNA gene sequencing data but also to quantify its abundance.

Agmatine

This gut metabolite/semi-essential amino acid may be an interesting target for the treatment of systemic metabolic inflammation since previous studies showed effects either from a computationally gut microbiota (62) or a nutritional (71) view point. Agmatine

production by the gut microbiota following metformin treatment is nutrition-dependent and is significantly increased in type 2 diabetes patients compared to solely obese patients (62). Further, in a rodent model, peripheral I_2 -imidazoline receptor is activated by agmatine and improves insulin activity in type 2 diabetes rats (71) and acts as a target for glucose metabolism research. Agmatine is known to inhibit iNOS in most tissues in response to systemic inflammation and stress (74). However, until now, most studies regarding agmatine have been based on rodents or on a molecular level and mostly investigated neurological diseases (78)(57). Therefore, the aim of this research was to investigate the effect of agmatine on human metabolism (through data on biomarkers and diseases), dietary intake (EPIC protocol (88)) and microbial composition in n=1,704 human subjects of the FoCus cohort in Kiel, Germany (86). Additionally, we performed functional cell culture experiments in five different cell lines (mouse and human tissues) to unravel molecular effects of agmatine. For this purpose we analyzed metabolic, inflammatory and dietary parameters in association to agmatine with bioinformatical models in the FoCus cohort. Further, we used 16S rRNA gene sequencing data to display human gut microbiota measures in relation to agmatine. Urine MS-metabolomics data was used to associate availability of agmatine in the blood with potential degradation products in the human urine. Genomic analysis gave insights into the association of agmatine with human SNPs via genome-wide association study (GWAS) method. Lastly, agmatine treatment was applied on mouse adipocytes, human colon adenocarcinoma cells, human hepatocytes and human monocytes and measured via the expression of particular antibodies through Western Blot. Human embryonic kidney cells were treated with agmatine and relative luciferase activity was measured after transfection experiments.

3 Material and methods

3.1 Study population and study design of the FoCus cohort, ATP cohort & Intervention cohort

FoCus cohort

The network of competence FoCus was funded by the German Ministry of Education and Research (BMBF). In this framework a cohort of n=2,000 individuals was established from 2011-2015 in Kiel (Germany). The aim of the FoCus cohort was to implement nutritional intervention studies, integrate genetic and environmental factors in the development of nutrition-associated diseases, develop functional food products and evaluate them in human intervention studies. One part (n=500) of the cohort was recruited from obesity outpatient clinic of the Department of Internal Medicine I of the University Hospital of Kiel. The other part (n=1,500) of the cohort was recruited from the regional registration office as cross-sectional controls. The study population of FoCus was extensively phenotyped and genotyped. The following measurements were included in the procedure: collection of blood samples for measuring several metabolic and inflammatory parameters, anthropometric measurements and microbiome investigations through 16S rRNA gene sequencing of collected stool samples. Study subjects were genotyped using the Illumina Immunochip and the Affymetrix Whole Exome Array as described elsewhere (89). In addition to these measurements subjects completed a 12-month retrospective food frequency questionnaire (FFQ) that was evaluated by EPICsoft database in order to gain more insights into nutritional intake. Prior to the study, a formally written consent was obtained from each subject. The German Clinical trial registration number is DRKS00005285 and the grant number is 0315540A.

Alberta's Tomorrow Project cohort

The ATP cohort from Alberta, Canada consists of an overall study population of n=52,810. In this analysis we used n=438 subjects as a cross sectional comparison. These included 242 healthy controls (with a BMI between 20-25 kg/m²), 120 subjects with cardiovascular disease, 36 with chronic metabolic disease and 44 with chronic inflammatory disease. Fecal samples from all n=438 ATP subjects were available for the present analysis and 16S rRNA gene sequencing was performed in the same laboratory and using the same methodology as for the FoCus cohort samples.

Intervention cohort

For validation of 16S rRNA gene sequencing data, we performed qPCR for *Parasutterella excrementihominis* of n=55 patients of an intervention cohort described elsewhere (90). In brief, this group of severely overweight patients underwent a dietary intervention that consisted of a very low calorie formula diet for the duration of 12 weeks, followed by a stabilization period of another 14 weeks. It is important to mention that the formula diet used was enriched in fish oil according to the EU regulations and contained low carbohydrate content.

Patients received extensive medical, dietary and psychological monitoring during the intervention and gave blood and stool samples at the beginning, mid-point and end of the study. All patients of the intervention study gave their informed consent.

3.1.1 16S rRNA gene sequencing

Stool samples of the study populations were stored at -80°C for microbiome gene sequencing. The Institute of Clinical Molecular Biology (IKMB) in Kiel (Germany) realized laboratory work, quality control and taxonomic classification.

16S rRNA gene sequencing was performed as explained previously (91). The gut microbiome of the probands was identified through DNA sequencing of the variable regions V1 V2 of the bacterial 16S rRNA gene. The QIAamp DNA stool mini kit and the QIAcube technology from Qiagen was used for DNA extraction. In order to amplify the variable regions V1 V2 primers such as 27F and 338R were integrated in a PCR. After normalization, the Illumina MiSeq technology was used for 16S rRNA gene sequencing. When sequences were below a quality of 30 and had less nucleotides than 95%, data was left out. Bioinformatic analysis was done using amplicon sequence variants (ASVs) in R (92). *Parasutterella* was generated for each sample through this method.

3.1.2 Metabolomics sample preparation

In general samples of the FoCus and ATP cohort were prepared according to the following procedure implemented by the group of Food Technology, Department of Human Nutrition, University of Kiel:

Serum samples were thawed on ice and extracted by a modified SIMPLEX approach according to Matyash et al. (93). From 100µl blood samples, a lipophilic methyl-tert-butyl

Material and methods

ether (MTBE) phase, a hydrophilic methanol-water phase and a protein pellet were obtained, dried under vacuum (speed-vac from Thermo Fisher, Germany) and resuspended with the following solvent: the lipophilic phase with a mixture of isopropanol/chloroform (3/1, v/v) with 0.1% acetic acid; the hydrophilic phase with water/methanol (50/50, v/v) with 0.1% acetic acid.

To each sample, 4 µl of an internal standard mixture were added. The hydrophilic standard contains a mixture of ¹³C-labeled tyrosine and tryptophan. The lipophilic standard contains synthetic lipids PC 5:0, PC 11:0, PC 19:0 and PG 17:0. All samples were stored at -80°C until the day of measurements.

Mass spectrometry was conducted using a FT-ICR-MS (7 Tesla, SolarixR, Bruker, Bremen, Germany) in the flow-injection mode. The injection was facilitated by a high performance liquid chromatography (HPLC) autosampler (1260 Infinity, Agilent, Waldbronn, Germany). The eluent for the hydrophilic samples was water/methanol (50/50, v/v) with 0.1% acetic acid and for the lipophilic samples, isopropanol / chloroform (3/1, v/v) with 0.1% acetic acid, respectively. The samples were ionized with an electrospray ionization source (in both modes). Different methods were used, each optimized to the respective detection range (in total, the range were from 65-3000 m/z). The average resolution at 400 m/z was 600,000. Evaluation of mass features was conducted with DataAnalysis 5.0 and MetaboScape 4.0.1 both from Bruker (Bremen, Germany). Molecular sum formulas were calculated based on the mass error and isotopic fine structure of mass features. To reduce false-positive results, the seven golden rules of Kind and Fiehn were applied (94).

In particular, agmatine was measured in n=473 samples and absence of agmatine existed in n=1,232 samples of the FoCus cohort that have been further used as a dependent variable in statistical calculations.

3.2 Bioinformatical analysis

The bioinformatical analysis was done in Rv3.6.0. for statistical calculations as well as graphical figures (95). Additionally, Graphpad Prism 5 was used to create graphical figures in particular for the experimental laboratory part. The following part will describe the particular analyses applied either for *Parasutterella* or agmatine.

3.2.1 Univariate analysis

Agmatine

For phenotypical data, we used Wilcoxon-rank sum test to calculate differences in two groups (agmatine absence vs. agmatine presence). Further, we applied Spearman correlation to test associations of continuous variables (phenotypical and nutritional) with agmatine intensities. For gender and diseases we used Chi-squared test in two groups of agmatine absence vs. agmatine presence. Statistical significance was set at $p < 0.05$. P-values were shown as FDR (False Discovery Rate) adjusted to correct for multiple hypotheses testing.

3.2.2 Multivariate analysis

Parasutterella

Data was tested for normality by Shapiro-Wilk-Test. Since *Parasutterella* distribution included various statistical zeros, hurdle models were chosen in order to handle the excess number of zeros and overdispersion in the data (96). Hurdle models are two-part (negative-)binomial regression models in which probabilities for the non-zero and zero abundances of *Parasutterella* are handled separately. In the first part of the model (henceforth called “count part”) the model is truncated at zero and a negative-binomial linear regression is fitted to the remaining abundance data. In the second part of the model (henceforth called “zero part”) a logistic regression is fitted to determine the binary probability of agmatine being zero vs. non-zero. ASV abundances of *Parasutterella* sp. lower than 10 counts were set to zero prior to using the hurdle algorithm to adjust for the error in determining low counts of 16S rRNA data. A multivariate hurdle algorithm was used to model the association of *Parasutterella* and the independent variable of interest including phenotypical as well as nutritional data. As confounding factors, we used variables such as inflammatory bowel disease (IBD), psoriasis and age that might influence our models, since previous publications reported significant influence of these conditions (97)(98). Additionally, when marked accordingly, we used BMI as a covariate.

Agmatine

Data was tested for normality by Shapiro-Wilk-Test. Since agmatine distribution included various statistical zeros, hurdle models were chosen as described in the previous section. A multivariate hurdle algorithm was used to model the association of agmatine and the independent variable of interest including phenotypical as well as nutritional data. As confounding factors, we used variables such as gender, age, metformin and BMI that might influence our models, since previous publications reported significant influence on the gut microbiome (62).

3.2.3 Nutritional analysis

Parasutterella & agmatine

A 12-months retrospective FFQ was filled in by the FoCus cohort' participants. The patients' medical record comprising all medications was included. Several amounts of the intake of macro- and micronutrients were calculated for each participant.

First of all, data were grouped into underreporter, average reporter and overreporter according to the Goldberg cut-off (99). This was done in order to identify participants that absorbed too little or too much energy with regard to total calculated energy intake. The basal metabolic rate (BMR) was calculated for each participant according to Schofield (100) and was multiplied by 4.184 to get kilojoule. Table 1 shows the equations after Schofield for estimating BMR from weight (W_t). It was adapted for the particular gender and age group.

Table 1: Equations for estimating BMR

Gender/Age (years)	BMR (kcal/d)
Males	
10-17	$17.7 \times W_t + 658.2$
28-29	$15.0 \times W_t + 692.1$
30-59	$11.5 \times W_t + 873.0$
60+	$11.7 \times W_t + 587.7$
Females	
10-17	$13.4 \times W_t + 692.6$
18-29	$14.8 \times W_t + 486.6$
30-59	$8.1 \times W_t + 845.6$
60+	$9.1 \times W_t + 658.4$

Abbreviations: BMR: Basal Metabolic Rate. Source: Schofield (1985), *Predicting basal metabolic rate, new standards and review of previous work, Hum Nutr Clin Nutr*;39 1:5-41.

The total energy intake (GJ) was divided by BMR for each participant. Afterwards, the lower and upper cut-off was calculated with the following formula, whereby the PAL-value is 1.6 for average activity, SD_{min} is -2, SD_{max} is 2, and n is 1:

Lower cut-off: $El: BMR > PAL \times \exp [SD_{min} \times (S/100/\sqrt{n})]$

Upper cut-off: $El: BMR > PAL \times \exp [SD_{max} \times (S/100/\sqrt{n})]$

S was calculated as the following: $S = \sqrt{(CV_{wEI}^2 / d) + CV_{wB}^2 + CV_{tP}^2}$

CV_{wEI} = 23%; for within-subject variation in energy intake

d = 365; for the number of days of diet assessment

CV_{wB} = 8.5%; for the within-subject variation in repeated BMR measurements

CV_{tP} = 15%; for the total between-subject variation in PAL

Finally, the cut-off variable consisted of three subgroups and was used for further multivariate modeling (hurdle model) as a confounding variable.

In total 134 macro- and micronutrients were used for statistical calculations. Next, nutrients such as protein, fat, short-chain fatty acids, medium-chain fatty acids, long-chain fatty acids, polysaturated fatty acids and polyunsaturated fatty acids were adjusted to the total GJ of each individual in order to further use the energy density for statistical models. All other nutrients except for water and kitchen waste were adjusted by using residuals

Material and methods

from regressing nutrients against total energy intake according to Willet et al. (101). Residuals were then added to the mean of one nutrient for all subjects. Negative values were replaced with zero since they could not be used for further statistical calculations. Finally, we applied the multivariate hurdle algorithm as described previously to investigate the association of *Parasutterella*/agmatine and the particular independent variable.

3.2.4 Microbiome analysis

Parasutterella & agmatine

For microbial data human subjects were grouped into absence and presence of *Parasutterella*/agmatine. A phyloseq object using the R package 'phyloseq' was used to combine phenotypical data, taxon-by-sample ASV abundance data and phylogenetic data. Furthermore, the phyloseq object was pruned to exclude ASVs that showed zero abundance in all probands. The file was grouped into six taxonomic ranks for each ASV: domain, phylum, class, order, family and genus classified with a certainty of > 80%. For further microbiome measurements the package 'microbiome' was used. The core measurable microbiome was defined that an ASV has to occur in 40% of the samples (prevalence) with a bacterial mean abundance of > 0.5% in the study cohort. The α -diversity was characterized by the Shannon diversity, Chao1 as well as Species Richness indices (102). The α -diversity reflects the intra-individual bacterial diversity based on ASV distribution within one sample. The Species Richness is the count of different species in one sample independently of the abundance. The Shannon diversity is defined by the proportion of each ASV as measured by the total microbial mass in one sample. It takes into account if the distribution of ASVs in one sample is evenly or if less ASVs dominate one sample's microbiome proportionally. The Chao1 Index assumes that the number of ASV observations has a Poisson distribution and corrects for variance. So, it takes into account the richness of a bacterial community by also integrating ASVs with a low abundance in one sample. The α -diversity indices were calculated with the 'vegan' package. Wilcoxon-rank sum tests were used to elaborate on differences in the two groups. β -diversity was characterized by the Bray-Curtis dissimilarity and Jaccard index. It defines the inter-individual diversity of microbial composition between samples. The Bray-Curtis index (103) focuses on the dissimilarity of two samples regarding ASV abundances. A dissimilarity matrix is calculated with indices ranging from 0 to 1 whereby 1 accounts for two samples having no bacteria in common. The Jaccard index (104) focuses on the ASV being present/absent in a sample pair comparison based on their core measurable microbiome only. It therefore includes a binary variable in the calculation instead of all

absolute abundances. Both indices were calculated with the package 'vegan' with the 'vegdist' function. Additionally, a permutational multivariate analysis of variance (PERMANOVA) (105) was used to calculate differences in β -diversity between absence/presence of *Parasutterella*/agmatine with 1,000 permutations to adjust for bias in parameter estimates.

3.2.5 Metabolomic analysis

Parasutterella

Metabolomics data was either K-nearest neighbor (KNN) (for samples with < 50% missingness) or limit of detection (LOD) (for samples with > 50% missingness) imputed and then log-transformed. For the metabolomics analysis once again the hurdle models were used as previously described.

3.2.5.1 Metabolomics pathway enrichment analysis

Parasutterella

Based on the results of mass spectrometry metabolite analysis, we performed an enrichment analysis in MetaboAnalyst 5.0 in order to find common pathways of all the metabolites that are significantly associated with *Parasutterella*. Out of 256 nominally significant metabolites, we made use of n=126 metabolites that were significantly associated with *Parasutterella* sp. abundance after correction of p-values in the count part of the hurdle model. Of the 126 a total 76 metabolites could be matched to terms of The Small Metabolites Pathway Database (SMPDB), whereas the other 40 were unidentified compounds.

3.2.5.2 Microbial community metabolism

Parasutterella

L-cysteine prediction models were implemented by the group of Medical System Biology, Institute of Experimental Medicine, University of Kiel.

Metabolic network modeling was used to elucidate to which extent *Parasutterella* and associated gut microbes are involved in the consumption or production of certain

Material and methods

metabolites, like L-cysteine. In order to predict L-cysteine consumption by bacteria of the gut microbiota, we employed gapseq (v1.2) to reconstruct metabolic models (106) based on genomic data originating from the reference set of 820 bacteria and archaea belonging to the human gut microbiota (AGORA collection (106)). Default settings of gapseq were used. For gap filling and modeling of in silico growth, we assumed a nutritional environment corresponding to the average dietary input recorded for a cohort of human participants as described previously ("Kiel cohort") (62). For each individual bacterial model, we used flux balance analysis (107) implemented in the package 'sybil' (version 2.2.0) (108) with biomass production as objective and unconstrained L-cysteine uptake as input to predict maximal L-cysteine consumption during optimal growth. We used information about the relative abundances of bacterial species from the FoCus cohort as references to determine average abundance of each bacterial species across human samples. Relative cysteine uptake was then determined by multiplying the maximal L-cysteine uptake of each bacterial species by the average relative abundance of the corresponding bacterial species in the FoCus cohort.

3.2.5.3 Urine metabolomics

Agmatine

For urine metabolomics data we had n=12 detectable positively ionized metabolites and n=3 detectable negatively ionized metabolites available. Those metabolites were previously determined through MetaboScape, belonging to the arginine and proline metabolism. The measurements, laboratory work and quality control were realized by the group of Food Technology, Department of Human Nutrition, University of Kiel.

Values of metabolites and agmatine were log-transformed. For continuous agmatine values (log-transformed) we used a hurdle model as described above. For the dichotomous variable of agmatine (agmatine absence and agmatine presence) we used a general logistic regression model for binomial distributions. In a second step, we additionally used confounder such as gender, age, BMI in our models.

3.2.6 Genomic analysis (GWAS)

Parasutterella

Information about 962,927 SNPs from 1,455 samples were available. GWAS was done in PLINK. 1,455 human individuals were selected for genotyping, and after genotype quality

control (QC) (109) 1,397 human individuals remained for association analyses, including 512 males and 885 females. These genotypes included 255 cases (*Parasutterella* > 10) and 1,142 controls.

Firstly, data excluded SNPs that were missing in a large proportion of the subjects (geno 0.2) and individuals who had high rates of genotype missingness (mind 0.2). After the first QC step 1,415 subjects remained. Secondly, the data was checked for discrepancies between sex of the individuals and their sex based on X chromosome heterozygosity/homozygosity rates (females: F-value of < 0.2, males: F-value of > 0.8). After the second QC step 1,397 subjects remained and 18 subjects were flagged as 'problem' in the dataset. With the help of a filtered dataset, those 18 subjects were deleted. In step three SNPs with low minor allele frequency (MAF 0.05) were excluded. An amount of 317,379 SNPs failed frequency test and were therefore deleted from the dataset. The fourth step deleted SNPs, which deviate from Hardy-Weinberg-Equilibrium and selected SNPs with p-value below 0.00001. There were 0 markers from cases and controls excluded. 579,666 SNPs remained for analysis. The fifth step checked for heterozygosity rate of subjects, and was performed on a set of SNPs which was not highly correlated (deviate ± 3 mean), and individuals who deviate more than 3 standard deviations from the heterozygosity rate mean were deleted. After, the dataset was tested for cryptic relatedness, meaning identity by descent of all sample pairs was calculated indicating a Pihat threshold of 0.2. There were no subjects with relatedness above the chosen threshold identified. Step seven would include population stratification that would have been checked through data from 1000 Genome-project, in order to remove subjects with non-European ethnic background. Since our population was collected and examined in Northern Germany, there might be less probability that there is a high amount of different ethics. In summary, in total 1,397 subjects and 579,666 SNPs of 962,927 SNPs remained for analyses, which were applied for a logistic regression.

Agmatine

Information about 937,641 SNPs from 1,486 samples were available. After genotype QC, 1,486 human individuals remained for association analyses, including 553 males and 933 females. These genotypes included 410 cases and 1,076 controls. In total 937,641 SNPs were used for logistic as well as linear analysis. Beforehand, the same QC procedure was applied as described in the previous part.

Material and methods

3.3 Cell culture

Agmatine was investigated in mouse as well as human cell lines in order to cover its effect of a wide spectrum of metabolic processes and tissues. Cell culture experiments of Caco-2 and Hep-G2 cells were completed by master students from our institute namely Ella Ubbelohde and Thea Bruns under the guidance of Lea Henneke.

3.3.1 3T3-L1 (mouse pre-adipocytes)

The mouse cell line was obtained from the American Type Culture Collection (ATCC, USA, no. CL-173)

3.3.2 Caco-2 (human colon adenocarcinoma cells)

The cells (no. HTB-37) were a generous donation from the IKMB, Kiel (group of Prof. Rosenstiel)

3.3.3 Hep-G2 cells (human hepatocytes)

The human cell line was purchased from the Leibniz Institute (DSMZ, Germany, no. ACC180).

3.3.4 THP-1 cells (human monocytes)

The human cell line was purchased from the Leibniz Institute (DSMZ, Germany, no. ACC16).

3.3.5 HEK293 cells (human embryonic kidney cells)

The cells (no. CRL-1573) were a generous donation from the IKMB, Kiel (group of Prof. Rosenstiel).

3.4 Material

3.4.1 Technical instruments

Table 2: Technical instruments

instrument	name	company
Blot-Equipment	Fastblot B34	Biometra GmbH (Göttingen, Germany)
Centrifuge I	VWR Micro Star 17R	Thermo Electron LED GmbH (Osterode,

		Germany)
Centrifuge II	Heraeus Multifuge 1S-R	Thermo Fisher
Centrifuge III	Mini-Zentrifuge Rotilabo Unifuge	Roth (Karlsruhe, Germany)
Heating block	TSC Thermo Shaker	Biometra GmbH (Göttingen, Germany)
Incubator	Heracell 150	Thermo Scientific
Luminometer	Mithras LB 940	Berthold Technologies (Bad Wildbad, Germany)
Magnetic stirrer	IKAMAG RCT	IKA Labortechnik (Staufen, Germany)
Microbiological safety workbenches	Heraeus	Thermo Fisher (Langenselbold, Germany)
Microscope	Motic AE31 E Series	Motic (Wetzlar, Germany)
PH-meter	FiveEasy FE20	Mettler-Toledo AG (Schwerzenbach, Switzerland)
Photometer	ChemiDoc XRS+ Imaging system	Bio Rad Laboratories GmbH (Feldkirchen, Germany)
Precision scale	Kern Gab	Kern & Sohn GmbH (Balingen, Germany)
Spectrophotometer	NanoDrop 2000 spectrophotometer	Thermo Fisher (Langenselbold, Germany)
Vortexer	Vortex-Genie 2	Scientific Industries (New York, USA)
Water bath	Wasserbad 1103	Gesellschaft für Labortechnik (Burgwedel, Germany)

3.4.2 Chemicals, antibodies and consumables

Table 3: Chemicals, antibodies and consumables

material	company
2-propanol	1.09634.2500, Merck
3-Isobutyl-1-Methylxanthine	I5879, Sigma-Aldrich
6-Aminocaproic acid	A2504, Sigma
Actrapid® Penfill	Novo Nordisk
Agmatin Sulfate (A7127)	MKCH3294, Sigma-Aldrich
Ampicillin	K029.1, Roth
Anti-rabbit secondary antibody	R10367, Thermo Fisher
Beta-Mercaptoethanol	M3148, Sigma-Aldrich
Cell culture plate (96 wells, 12 wells, 6 wells)	0020821, Sarstedt 3513, Costar 140675, Thermo Scientific
Cell scraper	83.3951, Sarstedt
Claudin 3 antibody	PA137469, Thermo Fisher
Dexamethasone	D4902, Sigma-Aldrich
Dimethylsulfoxid	Sc-358801, ChemCruz
Dual Luciferase Reporter Assay System	E1910, Promega
Dulbecco's Modified Eagle's Medium	10313021, Thermo Fisher
Dulbecco's Phosphate Buffered Saline (PBS)	56110008, Geyer
Endofree Plasmid Maxi Kit	12362, Qiagen
FABP4 antibody	PA530591, Thermo Fisher
Falcons	50ml: 62.559.001, Sarstedt
Fetale Bovine Serum	F7524, Sigma-Aldrich
FuGENE® HD	E2311, Promega
GAPDH antibody	14C10, Cell Signaling
Laemmli Sample Buffer	161-0747, Bio-Rad
LB-agar (Luria/Miller)	6675.1, Roth
LB-medium (Luria/Miller)	X968.2, Roth
L-Glutamine	X0550, Biowest
Methanol	4627.2, Roth
Micropipettes (1000µl, 200µl, 100µl, 20µl, 10µl, 2.5µl)	Eppendorf

Micropipette tips (1000µl, 2-200µl, 2,5µl)	1000µl: 70.3060.355, Sarstedt 200µl: 70.3030.100 Sarstedt 20µl: 70.1114.210, Sarstedt 2,5µl: 70.1130.212, Sarstedt
Milk powder	T145.2, Roth
Minimum Essential Medium	31095029, Thermo Fisher
Neutral Red Solution	sc-281691, Santa Cruz Biotechnology
Newborn Calf Serum	16010159, Gibco
NFκB (p105/p50) antibody	Ab32360, abcam
Nuklease-free water	R0582, Thermo Fisher
Oil Red O Solution	O0625-25G, Sigma-Aldrich
One Shot Chemically Competent <i>E. coli</i>	C4040-10, Invitrogen
Opti-MEM 100ml	31985062, Gibco
Parafilm	90026071, Roth
Pasteurpipettes	40567002, Hecht Assistent
Penicillin-Streptomycin Solution 100x	11681940, Geyer
Petri plates	83.3903.300, Sarstedt
pGL4.32 [luc2P/NF-κB-RE/Hygro]	AG Prof. Arlt (Molecular Gastroenterology, Kiel, Germany)
Phospho-NF-κB p65	3033T, Cell Signaling
PhosStop Easy pack tablets	04906845001, Roche
Phorbol-12-myristate-13-acetate (PMA)	P1585, Sigma-Aldrich
PowerUp Syber Master Mix	A25742, Thermo Fisher
PPAR-γ antibody	2435S, Cell Signaling,
Protease Inhibitor Cocktail	109M4068V, Sigma Aldrich
Protein Assay Dye Reagent Concentrate	500-0006, Bio-Rad
PVDF transfer membrane	Carl Roth
Restore™ Plus Western Blot Stripping Buffer	46430, Thermo Scientific
Roswell Park Memorial Institute -1640 W/O Glutamine	31870025, Thermo Fisher
SafeSeal tubes (2ml, 1,5ml)	72.695.500, Sarstedt 72.706.700, Sarstedt
Serological pipettes (50ml, 25ml, 10ml, 5ml)	86.1256.001, Sarstedt 86.1685.001, Sarstedt 86.1254.001, Sarstedt

S.O.C. medium	15544034, Invitrogen
SREBP1 antibody	MA511685, Thermo Fisher
SuperSignal West Dura	34076, Thermo Fisher
SuperSignal West Dura Luminol Enhancer	1856145, Thermo Scientific
SuperSignal West Dura Stable Peroxide	1856146, Thermo Scientific
TEMED	11652164, Geyer
Trypan Blue Stain	15250061, Gibco
Trypsin	25300062, Gibco
Tumor Necrosis Factor alpha	10716971, Geyer
Tween-20	P2287, Sigma-Aldrich
WesternSure Pre-Stained Chemiluminescent Protein Ladder	926-98000, LI-COR
Whatman™ filter paper	1003-917, GE Healthcare
ZO-2 antibody	2847S, Cell Signaling

3.4.3 Buffers

Table 4: Buffers

buffer	buffer composition
1x Sodium dodecyl sulphate (SDS) running buffer	100ml SDS 10x 1000ml dH ₂ O
10x SDS	60.4g Tris Base 288g Glycine 20g SDS 2000ml dH ₂ O
1x Tris buffered Saline/Tween (TBS/T)	100ml TBS 10x 1ml Tween-20 2000ml dH ₂ O
10x TBS	140g NaCl 4g KCl 60g Tris Base 2000ml dH ₂ O
Radioimmunoprecipitation assay buffer (RIPA)	2.5ml Tris-HCL (pH 7.4) (500mM) 2.5ml NaCl (1500mM)

	2.5ml Na-Deoxycholat (5%) 2.5ml SDS (1%) 2.5ml Nonidet P-40 (10%) 2.5ml EDTA (20mM) 10ml dH ₂ O
Transfer buffer A	36.34g Tris Base 200ml MeOH 1000ml dH ₂ O
Transfer buffer B	3.03g Tris Base 200ml MeOH 1000ml dH ₂ O
Transfer buffer C	3.03g Tris Base 200ml MeOH 0.5g/100ml aminocaproic acid 1000ml dH ₂ O

3.4.4 Composition of SDS-PAGE (30% acrylamide)

Table 5: Composition of small gels

small gels	composition
Seperation gel (2 gels)	4ml dH ₂ O 1.4ml SDS (1%) 2.8ml Tris-HCL (1.88M) 5.8ml Acrylamid (30%) 70µl APS 12µl TEMED
Stacking gel (2 gels)	2.2ml dH ₂ O 0.4ml SDS (1%) 0.8ml Tris-HCL (0.625M) 0.6ml Acrylamid (30%) 20µl APS 4µl TEMED

Table 6: Composition of large gels

large gels	composition
Separation gel (2 gels)	12ml dH ₂ O 4.2ml SDS (1%) 8.4ml Tris-HCL (1.88M) 17.4ml Acrylamid (30%) 210µl APS (10%) 36µl TEMED
Stacking gel (2 gels)	8.8ml dH ₂ O 1.6ml SDS (1%) 3.2ml Tris-HCL (0.625M) 2.4ml Acrylamid (30%) 80µl APS (10%) 16µl TEMED

3.5 Methods

3.5.1 Quantitative polymerase chain reaction

Parasutterella

Genomic DNA (gDNA) was extracted from stool samples using the Qia Amp Fast DNA Stool Mini Kit according to the manufacturer's protocol. For quantifying the amount of DNA in each fecal sample, we used a Thermo NanoDrop 2000 spectrophotometer. A concentration of 2.5ng/µl was used of each sample. For qPCR measurement a tenfold serial dilution of *Parasutterella excrementihominis* was generated to produce a standard curve (ordered from DSMZ, Germany). The qPCR system contained a PowerUp™ SYBR™ Green Master Mix (5µl), the forward primer and reverse primer (2.5µM each) and DNase free water (4.5µl). The primers for *Parasutterella excrementihominis* were selected according to a study of Chen and co-workers: GGAAGTACGGTCGCAAGA (forward) and TGTCAAGGGTTGGGTAAGACA (reverse) (104). Melt curves and relative quantification of *Parasutterella excrementihominis* were generated with Bio-Rad CFX Connect™ Real-Time System PCR instrument with the help of the following template: 50°C for 2 min, preliminary denaturation at 95°C for 2 min, 40 cycles at 95°C (15 sec), 40 cycles annealing at 60°C (30 sec), 40 cycles extension at 60°C (1 min). Melt curve analysis were performed between 65°C and 95°C (increment: 0.5).

Bio-Rad CFX Manager 3.0 was used to analyze melt curves and copy numbers of the target gene concentrations. C_t -values of the target gene were indicated with the help of a standard curve to obtain the final concentration through the following formula:

$y = -1.48\lg(x) + 13.854$ ($R^2 = 0.9979$). C_t -values of the reference gene (primer: EUB338F: ACTCCTACGGGAGGCAGCAG, EUB518R: ATTACCGCGGCTGCTGG) were calculated through the following formula: $y = -1.349\lg(x) + 14.338$ ($R^2 = 0.9942$). The formula used varied according to each plate. Afterwards, the C_t -value of the target gene was divided through the C_t -value of the reference gene.

In order to assure that the primers of the target gene were binding solely to gDNA of *Parasutterella*, three bacteria such as *Lactobacillus reuteri* (DSM20016), *Bifidobacterium bifidum* (DSM20082) and *E. coli* (DSM10725) were used as control in a previous experiment.

3.5.2 Cell cultivation 3T3-L1

Agmatine

To start up, an aliquot (2nd passage) was thawed at 37°C, quickly suspended in 9ml Dulbecco's Modified Eagle's Medium (DMEM) supplemented with 10% newborn calf serum (NBCS), 1% L-glutamine and 1% penicillin/streptomycin and centrifuged for 7 min at 125 xg. The cell pellet was resuspended in 6ml DMEM/10% NBCS and 2 x 3ml were added to two T25 flasks (25cm²) for adherent cells which contained 2ml pre-warmed medium each.

After two days, cell suspension was transferred to a T175 flask and DMEM/10% NBCS was added up to a total volume of 15ml. Cells were cultured at 37°C in a 5% CO₂ incubator. The cells were subcultured every three days when 70-80% confluence was reached at a split ratio between 1:6 and 1:8. Cells were then pre-washed with PBS (20ml) and became loose by trypsinization (7ml). Subsequent experiments were based on this starting point.

3.5.3 Cell cultivation Caco-2

Caco-2 cells (2nd passage) were thawed at 37°C and suspended in 15ml Minimum Essential Medium Eagle (MEM) supplemented with 20% FCS and centrifuged for 5 min at 300 xg. The cells were resuspended in 10ml MEM/20% FCS and added to a T175 flask

Material and methods

for adherent cells. Medium was added up to a total volume of 20ml and the flask was incubated at 37°C and 5% CO₂. The cells were subcultured every three to four days at a split ratio between 1:3 and 1:8 depending on the confluence of the cells (maximum 90%). Subsequent experiments were based on this starting point.

3.5.4 Cell cultivation Hep-G2

Hep-G2 cells (6th passage) were thawed at 37°C and suspended in 15ml in Roswell Park Memorial Institute Medium 1640 (RPMI) supplemented with 10% FCS, 1% L-glutamine and 1% penicillin/streptomycin and centrifuged for 5 min at 1100 xrpm. The cells were resuspended in 10ml RPMI/10% FCS and added to a T175 flask for adherent cells. Medium was added up to a total volume of 25ml and the flask was incubated at 37°C and 5% CO₂. The cells were subcultured every three to four days at a split ratio between 1:2 and 1:3 depending on the amount of total cells. Subsequent experiments were based on this starting point.

3.5.5 Cell cultivation THP-1

THP-1 cells (4th, 6th and 9th passage) were thawed at 37°C and suspended in 15ml RPMI medium (including 10% FCS, 2mM L-glutamine and 1% penicillin/streptomycin) and centrifuged for 5 min at 258 xg. The cells were resuspended in 10ml RPMI/10% FCS and added to a T175 flask for suspension cells. Medium was added up to a total volume of 20ml and the flask was incubated at 37°C and 5% CO₂. The cells were subcultured every three days at a split ratio between 1:4 and 1:5 depending on the amount of total cells. Subsequent experiments were based on this starting point.

3.5.6 Cell cultivation HEK293

HEK293 cells (2nd passage) were thawed at 37°C and suspended in 15ml DMEM medium (including 10% FCS without antibiotics) and centrifuged for 5 min at 300 xg. The cells were resuspended in 10ml DMEM/10% FCS and added to a T175 flask for adherent cells. Medium was added up to a total volume of 20ml and the flask was incubated at 37°C and 5% CO₂. The cells were subcultured two times a week at a split ratio between 1:6 and 1:10 depending on the amount of total cells. Subsequent experiments were based on this starting point.

3.5.7 General cell counting procedure

For the seeding procedure a constant cell concentration was attained through prior cell counting. Cell suspension of a T175 flask was pipetted into a falcon and centrifuged at the particular condition for the particular cell line. Supernatant was removed and the cell pellet was resuspended in 10ml medium. 90µl of trypan blue and 10µl of cell suspension were pipetted into an Eppendorf tube. 10µl of this suspension was pipetted on the Neubauer counting chamber and cells were counted for each counting grid (4 in total, 1 x 1 mm). Mean number of cells was calculated. The following formula was used to calculate the total concentration of cells in the falcon: $(\text{mean cell number}/0.1) \times 1000 \times 10 \times 10 = \text{total cells}/10\text{ml}$. For adherent cell lines the procedure was followed without trypan blue staining.

3.5.8 Cell culture experiment with 3T3-L1 cells

3T3-L1 mouse pre-adipocytes were cultured in DMEM supplemented with 10% NBCS, 1% L-glutamine and 1% penicillin/streptomycin until they reached 70-80% confluence. Then cells were harvested by trypsinization and seeded 25×10^4 in a 6-well plate. Cells were cultured at 37°C in a 5% CO₂ Incubator. Medium of 3T3-L1 was changed after 2-days post-confluence (100%) to DMEM supplemented with 10% FCS, 0.25µM dexamethasone, 0.5µM isobutylmethylxanthine, 0.83µM humane insulin, 1% L-glutamine, 1% penicillin/streptomycin to induce differentiation into adipocytes. After two more days medium was changed to DMEM supplemented with 10% FCS, 0.83µM humane insulin, 1% L-glutamine and 1% penicillin/streptomycin. After another two days medium consisted of DMEM supplemented with 10% FBS, 1% L-glutamine and 1% penicillin/streptomycin. Cells remained in medium for four days until lysis (see 3.5.12) with RIPA supplemented with PhosStop phosphatase inhibitor (PhosStop, dilution 1:10) and a Protease Inhibitor Cocktail (PIC, dilution 1:100) was done. Cells were scraped and stored at -80°C. Either agmatine (100µM or 500µM concentration) or phosphate buffered saline PBS (1%) as a control was added from 2-day post-confluence onwards during the whole differentiation procedure. The experiment was repeated four times.

Lipid (Oil Red O) staining

Right before the cell lysis of adipocytes took place, cells were fixed with 2ml formalin (10%) and incubated at room temperature for 30 min. After cells were washed two times

Material and methods

with 2ml dH₂O. The working solution of Oil Red O was prepared 10 min before usage. Oil Red O solution was suspended in dH₂O (3:2) and incubated at room temperature for 10 min. Isopropanol (60%) was suspended with dH₂O (3:2) and 2ml was added to each well and incubated at room temperature for 5 min. After removing isopropanol mixture, 2ml Oil Red O working solution was put on cells and incubated for 20 min. Cells were washed with 2ml dH₂O for three times and lipid droplets were stained red.

3.5.9 Cell culture experiment with Caco-2 cells

The following part consists of pre-experiments focusing on a three day differentiation procedure and a final experiment of three weeks differentiation.

Three days differentiation

For time- and dose- response experiments, Caco-2 cells were seeded at a density of 0.8×10^6 cells per well into a 6-well plate in 2ml MEM/20% FCS. After culturing for 2 days the cells reached 100% confluence. On day 3, all wells except of the positive control were incubated with TNF- α (100ng/ml) in serum-free MEM for 24h.

For the time-response experiment, 2h prior to finalising TNF- α incubation, agmatine was added directly into the medium (1mM). Afterwards, the plate was shaken gently and incubation at 37°C in 5% CO₂ followed. This step was repeated independently for all other wells regarding different time slots such as 0.25h, 0.5h and 1h. A negative control was left untreated. Cells were lysed with RIPA buffer supplemented with PhosStop (1:10) and PIC (1:100). The lysate was stored at -80°C.

For the dose-response experiment, the procedure was similar, except of cells being incubated with agmatine 1h prior to finalizing TNF- α incubation to all wells with different concentrations compromising 100 μ M, 500 μ M, 1mM, 5mM and 10mM. The experiments were repeated 4-5 times.

Three weeks differentiation

Caco-2 cells were cultured until 80% confluence and seeded at a density of 0.8×10^6 cells per well into a 6-well plate in MEM supplemented with 20% FCS without antibiotics. Cells were grown for six days while medium was changed every two to three days. On day seven the experiment started and cells were treated either with 1mM agmatine every second day or solely with medium. For TNF- α treated wells, cells were treated with 100

ng/ml TNF- α on day 20. Cells were lysed with RIPA on day 21, scraped and stored at -80°C. The experiment was repeated five times.

3.5.10 Cell culture experiment with Hep-G2 cells

Hep-G2 cells were cultured in RPMI supplemented with 10% FCS, 1% L-glutamine and 1% penicillin/streptomycin until 70-80% confluence, then harvested by trypsinization and seeded at a density of 15.7×10^6 into a 6-well plate. Cells were pre-washed with PBS and medium was changed after two to three days. On day seven the medium of Hep-G2 was changed to RPMI supplemented with 1% FCS, 1% L-glutamine and 1% penicillin/streptomycin. The next day the experiment started and medium was changed to RPMI with 1% FCS. The cells were treated with 500 μ M agmatine or with PBS as control and were incubated for 0.5h, 1h or 2h. Then the cells were lysed with RIPA (including PhosStop and PIC), scraped and stored at -80°C. The experiment was repeated four times.

3.5.11 Cell culture experiment with THP-1 cells

THP-1 cells were seeded at a density of 1.5×10^6 in 2ml RPMI per well into a 6-well plate. To differentiate monocytes (THP-1 cells) to macrophages, PMA (Phorbol-12-myristate-13-acetate) was added in dilution 1:10 to each well (stock solution of 160nM). Wells were incubated at 37°C in 5% CO₂ for 24h. Differentiation was proven with a microscope. Cells got adherent and had a polymorphic as well as dendritic structure. Cells were washed with PBS (2ml) and wells were filled up with 2ml RPMI medium and incubated for another 24h to start the experiment afterwards.

For the dose-response experiment, the cells were treated with different concentrations of agmatine: 100 μ M, 500 μ M, 1mM, 5mM and 10mM. PBS remained as a control. Cells were incubated for either 2h or 4h at 37°C in 5% CO₂. Afterwards, cells were lysed with RIPA (including PhosStop and PIC), scraped and stored at -80°C. The experiment was repeated four times for each time period.

For the time-response experiment, the cells were treated with the final concentration of 1mM agmatine and were incubated for either 0.25h, 0.5h, 1h or 2h at 37°C in 5% CO₂. PBS remained as a control. Afterwards, cells were lysed with RIPA (including PhosStop and PIC), scraped and stored at -80°C. The experiment was repeated four times for each time period.

Material and methods

3.5.12 General cell lysis procedure

Differentiated cells

For adherent cells, medium was removed and cells were washed with 2ml PBS per well. Cells were lysed in cold RIPA buffer including PhosStop and PIC (400µl for 6-well plate) and after treated with a cell scraper for pipetting total volume into an Eppendorf tube to store in the freezer at -80°C.

Suspension cells

Suspension cells were transferred into an Eppendorf tube and centrifuged at 258 xg for 5 min. Supernatant was removed by pipetting and the cell pellet was washed in 1ml cold PBS. After the second centrifugation and removing of supernatant, cell pellets were resuspended in cold RIPA buffer including PhosStop and PIC (400µl) and stored at -80°C.

3.5.13 Bradford protein quantification

Lysis sample was diluted 1:10 (2.5µl sample, 22.5µl dH₂O) and 10µl of each probe, standard and blank (dH₂O) were pipetted duplicate into a 96-well plate. BioRad-reagent was diluted 1:5 (1 part reagent, 4 parts dH₂O) and 200µl were added to each well to determine the amount of protein in each sample at 630nm (photometer). As standards, BSA solution (2mg/ml) was prepared as a stock solution and a dilution series (0.5mg/ml, 0.25mg/ml, 0.125mg/ml, 0.060mg/ml) was used. For analysis, means of samples, standards and blanks were calculated and blank mean was deducted of sample and standard means. Concentration of standards (dilution series, see above) and measured concentration (OD-value) were plotted in a linear regression ($y=mx+c$). To measure protein concentration, the OD-value was applied in the linear equation. Calculated results were multiplied by 20 in order to get the protein concentration for the whole sample (dilution factor= 20). For Western Blot, the volume (µl) was calculated for each sample of 30-50µg protein per slot of the gel. Volume of RIPA buffer and Laemmli buffer (4x) was calculated and added to the samples used for Western Blot.

3.5.14 Western Blot

Western Blot is a method for measuring specific proteins through transfer on a carrier membrane based on electrophoresis.

3.5.14.1 Preparation of small and large gels

Two glass plates were cleaned with ethanol and were put in a casting frame. Separating gel and stacking gel were prepared according to specific ingredients (see table 5).

Both gel ingredients were pipetted into a single falcon (50ml) and were well mixed. The separating gel was pipetted (1000 μ l- pipette) in between the glass plates until one centimetre above the top edge. 500 μ l of isopropanol was added to the edge in order to make it evenly. Isopropanol was removed with a filter paper after 30 min. Stacking gel was pipetted between glass plates until the edge and combs were stuck into glass plates for 15 min.

The same procedure was applied for large gels but amounts of ingredients differed (see table 6).

3.5.14.2 Preparation of samples

Samples were heated to 95°C with a heating block for 5 min. After several minutes of cooling down samples were transferred to gel (30-50 μ g per gel pocket). A protein ladder was used as a scale for measuring molar mass of proteins (in kDA).

3.5.14.3 Electrophoresis

Small gels

Firstly, gels operated for 15 min at 80V to gather proteins. Secondly, gels operated for 90 min at 120V to separate proteins. SDS running buffer (1x) was used inside and outside the equipment. This condition was used for THP-1 cells and nuclear factor kappa B (NF κ B) (p105/p50) antibody.

Large gels

Proteins were gathered for 20 min at 80V and separated for 120 min at 120V. This condition was used for THP-1 cells and NF κ B (p105/p50) antibody. Specific running conditions were adapted to the particular experiment and related antibodies as the following:

Table 7: Running conditions in relation to antibodies

Cell line	Antibody	Volt	Minutes
3T3-L1	PPAR- γ	120	75
3T3-L1	FABP4	120	75
Caco-2	ZO-2	140	125
Caco-2	Claudin 3	140	55
Caco-2	p-NF κ B	120	120
Hep-G2	SREBP1	140	150

3.5.14.4 Protein transmission (Semi Dry Blot)

Small gels

Gels were blotted on PVDF transfer membranes for 45 min at 140mA (for THP-1 cells and NF κ B antibody). Previously, membranes were activated for 1 min in methanol. Filter paper was used to ensure accurate blotting. Transfer buffer A-C were used (see table 4). See figure 3 for composition of blotting procedure.

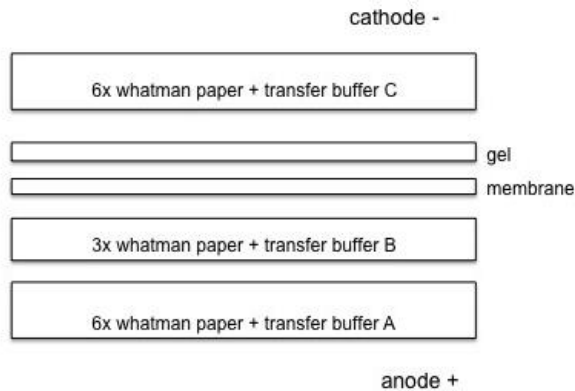


Figure 3: Composition of blotting procedure

Composition for small and large gels

Large gels

Gels were blotted on PVDF transfer membrane for 220mA for 1h generally. The blotting procedure was identical to small gels. Specific blotting conditions were adapted to the particular experiment and related antibodies as the following:

Table 8: Blotting conditions in relation to antibodies

Cell line	Antibody	mA	Minutes
3T3-L1	PPAR- γ	220	90
3T3-L1	FABP4	220	25
Caco-2	ZO-2	220	150
Caco-2	Claudin 3	220	30
Caco-2	p-NF κ B	220	120
Hep-G2	SREBP1	220	105

3.5.14.5 Membrane blocking and incubation of antibodies

Membranes were blocked in TBS with 5% milk powder for 60 min. Afterwards, membranes were washed for 3 x 5 min in TBS/T, the primary antibody with the corresponding dilution was incubated at 4°C overnight. The following day, membranes were washed 3 x 5 min in TBS/T. The secondary antibody with the corresponding dilution was incubated at room temperature for 45 min. Membranes were washed 3 x 5 min again. Proteins were detected by Chemiluminescence with luminol and peroxidase. As normalization, the housekeeping gene glyceraldehyd-3-phosphat-dehydrogenase (GAPDH) was selected. The following table 9 shows the particular antibody and corresponding dilutions.

Table 9: Dilutions of first and secondary antibody

Antibody (first)	Dilution	Antibody (secondary)	Dilution
PPAR- γ	1:1000	Anti-rabbit	1:2000
FABP4	1:1500	Anti-rabbit	1:2000
ZO-2	1:1000	Anit-rabbit	1:2000
Claudin 3	1:2000	Anti-rabbit	1:2000
p-NF κ B	1:3000	Anti-rabbit	1:2000
SREBP1	1:1000	Anti-rabbit	1:2000
NF κ B	1:10,000	Anti-rabbit	1:2000
GAPDH	1:5000	Anti-rabbit	1:2000

Material and methods

3.5.15 Viability assay

The level of cytotoxicity of agmatine was measured for 3T3-L1 as well as THP-1 cells with the help of a viability assay whereby a neutral red solution was used for the staining of the cells.

3T3-L1 cells

Cells were seeded at a density of 8×10^4 in a 6-well plate ($n=4$) in DMEM/NCBS and medium was changed every three days until the cells became 70-80% confluent. Cells were pre-washed with PBS and incubated another 24h in 37°C in 5% CO₂. Neutral-red dissolution was prepared 1:66 with one part being neutral-red and 66 parts DMEM/NCBS. Cells were incubated with medium, PBS, 1mM agmatine or ethanol (EtOH, 10%). After 24h medium was removed and 2ml of the neutral red solution was put on each well for 2h at 37°C in 5% CO₂. Neutral red solution was removed and cells were washed with PBS. Extraction buffer (50% EtOH, 49% dH₂O, 1% pure acetic acid) (2ml/well) was used and plates were vortexed at 600x rpm for 15 min. 200µl/well were transferred into a 96-well plate for the photometer measurement (540 nm).

THP-1 cells

Cells were seeded at a density of 1.5×10^6 in a 6-well plate ($n=3$). Monocytes were differentiated to macrophages with PMA (160nM). After 24h of incubation, cells were washed with PBS (2ml/well) and 2ml RPMI was used to incubate the cells for another 24h. PBS, 100µM agmatine, 500µM agmatine, 1mM agmatine, 5mM agmatine, 10mM agmatine and EtOH (10%) were added independently to the medium and incubated for 24h. Further proceeding was identical to the viability assay of 3T3-L1 cells.

3.5.16 Luciferase assay with HEK293 cells

3.5.16.1 Preparation

For Lysogeny Broth (LB)-medium (Luria/Miller), granulate (37g) was dissolved in 1500ml dH₂O and stirred for 30 min.

LB-agar (Luria/Miller) granulate (20g) was dissolved in 500ml dH₂O and stirred under heating for 1 min as well as autoclaved at 121°C for 20 min. LB-agar was cooled down to 50°C. Ampicillin (1g/20ml) was added to LB-agar. LB-agar was stored at 4°C. Sterile Petri-plates were prepared with 25ml LB-agar under the safety workbench. Petri-plates were incubated at 37°C overnight and stored at 4°C the next day.

One Shot Chemically Competent *E. coli* were stored at -80°C until usage.

The plasmid pGL4.32 (luc2P/NF-κB-RE/Hygro) (Firefly plasmid) for NFκB activity was a generous gift from Prof. Arlt (Molecular Gastroenterology, University Hospital Schleswig Holstein, Kiel). Further, plasmids namely pGL4.15 (luc2P Hygro) and pGL4.74 (hRluc/TK) were included as either transfection control or normal control and were also obtained from Prof. Arlt. The Eppendorf tubes were stored at -80°C until usage.

3.5.16.2 Transformation

In order to copy the plasmid pGL4.32 (1.13 µg/µl), the Eppendorf tube was centrifuged quickly. A dilution of 0.025µg/µl was used for transformation in *E. coli*. 2µl of the dilution was pipetted into one vial of One Shot Chemically Competent *E. coli* that was thawed on ice before (50µl). Vial was mixed gently and incubated on ice for 30 min. After that, vial was heat-shocked for 30 sec. at 42°C in the water bath. Vial was placed on ice for 2 min. 250µl of pre-warmed S.O.C medium (2% Trypton, 0.5% yeast, 10mM NaCl, 2.5mM KCl, 10mM MgCl₂, 10mM MgSO₄, 20mM glucose) was added to the vial and vial was shook horizontally at 37°C for 1h at 225 rpm in a shaking incubator. 20µl were used from the transformation mix and were added to 100µl of LB-medium (including Ampicillin (1g/20ml)) on a pre-warmed Petri-plate with LB-agar. The Petri-plate was inverted and incubated overnight at 37°C. The procedure was repeated and Petri-plates were closed with Parafilm and put into plastic bags.

3.5.16.3 Colony picking

LB-medium was pre-warmed at 37°C and was pipetted into falcons (2x 2ml) for the starting culture. Near a Bunsen burner, colonies on Petri-plates were picked with a sterile pipette tip and pipette tip was discarded into a falcon and the procedure was repeated. Falcons were then incubated at 37°C for 8h at 225 rpm.

LB-medium was pipetted into two Erlenmeyer flasks and pre-warmed at 37°C. Starting culture of falcons was pipetted into Erlenmeyer flasks (dilution 1:500) and incubated for 16h at 37°C and 225 rpm. For low-copy plasmids 250ml LB-medium and 500µl starting culture was used.

Cultures of Erlenmeyer flasks were filled into 50ml falcons and centrifuged at 4618 xg for 15 min at 4°C. Supernatant was decanted and pellets were stored at -20°C.

Material and methods

3.5.16.4 Purification

The purification of plasmids was done with the Endofree Plasmid Maxi Kit according to the manufacturer's protocol. There were some slight changes as follows: DNA was eluted with Qiagen tip 500 and QN buffer. Isopropanol was added to the eluted DNA and dissolutions were pipetted into 1.5ml Eppendorf tubes for further centrifugation at 15,000 xg for 30 min at 4°C. Supernatant was decanted and pellet was washed in EtOH (70%) and centrifuged at 15,000 xg for 10 min at 4°C. Again supernatant was decanted and TE buffer was used to dissolve the pellet. A Nanodrop (260nm) was used to measure concentration of plasmids (in ng/μl).

3.5.16.5 Transfection into HEK293 cells

In order to investigate the activity of the NFκB promoter in HEK293 cells through pro-inflammatory cytokines (TNF-α) and the effect of agmatine, we used the following reporter genes (tab. 10) and a Dual-Luciferase Reporter® Assay.

Table 10: Reporter genes

Plasmid	Description	Vector	Reference
pGL4.32 (luc2P/NF-κB- RE/Hygro)	Firefly-luciferase with NFκB-promoter	pGL4.32 (reporter gene vector)	Prof. Dr. Arlt
pGL4.74 (hRluc/TK)	Renilla-luciferase with HSV-TK promoter	hRluc (control vector)	Prof. Dr. Arlt
pGL4.15 (luc2P/Hygro)	Firefly-luciferase with no promoter	luc2P (reporter gene vector)	Prof. Dr. Arlt

luc2P (Photinus pyralis) is a luciferase reporter gene and designed for high expression. It contains hPEST, a protein destabilization sequence. hRluc (Renilla reniformis) is a luciferase reporter gene and contains an HSV-TK promoter for high expressions used as a control.

We used the reporter gene vector pGL4.32, which carries a Firefly-luciferase gene controlled by the NFκB-promoter. The promoter activity can be indirectly measured through the activity of the reporter gene. The measurement of the activity of the Firefly-luciferase is based on the luciferase enzyme, which is able to express luminescent

products through oxidation of beetle luciferin (111). We utilized pGL4.74 as an internal control vector, which carries a Renilla-luciferase gene and oxidizes coelenterazine luciferin through oxidation of oxygen (111). Additionally, we used pGL4.15 as a transfection control vector to guarantee stable transfections.

HEK293 cells were co-transfected with the pGL4.15 reporter plasmid as a transfection control plasmid and with pGL4.74 as an internal control plasmid. Furthermore, HEK293 cells were also co-transfected with the pGL4.32 reporter plasmid and with pGL4.74 as an internal control plasmid (tab. 11).

Table 11: Pipetting scheme (12-well plate)

	1	2	3	4
A	pGL4.15 + pGL4.74	pGL4.15 + pGL4.74 + TNF- α	pGL4.15 + pGL4.74 + TNF- α + 500 μ M AGM	pGL4.15 + pGL4.74 + 500 μ M AGM
B	pGL4.32 + pGL4.74	pGL4.32 + pGL4.74 + TNF- α	pGL4.32 + pGL4.74 + TNF- α + 500 μ M AGM	pGL4.32 + pGL4.74 + 500 μ M AGM

HEK293 cells were seeded at a density of 2×10^5 cells per well in a 12-well plate ($n=3$) with 1ml DMEM medium containing 10% FCS. Afterwards, cells were incubated overnight until they reached 80% confluence the next morning. The next day, Opti-MEM medium, pGL4.15 and pGL4.74 (or pGL4.32 and pGL4.74) followed by FuGene® HD were pipetted into an Eppendorf tube and incubated at room temperature for 15 min to form a complex of FuGene and nucleic acid (see tab. 11). Meanwhile cells were washed with 1ml PBS and 900 μ l DMEM medium containing 1% FCS without antibiotics was put on cells. Afterwards, the complex was added to the particular well drop by drop and cells were incubated another 24h at 37°C and 5% CO₂. The next day, cells were washed with PBS (1ml/well) and 1ml DMEM containing 10% FCS was added to each well. Cells were further incubated for 24h. Then, HEK293 cells were stimulated with either TNF- α (20ng/ μ l) or/and 500 μ M agmatine (see tab. 11) and incubated for 1h. Cells were washed with 1ml PBS. Afterwards, cells were harvested according to an active lysis procedure using 100 μ l lysis buffer/well. Cells were scraped and lysate was stored in Eppendorf tubes. To improve cell disruption, Eppendorf tubes were quick-frozen at -20°C before measurement.

Material and methods

3.5.16.6 Measurement

The Dual-Luciferase Reporter® Assay was used for measuring n=3 independent transfection experiments. 25µl of cell lysate was pipetted into a 96-well plate (duplicates) and was measured with a luminometer. The luminometer firstly added 100µl Luciferase Assay Reagent II (LARII) and the light emission of Firefly-luciferase was measured for 10 sec. Secondly, the luminometer added 100µl of Stop & Glo Reagent and measured the Renilla-luciferase for 2 sec. Both reporter genes were quantified consecutively. Data analysis was done in MicroWin 2000 and in GraphPad for statistical measurements. The ratio of Firefly/Renilla was calculated for each wells' reporter genes. The relative luciferase activity was compared through Kruskal-Wallis for overall non-parametric distribution and Dunn's test for multiple comparison.

4 Results

4.1 Characterization of the FoCus cohort, ATP cohort and Intervention cohort

A comparison of three cohorts, which were involved in the study, was done in order to increase reliability of the statistical data. The number of subjects in each cohort differed and is described in table 12.

Table 12: Overview of three cohorts involved in the study

parameter	<i>FoCus cohort</i> (n=1,544)	<i>ATP cohort</i> (n=438)	<i>Intervention cohort</i> (n=55)
Age (years)	51.62 ^a ± 14.22	56.9 ± 6.27	45.79 ± 10.89
Sex (% female)	63	72	69
BMI (kg/m²)	27.8 ^b (23.68; 35.9)	30.62 (26.55; 36.88)	45.25 (43.36; 48.13)
Underweighted (<20 kg/m²) (%)	4.5 ^c	-	-
Normal weighted (20-25 kg/m²) (%)	28.6	2.9	-
Overweighted (25- 30 kg/m²) (%)	27	46	-
Obese (>30 kg/m²) with type 2 diabetes (%)	10.6	5.2	17.3
Obese (>30 kg/m²) without type 2 diabetes (%)	29.2	45.8	82.7

^amean ± sd (all such values); ^bmedian: 25th, 75thpercentile (all such values); ^cpercentage (all such values). Abbreviations: BMI: body mass index; sd: standard deviation

4.2 *Parasutterella* – descriptive statistics

For multivariate modeling of *Parasutterella* sp., a subset of the FoCus cohort (n=1,544) was used for calculations and is outlined in table 13. Due to combining of various data sets the number of subjects included in each sub analysis differed. *Parasutterella* sp. data included various statistical zeros (suppl. fig. 1).

Table 13: Descriptive statistics of the FoCus cohort (*Parasutterella* sp.)

parameter	median (25 th and 75 th percentile) or mean \pm sd
Age (years)	51.62 ^a (14.22)
Sex (% female)	62.89 ^c
BMI (kg/m ²)	27.80 ^b (23.68; 35.89)
Glucose (mg/dl)	95 (88; 104)
Diabetes type 2 (%)	11.79
CRP (mg/l)	3.3 (1.6; 7.1)
IL-6 (pg/ml)	3.7 (2.6; 5.4)
Triglycerides (mg/dl)	108
HOMA-IR index	2.42
<i>Parasutterella</i> sp.	97.5 (0.00; 764.75)

^amean \pm sd (all such values); ^bmedian: 25th, 75th percentile (all such values); ^cpercentage (all such values). Abbreviations: BMI: body mass index; CRP: C-reactive protein; IL-6: interleukin-6; HOMA-IR index: Homeostasis Model Assessment insulin resistance index; sd: standard deviation

4.2.1 *Parasutterella* in relation to various phenotypes

To generate a comprehensive overview of *Parasutterella* on the development of obesity and type 2 diabetes we decided to investigate the bacterium on metabolic, inflammatory, dietary, microbiome, metabolome and genetic level. Additionally, we examined qPCR-determined *Parasutterella* abundances in a weight loss intervention study to further validate bioinformatical calculations and to gain insight into the functional capabilities of this species.

Parasutterella and measures of obesity

Firstly, 1,544 subjects were examined of the FoCus cohort regarding the obesity phenotype. Therefore, we used *Parasutterella* sp. > 10 counts (n=1,132 samples that met the threshold of *Parasutterella* sp. > 10 counts) for multivariate modeling in regard to different metric variables such as BMI and body weight. This threshold was recommended by QIIME pipeline (<https://docs.qiime2.org/2021.4/>) in order to only incorporate values of *Parasutterella* sp. that were truly measured through 16S rRNA gene sequencing. We found a significant positive association between positive counts of *Parasutterella* sp.

abundance and BMI (3.71e^{-2} , $p = 3.11\text{e}^{-3}$) (fig. 4A), meaning there was an increased *Parasutterella* sp. abundance in subjects with higher BMI. The results were in line with data regarding weight measurements: there was a nominally significantly positive association between *Parasutterella* sp. abundance and weight of the subjects (7.95e^{-3} , $p = 2.0\text{e}^{-2}$) (tab. 14). After additional correction for BMI, the association with weight measure diminished (tab. 15).

Table 14: Association of *Parasutterella* sp. with the particular phenotypical parameter (hurdle model)

parameter	confounder	model	estimate	p	significance	p-adjusted
BMI	Age, IBD, Psoriasis	count	3.71e^{-2}	3.89e^{-4}	***	3.11e^{-3}
		zero	-1.06e^{-2}	3.63e^{-1}		1
Triglycerides	Age, IBD, Psoriasis	count	2.61e^{-3}	3.34e^{-2}	*	2.67e^{-1}
		zero	-7.93e^{-5}	9.5e^{-1}		1
Weight	Age, IBD, Psoriasis	count	7.95e^{-3}	2.0e^{-2}	*	1.6e^{-1}
		zero	-3.41e^{-3}	3.67e^{-1}		1
Glucose	Age, IBD, Psoriasis	count	6.81e^{-3}	5.37e^{-2}		4.3e^{-1}
		zero	2.11e^{-3}	6.48e^{-1}		1
Insulin	Age, IBD, Psoriasis	count	3.02e^{-2}	1.73e^{-3}	**	1.38e^{-2}
		zero	-1.2e^{-2}	7.36e^{-2}		5.88e^{-1}
HOMA	Age, IBD, Psoriasis	count	9.88e^{-2}	1.87e^{-3}	**	1.5e^{-2}
		zero	-3.39e^{-2}	8.43e^{-2}		6.74e^{-1}
CRP	Age, IBD, Psoriasis	count	2.38e^{-2}	1.9e^{-1}		1
		zero	3.47e^{-3}	8.61e^{-1}		1
IL-6	Age, IBD, Psoriasis	count	1.07e^{-2}	1.52e^{-1}		1
		zero	4.37e^{-4}	9.58e^{-1}		1

Results

Association of phenotypical parameter and *Parasutterella* sp. abundance tested with a two-part hurdle model consisting of count and zero part. Confounder such as age, IBD and psoriasis were included. Results were reported through estimate, p-value, significance level and p-adjusted according to FDR-correction in the respective part. Statistical significance was set at $p < 0.05$. Abbreviations: BMI: body mass index; CRP: C-reactive protein; IL-6: interleukin-6; HOMA-IR index: Homeostasis Model Assessment insulin resistance index; IBD: inflammatory bowel disease.

Table 15: Association of *Parasutterella* sp. with the particular phenotypical parameter (hurdle model) including BMI as a covariate

parameter	confounder	model	estimate	p	significance	p-adjusted
Triglycerides	Age, IBD, Psoriasis, BMI	count	1.37e ⁻³	1.90e ⁻¹		1
		zero	3.65e ⁻⁴	7.90e ⁻¹		1
Weight	Age, IBD, Psoriasis, BMI	count	-1.76e ⁻²	6.83e ⁻²		4.79e ⁻¹
		zero	4.44e ⁻³	6.55e ⁻¹		1
Glucose	Age, IBD, Psoriasis, BMI	count	1.11e ⁻³	7.74e ⁻¹		1
		zero	4.16e ⁻³	4.13e ⁻¹		1
Insulin	Age, IBD, Psoriasis, BMI	count	1.74e ⁻²	9.7e ⁻²		6.79e ⁻¹
		zero	-1.18e ⁻²	1.23e ⁻¹		8.64e ⁻¹
HOMA	Age, IBD, Psoriasis, BMI	count	5.03e ⁻²	1.77e ⁻¹		1
		zero	-3.28e ⁻²	1.34e ⁻¹		9.37e ⁻¹
CRP	Age, IBD, Psoriasis, BMI	count	8.7e ⁻³	6.14e ⁻¹		1
		zero	1.1e ⁻²	6.17e ⁻¹		1

IL-6	Age, IBD, count	7.1e ⁻³	2.54e ⁻¹	1
	Psoriasis, BMI			
	zero	8.93e ⁻⁴	9.16e ⁻¹	1

Association of phenotypical parameter and Parasutterella sp. abundance tested with a two-part hurdle model consisting of count and zero part. Confounder such as age, IBD, psoriasis and BMI were included. Results were reported through estimate, p-value, significance level and p-adjusted according to FDR-correction in the respective part. Statistical significance was set at $p < 0.05$. Abbreviations: BMI: body mass index; CRP: C-reactive protein; IL-6: interleukin-6; HOMA-IR index: Homeostasis Model Assessment insulin resistance index, IBD: inflammatory bowel disease.

The significant positive association of *Parasutterella* sp. and BMI found in the European FoCus cohort was validated in the independent Canadian ATP cohort (n=305 samples that met the threshold of *Parasutterella* sp. > 10 counts). Of interest, we found that *Parasutterella* sp. abundance was increased in subjects with higher BMI ($p = 2.0e^{-3}$) in the Canadian cohort as well.

Parasutterella and diabetes phenotypes

In a next step, we analyzed glucose metabolism and found an association of *Parasutterella* sp. abundance with HOMA ($9.87e^{-2}$, $p = 1.87e^{-3}$) and fasting insulin ($3.01e^{-2}$, $p = 1.73e^{-3}$) (tab. 14) (fig. 4B). After correction with BMI, the association diminished as well (tab. 15). In addition, we found a positive association between *Parasutterella* sp. abundance and fasting glucose ($6.81e^{-3}$, $p = 5.38e^{-2}$), but after correction with BMI there was no significance. Furthermore, there was a significantly positive association between *Parasutterella* sp. abundance and the presence of type 2 diabetes ($7.67e^{-1}$, nominal significant, $p = 9.42e^{-3}$) (tab. 16) (fig. 4C). With regard to lipid metabolism, *Parasutterella* sp. was nominally positively associated with serum triglyceride levels ($2.61e^{-3}$, $p = 3.34e^{-2}$) (tab. 14), whereas no association was present after correction with BMI (tab. 15).

However, when adapting for BMI, the significant association to these measures of insulin sensitivity diminished, suggesting the association of *Parasutterella* with insulin resistance to be indirectly mediated via its effect on body weight gain.

In a subsequent analysis we grouped the FoCus cohort into five groups concerning BMI and diabetes status and found a significant difference in a hurdle count model between groups of *Parasutterella* abundance (fig. 5A). Interestingly, the difference in *Parasutterella* abundance between probands with a BMI greater than 30 without type 2 diabetes and

Results

probands with a BMI greater than 30 with type 2 diabetes was significant ($p = 3.6e^{-2}$), whereby probands with type 2 diabetes had around 70% higher *Parasutterella* abundance. The ATP cohort also showed higher abundance of *Parasutterella* sp. in probands with a BMI greater than 30 without type 2 diabetes as well as in probands with a BMI greater than 30 with type 2 diabetes in comparison to probands with a BMI between 20 and 25 kg/m² ($p = 9.6e^{-3}$, $p = 1.7e^{-3}$) (fig. 5B).

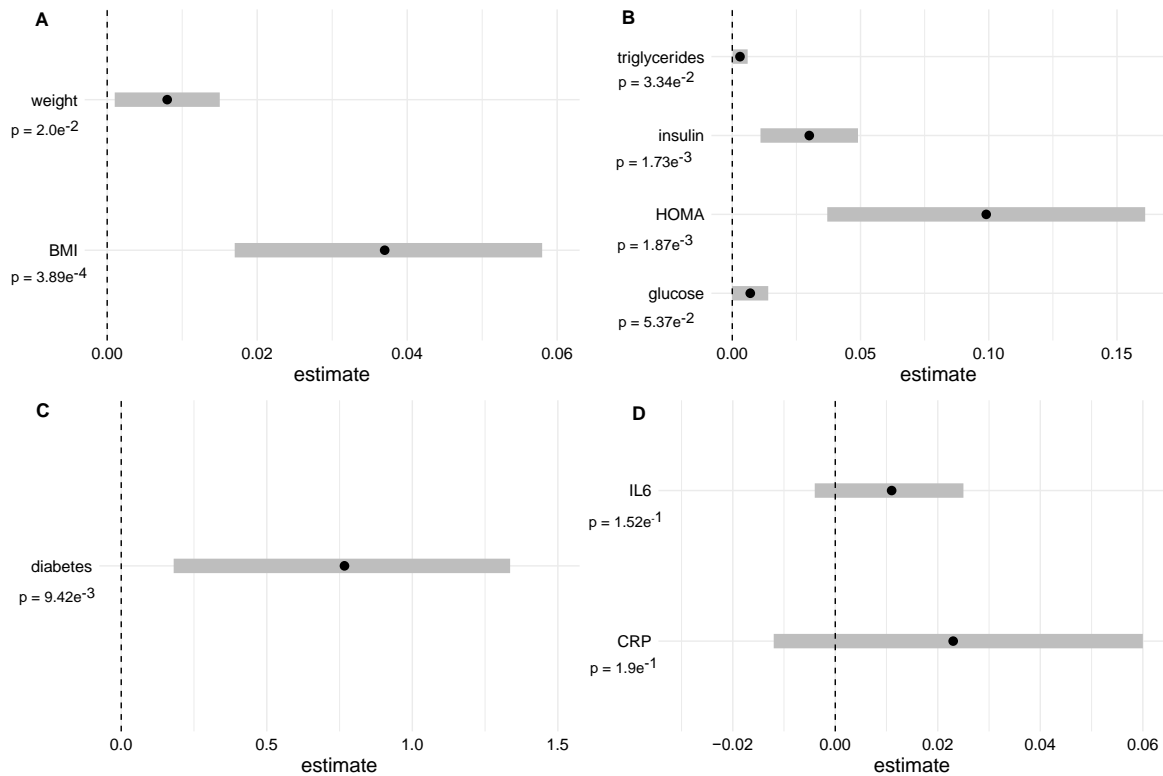


Figure 4: Association of *Parasutterella* sp. with the particular parameter (count model) without BMI as a covariate

Association of phenotypical parameter (including diabetes) and *Parasutterella* sp. abundance tested with a two-part hurdle model displaying only the count part here. Confounder such as age, IBD and psoriasis were included. Results were reported through estimate and nominal p-values. Statistical significance was set at $p < 0.05$. Abbreviations: BMI: body mass index; CRP: C-reactive protein; IL-6: interleukin-6; HOMA-IR index: Homeostasis Model Assessment insulin resistance index.

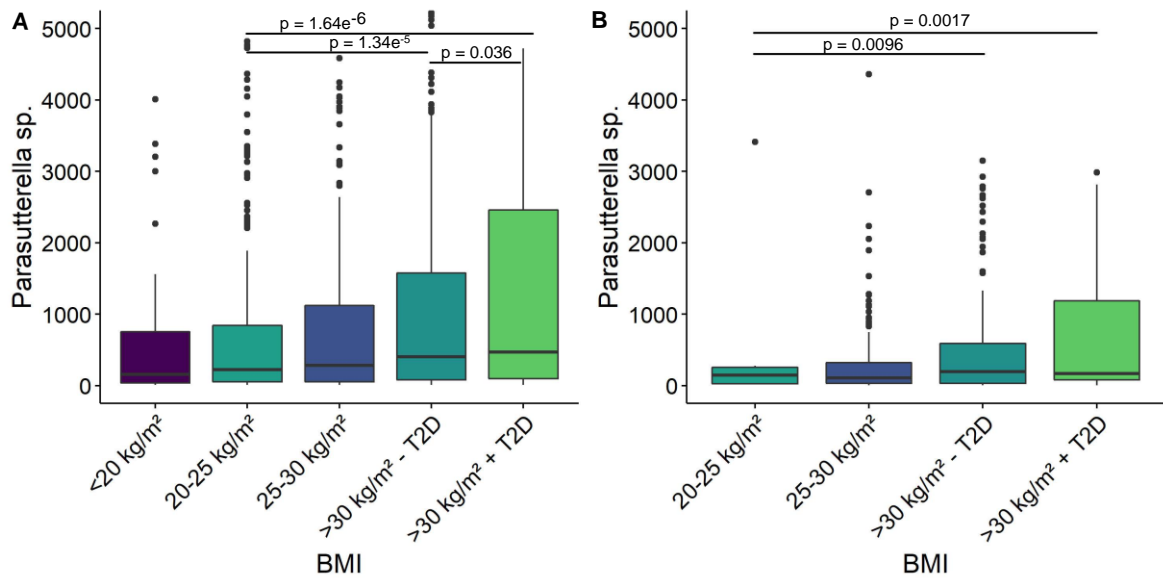


Figure 5: *Parasutterella* sp. abundance in relation to BMI and type 2 diabetes (T2D) groups in the FoCus cohort (A) and ATP cohort (B)

Distribution of *Parasutterella* sp. abundance in groups divided according to BMI and T2D (see table 12). The sequencing depth of the ATP cohort was slightly lower overall than in FoCus (median: ATP: 22,931; median FoCus: 36,048). Nevertheless the distribution of *Parasutterella* sp. abundance in relation to groups was comparable in both cohorts. Abbreviations: BMI: body mass index, T2D: type 2 diabetes.

Table 16: Association of *Parasutterella* sp. with the particular disease (hurdle model)

parameter	confounder	model	estimate	p	significance	p-adjusted
IBD	Age, Psoriasis	count	$1.74e^{-1}$	$7.62e^{-1}$		1
		zero	-1.36	$3.11e^{-3}$	**	$2.49e^{-2}$
Rheumatoid arthritis	Age, IBD, Psoriasis	count	$6.4e^{-2}$	$8.34e^{-1}$		1
		zero	$5.25e^{-1}$	$2.23e^{-1}$		1
Parodontitis	Age, IBD, Psoriasis	count	$7.67e^{-2}$	$7.71e^{-1}$		1
		zero	$8.73e^{-1}$	$1.26e^{-2}$	*	$1.01e^{-1}$
Psoriasis	Age, IBD	count	$4.68e^{-1}$	$4.6e^{-2}$	*	$3.68e^{-1}$

Results

			zero	1.18e ⁻¹	6.72e ⁻¹		1
Atopic eczema	Age,	IBD,	count	2.31e ⁻¹	3.62e ⁻¹		1
	Psoriasis						
			zero	-5.2e ⁻²	8.63e ⁻¹		1
IBS	Age,	IBD,	count	-8.03e ⁻¹	8.68e ⁻²		6.95e ⁻¹
	Psoriasis						
			zero	-6.05e ⁻¹	1.70e ⁻¹		1
Phlebitis	Age,	IBD,	count	-5.41e ⁻¹	3.33e ⁻¹		1
	Psoriasis						
			zero	-1.16	2.06e ⁻²	*	1.64e ⁻¹
Diabetes	Age,	IBD,	count	7.67e ⁻¹	9.42e ⁻³	**	7.95e ⁻²
	Psoriasis						
			zero	2.94e ⁻¹	4.49e ⁻¹		1

Association of diseases and Parasutterella sp. abundance tested with a two-part hurdle model consisting of count and zero part. Confounder such as age, IBD and psoriasis were included. Results were reported through estimate, p-value, significance level and p-adjusted according to FDR-correction in the respective part. Statistical significance was set at $p < 0.05$. Abbreviations: IBD: inflammatory bowel disease; IBS: irritable bowel syndrome.

Parasutterella and inflammatory phenotypes

In order to gain insights into the inflammatory properties of *Parasutterella* sp. we examined two biomarkers that mirror the inflammatory state of the subjects. *Parasutterella* sp. abundance was neither associated with CRP nor with IL-6 ($2.39e^{-2}$, $p = 1.9e^{-1}$; $1.07e^{-2}$, $p = 1.52e^{-1}$) (tab. 14) (fig. 4D). This finding indicates no major association of *Parasutterella* sp. to systemic metabolic inflammation.

Parasutterella and dietary phenotypes

Dietary data were derived from the 12-month FFQ ($n=1,443$). Analysis of 19 dietary components revealed that the intake of total carbohydrates showed a significant positive association with *Parasutterella* sp. abundance ($5.7e^{-2}$, $p = 4.09e^{-3}$) (tab. 17, fig. 6A) falling in line with the data on diabetes phenotypes. The composition of total carbohydrate intake consisted of 22.09% monosaccharides, 31.56% disaccharides and 44.22% polysaccharides and minor parts of sugar alcohol and oligosaccharides. Appropriately, monosaccharides showed a significant positive association with *Parasutterella* sp. abundance ($1.28e^{-2}$, $p = 2.05e^{-3}$). In contrast, total fat intake of the subjects was

significantly negatively associated with *Parasutterella* sp. abundance ($-6.18e^{-2}$, $p = 1.01e^{-2}$) (tab. 17). In more detail, we found the polyunsaturated fatty acid (PUFA) linolenic acid ($\omega 3$ -fatty acid) significantly negatively associated with *Parasutterella* sp. abundance ($-4.64e^{-1}$, $p = 5.05e^{-2}$) (tab. 17) (fig. 6B). Furthermore, eicosenoic acid was nominally significantly negatively associated with *Parasutterella* sp. (-3.86 , $p = 3.96e^{-3}$) (fig. 6C).

Table 17: Association of *Parasutterella* sp. with the particular dietary parameter (hurdle model)

parameter	confounder	model	estimate	p	significance	p-adjusted
Carbohydrates	Age, IBD, Psoriasis	count	$5.7e^{-2}$	$2.15e^{-4}$	***	$4.09e^{-3}$
		zero	$-2.76e^{-2}$	$1.58e^{-1}$		1
Monosaccharides	Age, IBD, Psoriasis	count	$1.28e^{-2}$	$1.08e^{-4}$	***	$2.05e^{-3}$
		zero	$-1.51e^{-3}$	$6.46e^{-1}$		1
Fat	Age, IBD, Psoriasis	count	$-6.18e^{-2}$	$5.32e^{-4}$	***	$1.01e^{-2}$
		zero	$2.15e^{-2}$	$3.2e^{-1}$		1
Protein	Age, IBD, Psoriasis	count	$1.02e^{-1}$	$7.46e^{-2}$		1
		zero	$-4.36e^{-2}$	$4.97e^{-1}$		1
Linolenic acid	Age, IBD, Psoriasis	count	$-4.64e^{-1}$	$2.66e^{-3}$	**	$5.05e^{-2}$
		zero	$-1.25e^{-2}$	$9.52e^{-1}$		1
Eicosenoic acid	Age, IBD, Psoriasis	count	-3.86	$3.96e^{-3}$	**	$7.52e^{-2}$
		zero	1.26	$4.43e^{-1}$		1
Butanoic acid	Age, IBD, Psoriasis	count	$-4.05e^{-1}$	$7.27e^{-2}$		1
		zero	$3.88e^{-1}$	$1.72e^{-1}$		1
Hexanoic acid	Age, IBD, Psoriasis	count	$-6.34e^{-1}$	$7.2e^{-2}$		1
		zero	$6.05e^{-1}$	$1.74e^{-1}$		1
Vitamin D	Age, IBD, Psoriasis	count	-83.06	$6.02e^{-2}$		1

Results

	Psoriasis				
		zero	92.27	$1.17e^{-1}$	1
Vitamin B9F	Age, IBD, Psoriasis	count	$-2.80e^{-1}$	$9.45e^{-1}$	1
		zero	$1.63e^{-1}$	$9.77e^{-1}$	1
Vitamin B6	Age, IBD, Psoriasis	count	$-9.02e^{-1}$	$1.01e^{-2}$ *	$1.92e^{-1}$
		zero	$6.09e^{-2}$	$8.78e^{-1}$	1
Vitamin C	Age, IBD, Psoriasis	count	$1.57e^{-4}$	$9.36e^{-1}$	1
		zero	$2.94e^{-3}$	$2.05e^{-1}$	1
Vitamin B12	Age, IBD, Psoriasis	count	-35.15	$5.90e^{-1}$	1
		zero	-77.17	$2.47e^{-1}$	1
Vitamin E	Age, IBD, Psoriasis	count	$-5.84e^{-2}$	$6.33e^{-2}$	1
		zero	$3.54e^{-2}$	$3.75e^{-1}$	1
Iodine	Age, IBD, Psoriasis	count	5.52	$4.83e^{-2}$ *	$9.17e^{-1}$
		zero	$-5.86e^{-1}$	$8.65e^{-1}$	1
Iron	Age, IBD, Psoriasis	count	$2.2e^{-1}$	$2.44e^{-3}$ **	$4.64e^{-2}$
		zero	$7.42e^{-2}$	$3.72e^{-1}$	1
Calcium	Age, IBD, Psoriasis	count	$5.3e^{-1}$	$3.27e^{-1}$	1
		zero	$-9.04e^{-1}$	$1.12e^{-1}$	1
Magnesium	Age, IBD, Psoriasis	count	-2.42	$1.67e^{-1}$	1
		zero	$4.82e^{-1}$	$8.33e^{-1}$	1
Zinc	Age, IBD, Psoriasis	count	$-5.24e^{-2}$	$3.09e^{-1}$	1
		zero	$-1.18e^{-2}$	$8.53e^{-1}$	1

Association of dietary parameter and Parasutterella sp. abundance tested with a two-part hurdle model consisting of count and zero part. Confounder such as age, IBD and psoriasis were included. Results were reported through estimate, p-value, significance level and p-adjusted according to FDR-correction in the respective part. Statistical significance was set at $p < 0.05$. Abbreviations: vitamin B9F: free folic acid; IBD: inflammatory bowel disease.

Table 18: Association of *Parasutterella* sp. with the particular dietary parameter (hurdle model) including BMI as a covariate

parameter	confounder	model	estimate	p	significance	p-adjusted
Carbohydrates	Age, IBD, Psoriasis, BMI	count	4.5e ⁻²	4.24e ⁻³	**	8.06e ⁻²
		zero	-2.48e ⁻²	2.12e ⁻¹		1
Monosaccharides	Age, IBD, Psoriasis, BMI	count	1.15e ⁻²	1.19e ⁻³	**	2.26e ⁻²
		zero	-7.51e ⁻⁴	8.25e ⁻¹		1
Fat	Age, IBD, Psoriasis, BMI	count	-5.13e ⁻²	5.97e ⁻³	**	1.13e ⁻¹
		zero	1.86e ⁻²	3.94e ⁻¹		1
Protein	Age, IBD, Psoriasis, BMI	count	3.76e ⁻²	5.32e ⁻¹		1
		zero	-3.36e ⁻²	6.07e ⁻¹		1
Linolenic acid	Age, IBD, Psoriasis, BMI	count	-3.30e ⁻¹	4.1e ⁻²	*	9.5e ⁻¹
		zero	-5.32e ⁻²	8.01e ⁻¹		1
Eicosenoic acid	Age, IBD, Psoriasis, BMI	count	-3.26	3.05e ⁻²		5.79e ⁻¹
		zero	9.89e ⁻¹	5.54e ⁻¹		1
Butanoic acid	Age, IBD, Psoriasis, BMI	count	-3.07e ⁻¹	2.20e ⁻¹		1
		zero	3.61e ⁻¹	2.05e ⁻¹		1
Hexanoic acid	Age, IBD, Psoriasis, BMI	count	-4.84e ⁻¹	2.17e ⁻¹		1
		zero	5.63e ⁻¹	2.07e ⁻¹		1

Results

Vitamin D	Age, IBD, count Psoriasis, BMI		-72.75	9.68e ⁻²		1
		zero	86.89	1.42e ⁻¹		1
Vitamin B9F	Age, IBD, count Psoriasis, BMI		2.61	5.63e ⁻¹		1
		zero	-2.96e ⁻¹	9.57e ⁻¹		1
Vitamin B6	Age, IBD, count Psoriasis, BMI		-7.51e ⁻¹	4.37e ⁻²	*	8.29e ⁻¹
		zero	8.20e ⁻³	9.84e ⁻¹		1
Vitamin C	Age, IBD, count Psoriasis, BMI		2.04e ⁻³	3.39e ⁻¹		1
		zero	2.82e ⁻³	2.2e ⁻¹		1
Vitamin B12	Age, IBD, count Psoriasis, BMI		-45.82	4.88e ⁻¹		1
		zero	-77.04	2.48e ⁻¹		1
Vitamin E	Age, IBD, count Psoriasis, BMI		-3.65e ⁻²	2.68e ⁻¹		1
		zero	2.98e ⁻²	4.62e ⁻¹		1
Iodine	Age, IBD, count Psoriasis, BMI		4.16	1.41e ⁻¹		1
		zero	-5.18e ⁻¹	8.80e ⁻¹		1
Iron	Age, IBD, count Psoriasis, BMI		2.28e ⁻¹	2.55e ⁻³	**	4.85e ⁻²
		zero	7.54e ⁻²	3.63e ⁻¹		1
Calcium	Age, IBD, count Psoriasis, BMI		3.55e ⁻¹	5.23e ⁻¹		1
		zero	-8.70e ⁻¹	1.28e ⁻¹		1

Magnesium	Age, IBD, count	-5.35e ⁻¹	7.83e ⁻¹	1
	Psoriasis, BMI			
	zero	2.34e ⁻²	9.92e ⁻¹	1
Zinc	Age, IBD, count	-3.99e ⁻²	4.85e ⁻¹	1
	Psoriasis, BMI			
	zero	-1.50e ⁻²	8.11e ⁻¹	1

Association of dietary parameter and Parasutterella sp. abundance tested with a two-part hurdle model consisting of count and zero part. Confounder such as age, IBD, psoriasis and BMI were included. Results were reported through estimate, p-value, significance level and p-adjusted according to FDR-correction in the respective part. Statistical significance was set at $p < 0.05$. Abbreviations: vitamin B9F: free folic acid; IBD: inflammatory bowel disease, BMI: body mass index.

Results

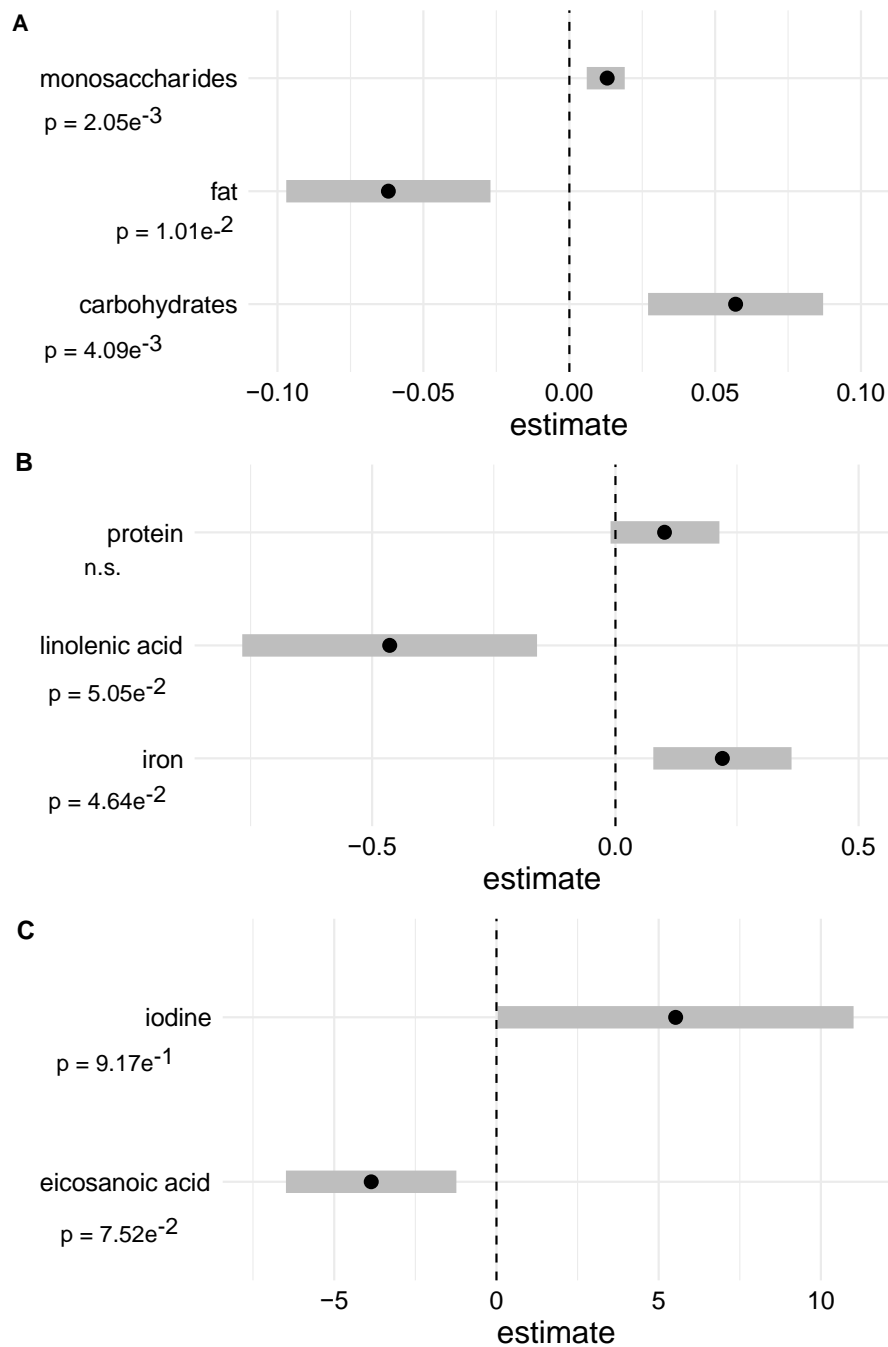


Figure 6: Association of *Parasutterella* sp. with the particular dietary parameter (count model) without BMI as a covariate

Association of dietary parameter and *Parasutterella* sp. abundance tested with a two-part hurdle model displaying only the count part here. Confounder such as age, IBD and psoriasis were included. Dietary parameter were shown and separated according to resembling estimates (A,B,C). Results were reported through estimate and p-adjusted according to FDR-correction. Statistical significance was set at $p < 0.05$.

Besides macronutrients, several micronutrients were examined, whereby iron was significantly positively associated with *Parasutterella* sp. abundance ($2.2e^{-1}$, $p = 4.64e^{-2}$) and remained significantly positively associated after adjustment for BMI ($2.28e^{-1}$, $p = 4.85e^{-2}$) (tab. 18). When dietary data were additionally adjusted by BMI (tab. 18), the above-described associations remained nominally significant except of eicosenoic acid and iodine.

4.2.2 *Parasutterella* and gut microbiomics

Concerning microbiomics, we investigated *Parasutterella* sp. groups (low vs. high *Parasutterella* sp.) with respect to the general microbiome composition, which indicates significant differences in β -diversity measures (Bray Curtis: $p = 9.0e^{-3}$, Jaccard index: $p = 8.0e^{-4}$) (fig. 7).

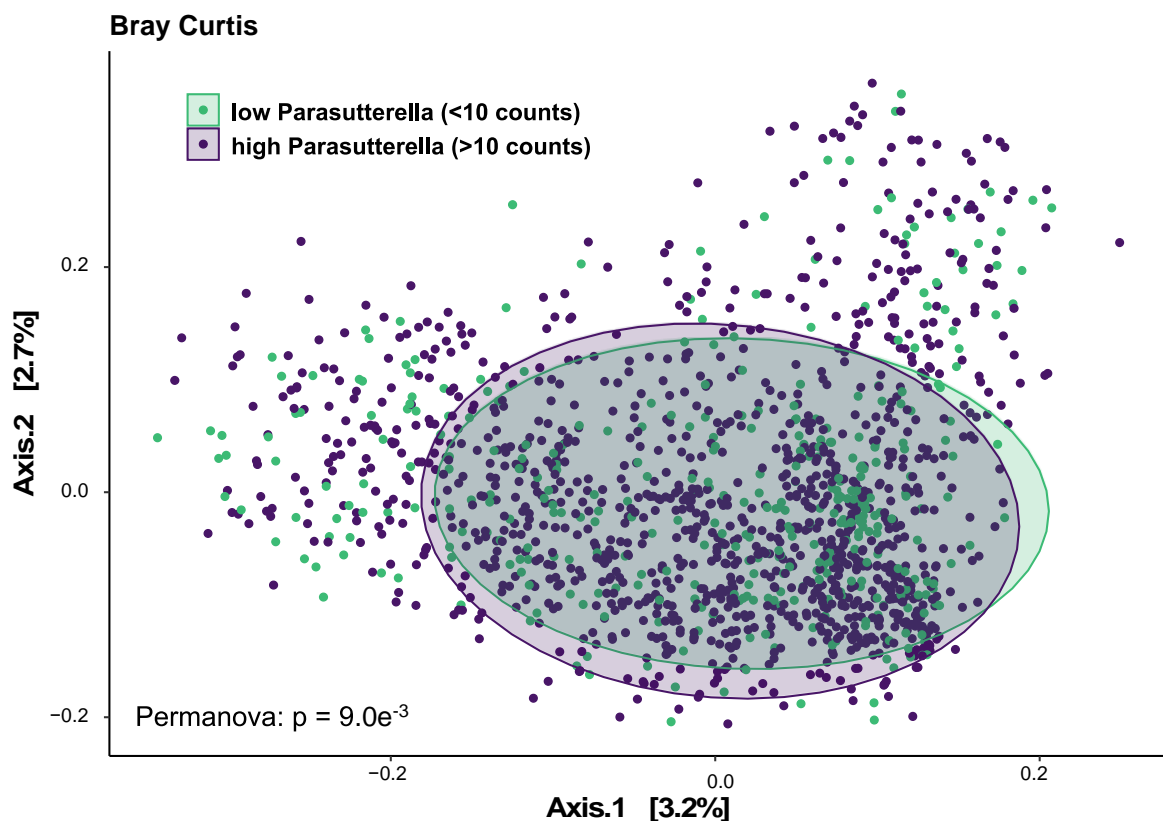


Figure 7: β -diversity displayed through Bray Curtis distance between *Parasutterella* sp. groups

*β -diversity in subjects with low and high (threshold < 10 counts) *Parasutterella* sp. abundance. Statistical significance was set at $p < 0.05$.*

Results

Additionally, α -diversity was significantly reduced in subjects with low *Parasutterella* sp. abundance (zero part of the hurdle model: Species Richness: $p = 2.6e^{-26}$, Shannon Index: $p = 2.4e^{-23}$, Chao1 Index: $p = 2.8e^{-25}$) (fig. 8). There were no significant associations in the count part of the hurdle model.

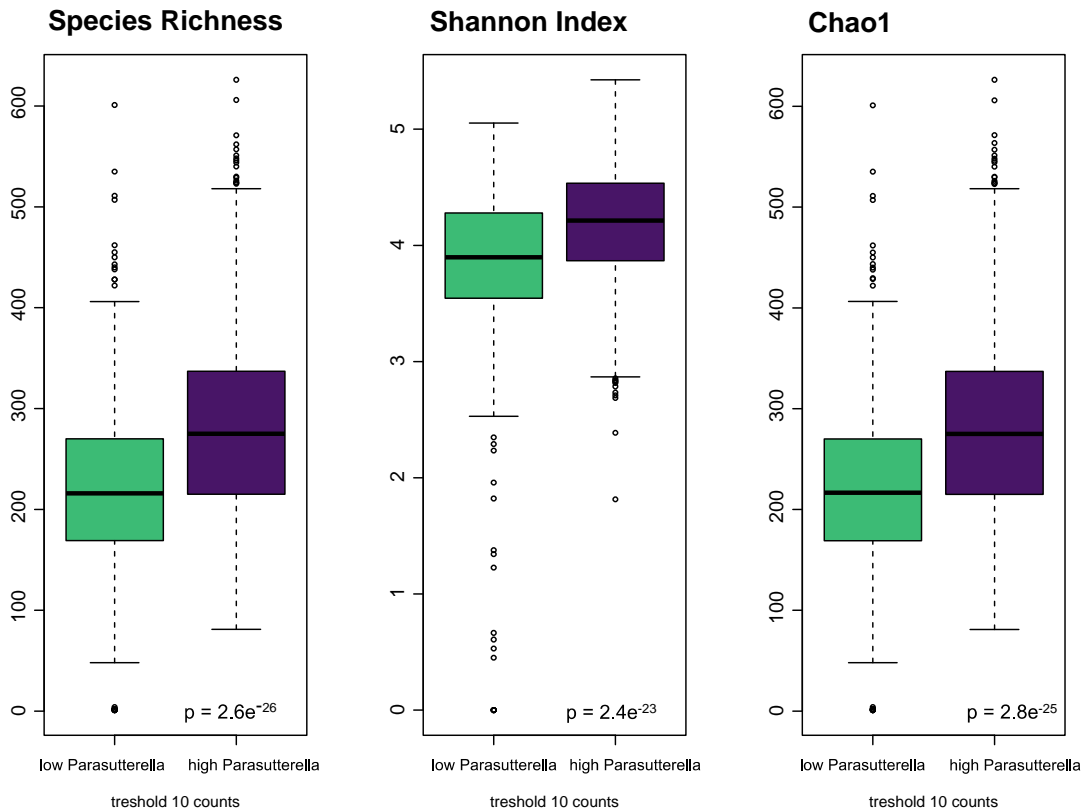


Figure 8: α -diversity displayed through Species Richness, Shannon Index and Chao1 Index between *Parasutterella* sp. groups

*α -diversity shown through three indices in subjects with low and high *Parasutterella* sp. Statistical significance was set at $p < 0.05$.*

4.2.3 *Parasutterella* and host metabolomics

Presently, MS-metabolomics analysis data were available of $n=470$ subjects of the FoCus cohort, consisting of $n=178$ metabolically diseased subjects and 292 healthy controls. This analysis took $n=955$ detectable metabolites into account. 256 metabolites were nominally associated with *Parasutterella* abundance (suppl. tab. 1), of which 126 remained significant after FDR adjustment for multiple comparisons. Interestingly, we were able to identify L-cysteine as a metabolite that showed an inverse association with *Parasutterella*

sp. abundance in the count part of the hurdle model (-13.00 , $p = 1.78e^{-3}$). In figure 9 are displayed the metabolites with the five highest negative and positive estimates, which were significant out of in total $n=126$ significant metabolites in association with *Parasutterella* sp. abundance in the count part (tab. 19, tab. 20). In a suppl. figure 2 we show the ranges of raw values of each metabolite in $n=470$ subjects.

Table 19: Association of *Parasutterella* sp. with the particular metabolite (hurdle model) displaying the five highest negative estimates

parameter	model	estimate	p	significance	p-adjusted
L-cysteine	count	-13.00	$1.5e^{-5}$	***	$1.78e^{-3}$
	zero	$3.77e^{-1}$	$9.31e^{-1}$		$9.83e^{-1}$
19,20-DiHDPA	count	-6.74	$3.7e^{-4}$	***	$1.12e^{-2}$
	zero	-2.98	$6.05e^{-2}$		$9.82e^{-1}$
Hydroxycholesterol	count	-4.60	$1.41e^{-3}$	***	$1.1e^{-2}$
	zero	-1.39	$3.37e^{-1}$		$9.82e^{-1}$
Tetrahydrocortisone	count	-3.93	$4.14e^{-3}$	***	$3.94e^{-2}$
	zero	-2.43	$1.37e^{-1}$		$9.82e^{-1}$
Tetracosatetraenoic acid	count	-3.62	$3.0e^{-5}$	***	$3.04e^{-3}$
	zero	1.29	$3.82e^{-1}$		$9.82e^{-1}$

Association of metabolites and Parasutterella sp. abundance tested with a two-part hurdle model consisting of count and zero part. Results were reported through estimate, p-value, significance level and p-adjusted according to FDR-correction in the respective part. The five highest negative estimates were shown. Statistical significance was set at $p < 0.05$. Abbreviations: 19,20-DiHDPA: X19,20,DiHDPA.C22H34O4.

Table 20: Association of *Parasutterella* sp. with the particular metabolite (hurdle model) displaying the five highest positive estimates

parameter	model	estimate	p	significance	p-adjusted
PE(P-18:1(11Z)/18:3(9Z,12Z,15Z))	count	3.53	4.25e ⁻³	***	3.99e ⁻²
	zero	9.93e ⁻²	9.40e ⁻¹		9.83e ⁻¹
Oxoglutaric acid	count	1.99	6.97e ⁻³	***	5.36e ⁻²
	zero	5.29e ⁻²	9.44e ⁻¹		9.84e ⁻¹
Hydroxynicotinic acid	count	1.57	5.7e ⁻⁴	***	1.22e ⁻²
	zero	-3.15e ⁻¹	4.78e ⁻¹		9.82e ⁻¹
Prostaglandin F1a	count	1.33	9.88e ⁻⁷	***	1.5e ⁻⁴
	zero	-3.8e ⁻¹	2.16e ⁻¹		9.82e ⁻¹
Isocaproic acid	count	1.25	1.1e ⁻⁴	***	5.51e ⁻³
	zero	4.05e ⁻¹	2.95e ⁻¹		9.82e ⁻¹

Association of metabolites and Parasutterella sp. abundance tested with a two-part hurdle model consisting of count and zero part. Results were reported through estimate, p-value, significance level and p-adjusted according to FDR-correction in the respective part. The five highest positive estimates were shown. Statistical significance was set at $p < 0.05$.

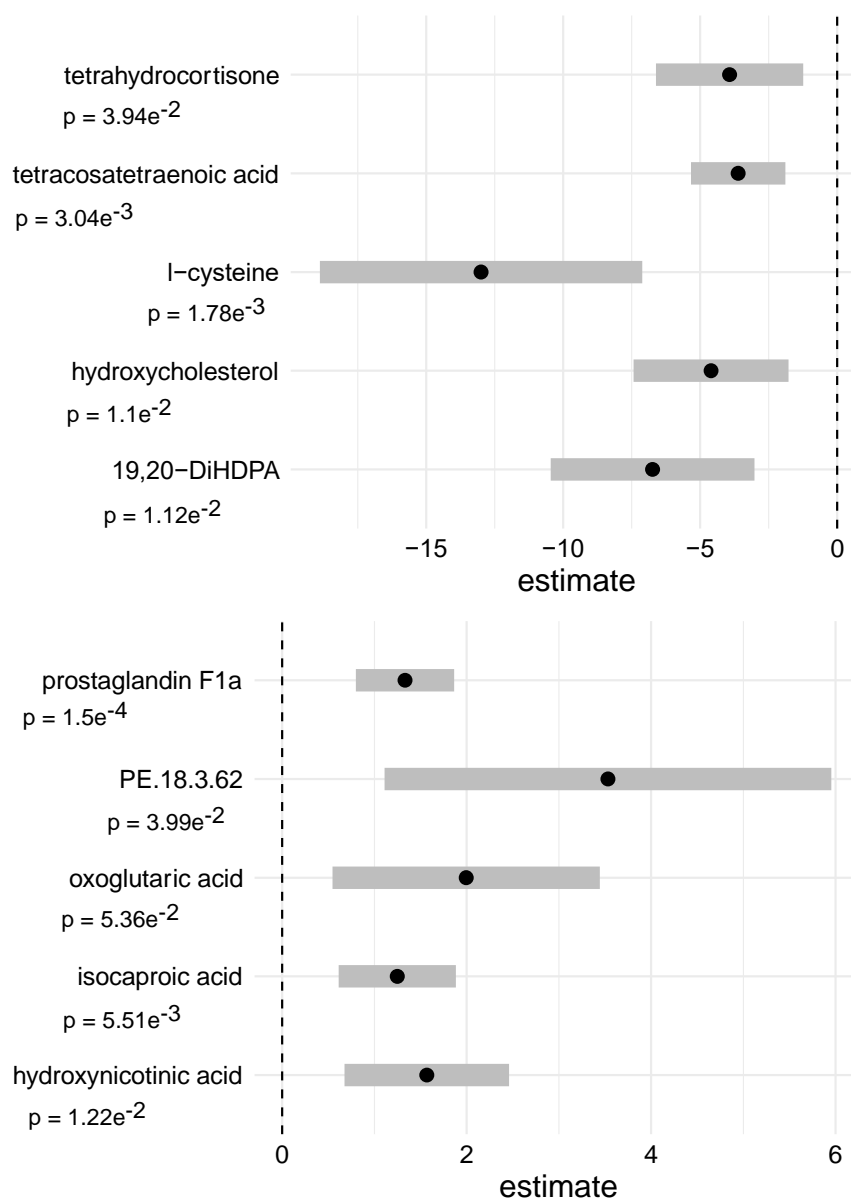


Figure 9: Association of *Parasutterella* sp. with the particular metabolite (count model) without BMI as a covariate

Association of metabolites and Parasutterella sp. abundance tested with a two-part hurdle model displaying only the count part here. No confounders were included. Results were reported through estimate and p-adjusted according to FDR-correction. Statistical significance was set at $p < 0.05$.

There were no significant associations in the zero part of the hurdle model for all metabolites analyzed. Furthermore, we added covariates such as BMI and age to our model. It is important to mention that L-cysteine remained significantly associated with *Parasutterella* sp. abundance in the count part of the hurdle model (-11.06, $p = 1.88 \times 10^{-2}$) (tab. 21). Prostaglandin F1a (with a positive estimate) was significantly associated with

Results

Parasutterella sp. abundance in the count part of the hurdle model when BMI and age were included as covariates ($9.63e^{-1}$, $p = 2.49e^{-2}$) (tab. 22). Again, for the zero part of the hurdle model we found no associations.

Table 21: Association of *Parasutterella* sp. with the particular metabolite (hurdle model) including covariates such as BMI and age, displaying the five highest negative estimates

parameter	confounder	model	estimate	p	significance	p-adjusted
L-cysteine	BMI, age	count	-11.06	$2.0e^{-4}$	***	$1.88e^{-2}$
		zero	$-5.26e^{-1}$	$9.03e^{-1}$		$9.97e^{-1}$
Prolylhydroxyproline	BMI, age	count	-3.55	$2.96e^{-9}$	***	$2.82e^{-6}$
		zero	2.07	$2.28e^{-1}$		$9.96e^{-1}$
X4a.Carboxy.4b.methyl.5a.cholesta.8.24.dien.3b.ol.C29H46O3	BMI, age	count	-2.85	$2.7e^{-4}$	***	$1.92e^{-2}$
		zero	1.29	$3.15e^{-1}$		$9.96e^{-1}$
dUDP.C9H14N2O11P2	BMI, age	count	-2.55	$2.17e^{-5}$	***	$3.43e^{-3}$
		zero	$-5.98e^{-1}$	$3.76e^{-1}$		$9.96e^{-1}$
PG.16.1.9Z.18.3.6Z.9Z.12Z...C40H71O10P	BMI, age	count	-2.18	$1.09e^{-3}$	***	$4.97e^{-2}$
		zero	$4.47e^{-2}$	$9.64e^{-1}$		$9.97e^{-1}$

Association of metabolites and Parasutterella sp. abundance tested with a two-part hurdle model consisting of count and zero part. Confounder such as BMI and age were included. Results were reported through estimate, p-value, significance level and p-adjusted according to FDR-correction in the respective part. The five highest negative estimates were shown. Statistical significance was set at $p < 0.05$.

Table 22: Association of *Parasutterella* sp. with the particular metabolite (hurdle model) including covariates such as BMI and age, displaying the two highest positive estimates

parameter	confounder	model	estimate	p	significance	p-adjusted
Prostaglandin F1a	BMI, age	count	9.63e ⁻¹	4.4e ⁻⁴	***	2.5e ⁻²
		zero	-3.06e ⁻¹	3.27e ⁻¹		9.96e ⁻¹
DG.15.0.18.2.9 Z.12Z..0.0..C36 H66O5	BMI, age	count	5.66e ⁻¹	1.5e ⁻⁴	***	1.63e ⁻²
		zero	-2.39e ⁻¹	1.85e ⁻¹		9.96e ⁻¹

Association of metabolites and Parasutterella sp. abundance tested with a two-part hurdle model consisting of count and zero part. Confounder such as BMI and age were included. Results were reported through estimate, p-value, significance level and p-adjusted according to FDR-correction in the respective part. The two highest positive estimates were shown. Statistical significance was set at $p < 0.05$.

Secondly, the pathway enrichment analysis of 76 metabolites that were successfully matched to terms of the SMPDB database resulted in two nominally significant pathways: fatty acid biosynthesis and α -linolenic acid metabolism ($p = 1.16e^{-2}$, $p = 4.62e^{-2}$) (fig. 10). All other pathways in the figure were not significantly enriched (suppl. tab. 2).

Results

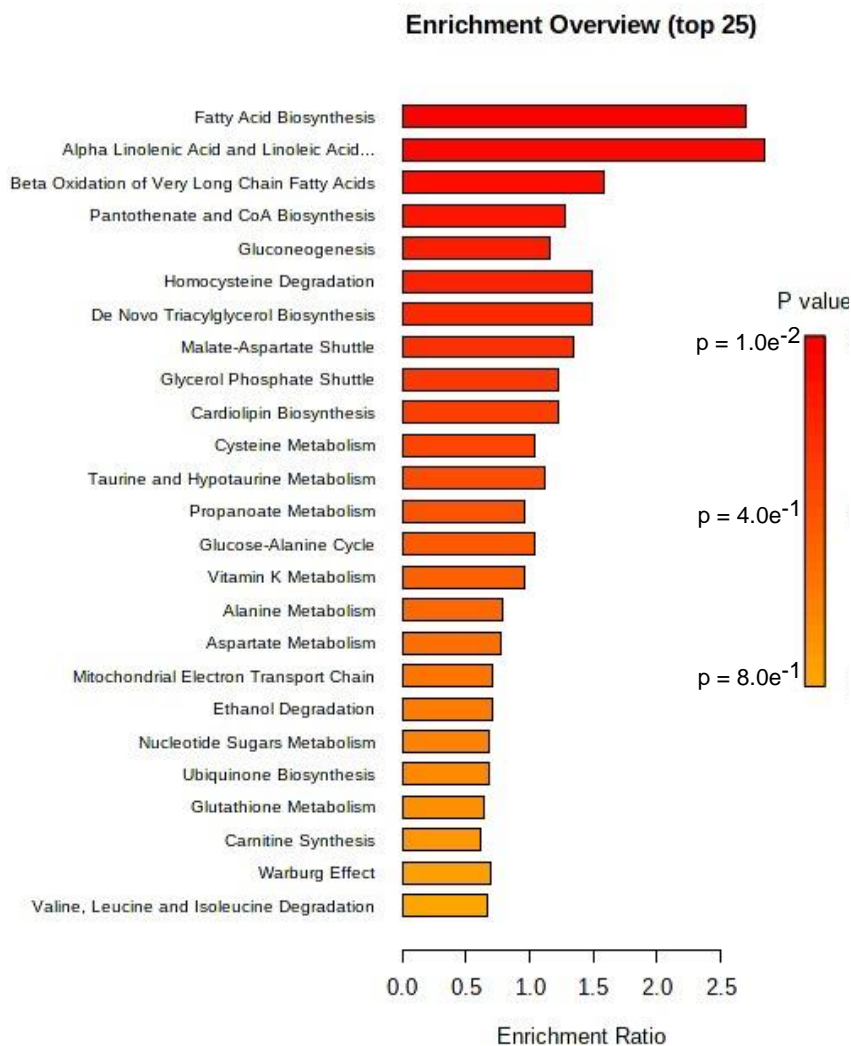


Figure 10: Pathway enrichment analysis (SMPDB database) of metabolites associated with *Parasutterella* sp.

Enrichment ratio and related nominal *p*-value of the metabolic pathway enrichment analysis (SMPDB database), displaying fatty acid biosynthesis and α -linolenic acid metabolism as significant. Statistical significance was set at $p < 0.05$.

Thirdly, we used metabolic network modeling to investigate maximal L-cysteine consumption by member species of the human gut microbiota. This analysis revealed that *Parasutterella* is amongst the top five consumers, together with *Dialister invisus*, *Enterobacter cancerogenus*, *Prevotella copri*, and *E. coli* K12. Hence, the fact that *Parasutterella* is a high L-cysteine consumer fits with the findings of reduced L-cysteine levels in the serum of human subjects with high *Parasutterella* abundance. Table 23 gives an overview of the top L-cysteine consumers in the gut microbiome.

Table 23: Gut bacteria of the human gut microbiota with the highest relative L-cysteine consumption in human samples

species (strain designation in the AGORA collection)	maximal L-cysteine consumption (mmol/gDW/h)	average relative abundance	abundance-weighted cystein consumption	relative L-cysteine consumption
<i>Dialister invisus</i> DSM 15470	40.8	7.8e ⁻²	3.20	13.72%
<i>Enterobacter cancerogenus</i> ATCC 35316	97.7	2.7e ⁻²	2.68	11.53%
<i>E. coli</i> K12 MG1655	47.1	5.2e ⁻²	2.47	10.59%
<i>Prevotella copri</i> CB7 DSM 18205	38.9	5.8e ⁻²	2.27	9.77%
<i>Parasutterella excrementihominis</i> YIT 11859	81.9	2.6e ⁻²	2.12	9.10%
<i>Sutterella wadsworthensis</i> 3145B	96.3	8.0e ⁻³	0.81	3.48%
<i>Roseburia hominis</i> A2 183	89.4	8.0e ⁻³	0.70	3.02%
<i>Hafnia alvei</i> BIDMC 31	98.1	7.0e ⁻³	0.70	3.01%
<i>Bilophila wadsworthia</i> 316	96.3	5.0e ⁻³	0.51	2.17%
<i>Acidaminococcus intestini</i> RyC MR95	88.2	4.0e ⁻³	0.39	1.68%

Gut bacteria on species level with the highest relative L-cysteine consumption in human samples. The second column indicates the maximal predicted L-cysteine consumption of each strain during optimal growth, the third column the average abundance in the FoCus cohort and the forth column the abundance weighted cysteine consumption. The fifth column shows the relative L-cysteine consumption as a sum of 1 regarding microbiome abundance in the FoCus cohort.

Results

4.2.4 *Parasutterella* and host genomics

Regarding genomic analysis, we applied a GWAS for $n=1,397$ subjects. In the logistic model, that included *Parasutterella* sp. presence and *Parasutterella* sp. absence in association to 579,666 SNPs, covariates such as BMI and age were included for modeling. There was no SNP genome-wide significantly associated with *Parasutterella* sp. presence/*Parasutterella* sp. absence. A few SNPs (chr6:43752536, chr11:97176319, chr15:70463992) were suggestively significant at a threshold of $p < 0.00001$ but were not further investigated (fig. 11). Q-Q-plot displayed p-values included in the analysis (suppl. fig. 3).

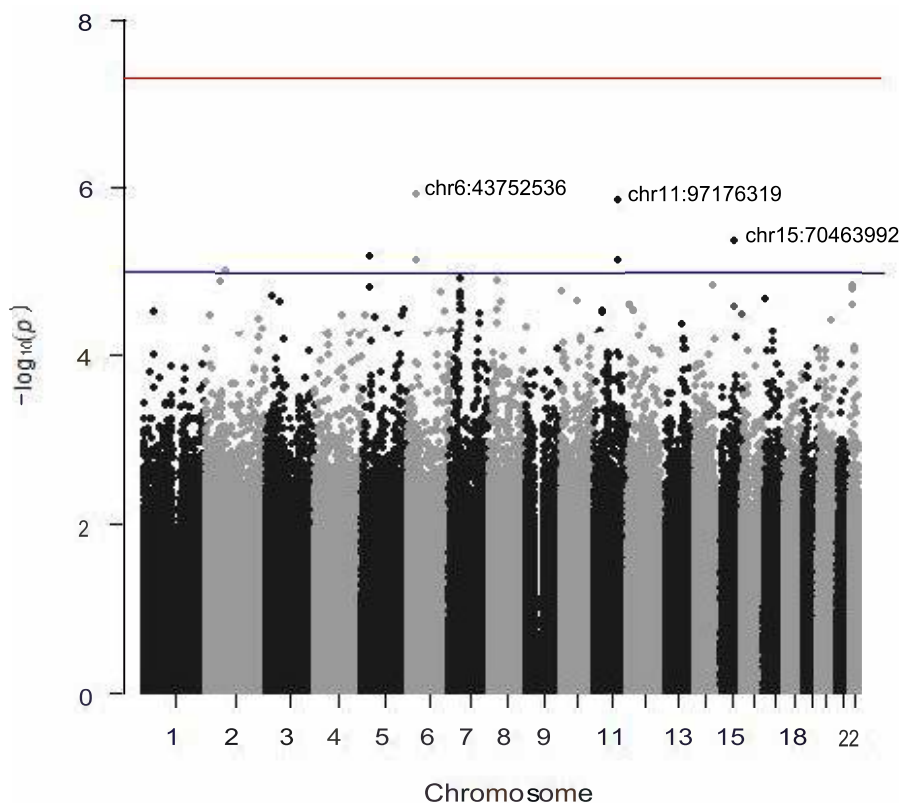


Figure 11: Association of *Parasutterella* sp. and SNPs (logistic model) of $n=1,397$ subjects

Manhattan plot showed no genome wide association of SNPs with *Parasutterella* sp. absence/presence. A logistic regression model including $n=1,397$ subjects and 579,666 SNPs as well as BMI and age as covariates was used. The blue line typifies a suggestive threshold of $p < 1 \times 10^{-5}$. The x-axis shows autosomal chromosomes. The y-axis shows negative logarithm of p-values ($-\log_{10}(p)$).

4.2.5 *Parasutterella* and weight loss intervention

The patients of the weight loss intervention lost a significant amount of weight (mean of 23 kg; Wilcoxon signed-rank test, $p = 5.30 \times 10^{-10}$). BMI dropped from 45.2 kg/m² to 38.5 kg/m² (fig. 12A). Interestingly, *Parasutterella excrementihominis* was significantly reduced during the intervention (fig. 12B). The median value of relative *Parasutterella excrementihominis* abundance at baseline was 1.62% in comparison to 0.62% of *Parasutterella excrementihominis* after the intervention. These data indicate that *Parasutterella* is not only associated to the obesity phenotype in a steady state but also reacts significantly to variations in body weight. It has to be mentioned that the formula diet used within the human intervention study has a low carbohydrate content.

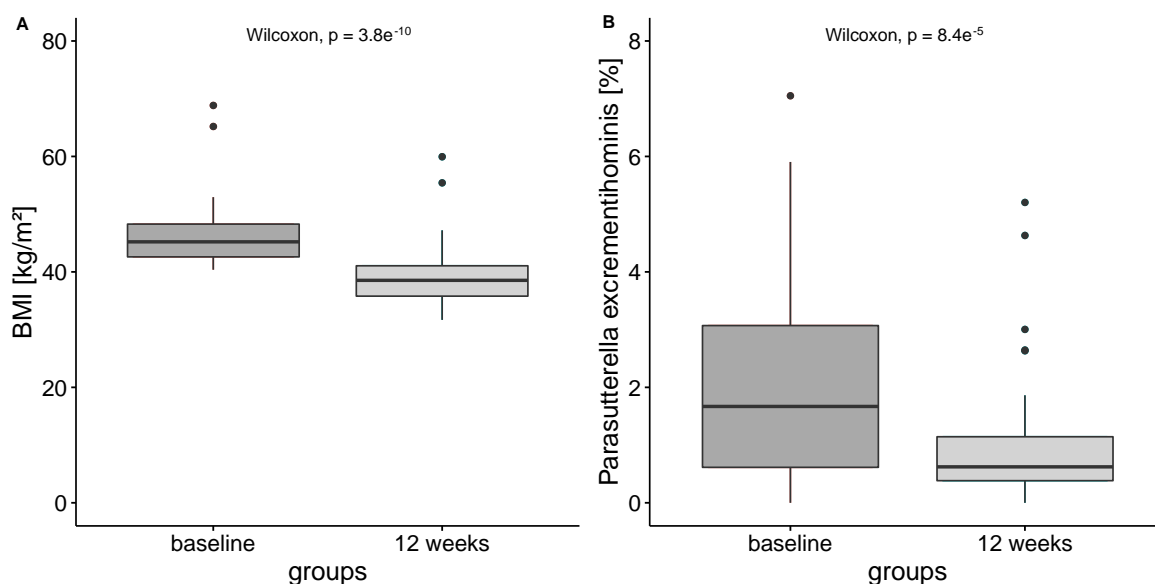


Figure 12: Difference of BMI (A) and abundance of *Parasutterella excrementihominis* (B) in subjects of intervention at baseline compared with 12 weeks

Difference between two groups was calculated through Wilcoxon signed-rank test for $n=55$ human subjects. Statistical significance was set at $p < 0.05$. Abbreviations: BMI: body mass index.

4.3 Agmatine – descriptive statistics

For univariate and multivariate modeling of agmatine, a subset of the FoCus cohort ($n=1,704$) was used for further calculations and is outlined in table 24. Due to combining

Results

of various data sets the number of subjects included differs. Agmatine variable includes various statistical zeros (suppl. fig. 4).

Table 24: Descriptive statistics of the FoCus cohort (agmatine)

parameter	median (25 th and 75 th percentile) or mean \pm sd
Age (years)	49.95 ^a (14.14)
Sex (% female)	62.62
BMI (kg/m ²)	27.79 ^b (23.61; 35.87)
Normal weighted (19-25 kg/m ²) (%)	30.81 ^c
Over weighted (25-30 kg/m ²) (%)	26.76
Obese (>30 kg/m ²) (%)	39.20
Glucose (mg/dl)	95.0 (88.0; 104.0)
Diabetes type 2 (%)	13.98
CRP (mg/l)	1.7 (0.9; 4.12)
IL-6 (pg/ml)	3.2 (1.9; 4.9)
Agmatine	645064.2 (1363328)

^amean \pm sd (all such values); ^bmedian: 25th, 75th percentile (all such values); ^cpercentage (all such values). Abbreviations: sd: standard deviation; BMI: body mass index; CRP: C-reactive protein; IL-6: interleukin-6.

4.3.1 Agmatine regarding phenotypical parameter and diseases

Data pre-analysis of the metabolite agmatine measured in human serum samples and various phenotypical parameters showed an elevated BMI and waist median value in the agmatine presence group (n=1,704) (fig. 13, A+B). All other parameters tested showed no significant difference (tab. 25).

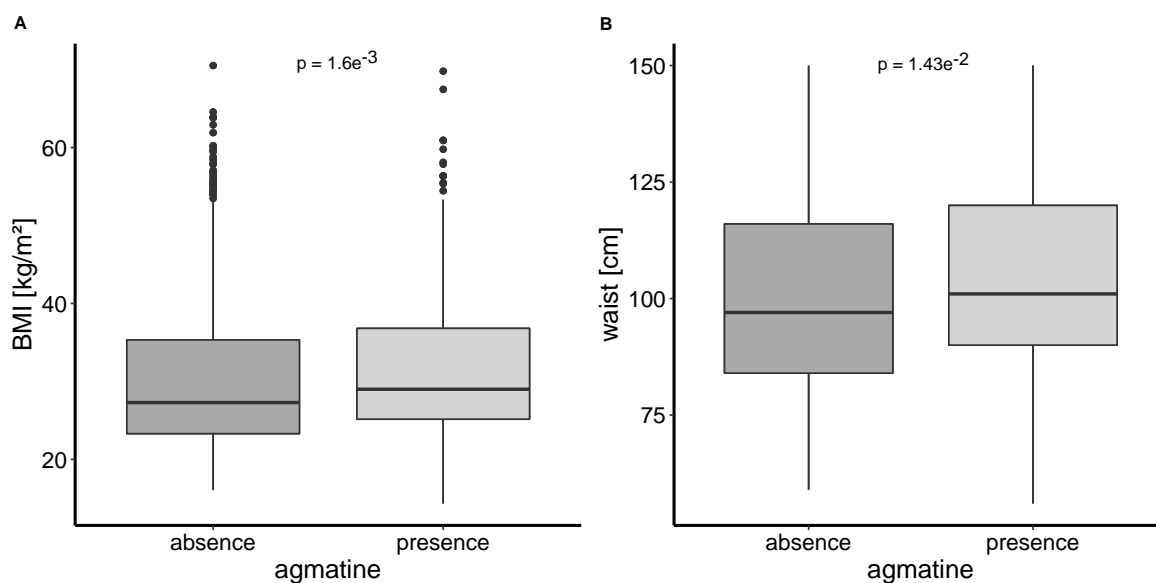


Figure 13: Differences in agmatine absence and agmatine presence regarding BMI (A) and waist (B)

Wilcoxon-rank sum test was used to determine between group differences for continuous variables. P-adjusted according to FDR-correction was displayed. Statistical significance was set at $p < 0.05$. Statistical analysis includes $n=1,704$ subjects for A and $n=1,703$ subjects for B. Abbreviations: BMI: body mass index.

Table 25: Differences in agmatine absence and agmatine presence regarding the particular parameter

parameter	p	p-adjusted
CRP	3.47e ⁻²	3.47e ⁻¹
Glucose	3.08e ⁻¹	1
HOMA	8.13e ⁻¹	1
IL-6	6.84e ⁻¹	1
TNF-α	3.90e ⁻¹	1
Triglycerides	9.45e ⁻¹	1
Visceral fat	2.49e ⁻²	2.49e ⁻¹
Waist	1.44e ⁻³	1.43e ⁻²
Age	1.67e ⁻¹	1
BMI	1.69e ⁻⁴	1.6e ⁻³

Wilcoxon-rank sum test was used to determine between group differences for continuous parameter. Results were reported through p-value and p-adjusted according to FDR-correction. Statistical significance was set at $p < 0.05$. Abbreviations: BMI: body mass index; CRP: C-reactive protein; IL-6: interleukin-6; HOMA-IR index: Homeostasis Model Assessment insulin resistance index; TNF- α : tumor necrosis factor-alpha.

For the variable gender, we looked at different distributions in either male or female subjects concerning agmatine absence or agmatine presence (χ^2 -test). We found a significant difference in male and female subjects regarding agmatine availability whereby 43% of females and solely 31% of males were displayed with agmatine presence ($p = 6.5e^{-3}$) (fig. 14A). In addition, we calculated if there is a difference in male or female subjects in agmatine intensity. Data revealed higher intensity of agmatine in female subjects (Wilcoxon-rank sum, $p = 4.0e^{-3}$) (fig. 14B).

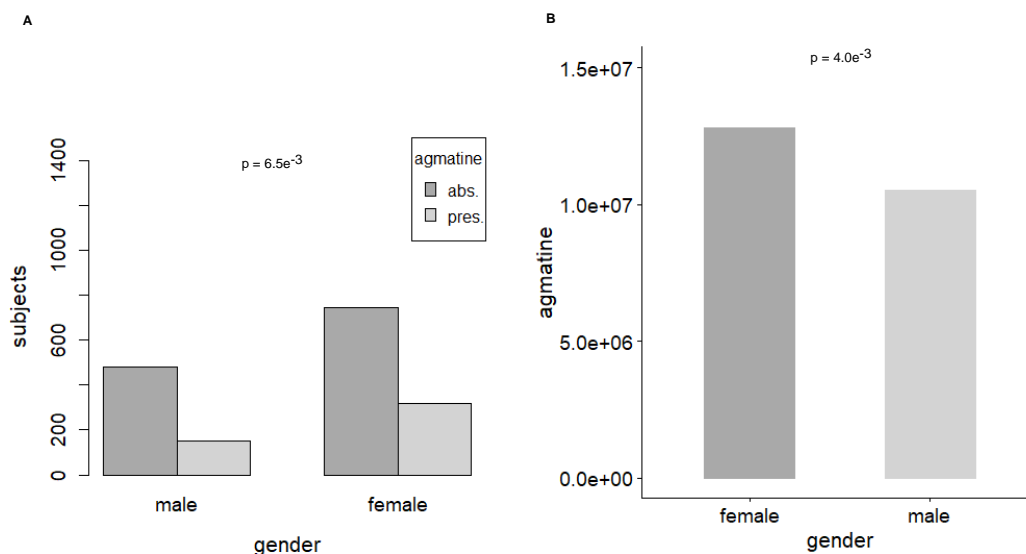


Figure 14: (A) Differences in prevalence of agmatine absence and agmatine presence in male or female subjects, (B) Differences in female or male subjects regarding agmatine intensity.

(A) χ^2 -test was used to determine group differences for categorical parameter. Nominal p -value was displayed. Statistical significance was set at $p < 0.05$. (B) Wilcoxon-rank sum test was used to determine between group differences for continuous parameter. Nominal p -value was displayed. Statistical significance was set at $p < 0.05$.

We were curious to know if in female subjects there is a difference in BMI less than 25 kg/m² compared to women with a BMI greater than 25 kg/m² in agmatine intensity. Figure 15 showed that agmatine is elevated in obese female subjects ($p = 8.5e^{-5}$).

Results

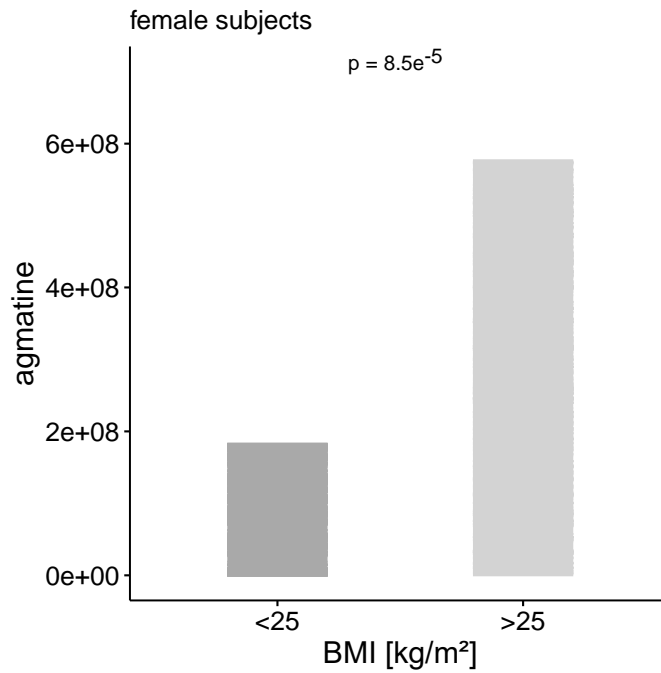


Figure 15: Differences in BMI groups regarding agmatine intensity in female subjects

Wilcoxon-rank sum test was used to determine between group differences for continuous parameter. Nominal p-value was displayed. Statistical significance was set at $p < 0.05$. Statistical analysis includes $n=1,067$ subjects. Abbreviations: BMI: body mass index.

Further, association analysis revealed that agmatine was positively associated with BMI and waist (spearman correlation) ($p = 1.90e^{-5}$, $p = 2.31e^{-4}$) (fig. 16). Table 26 showed no further significant associations of agmatine and phenotypical parameter for p-adjusted according to FDR-correction.

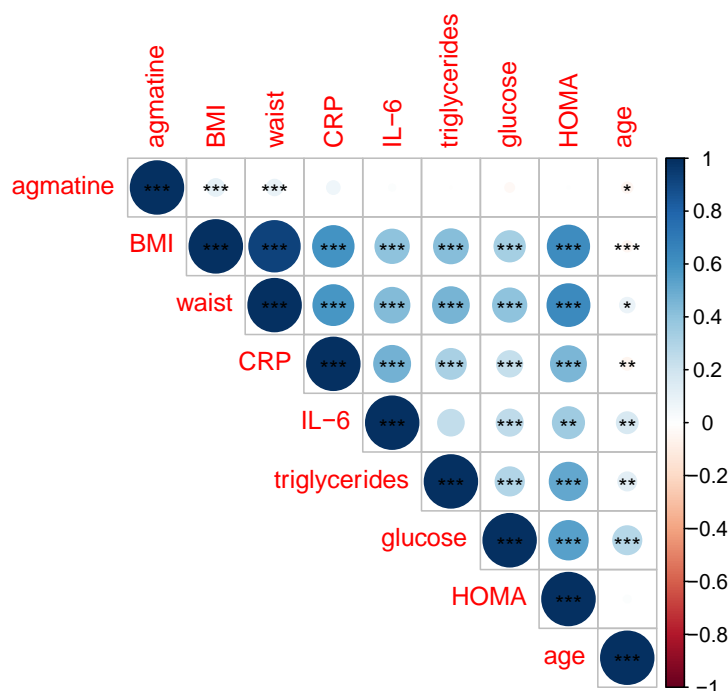


Figure 16: Association of agmatine with phenotypical parameter

Spearman correlation test was used to determine associations between two continuous parameters. Nominal p-values were displayed. Statistical significance was set at $p < 0.05$. Abbreviations: BMI: body mass index; CRP: C-reactive protein; IL-6: interleukin-6; HOMA-IR index: Homeostasis Model Assessment insulin resistance index.

Table 26: Associations of agmatine and phenotypical parameters

parameter	r	p	p-adjusted
CRP	$6.37e^{-2}$	$8.5e^{-3}$	$8.53e^{-2}$
Glucose	$-3.08e^{-2}$	$2.04e^{-1}$	1
HOMA	$-5.92e^{-5}$	$9.98e^{-1}$	1
IL-6	$1.73e^{-2}$	$4.76e^{-1}$	1
TNF- α	$8.37e^{-2}$	$4.03e^{-1}$	1
Triglycerides	$-2.04e^{-3}$	$9.33e^{-1}$	1
Visceral fat	$-2.61e^{-1}$	$9.07e^{-2}$	$9.07e^{-1}$
Waist measure	$8.93e^{-2}$	$2.31e^{-4}$	$2.31e^{-3}$
Age	$-3.96e^{-2}$	$1.02e^{-1}$	1
BMI	$1.03e^{-1}$	$1.90e^{-5}$	$1.9e^{-4}$

Spearman correlation test was used to determine associations between two continuous parameters. Results were reported through r, p-value and p-adjusted according to FDR-correction.

Results

Statistical significance was set at $p < 0.05$. Abbreviations: BMI: body mass index; CRP: C-reactive protein; IL-6: interleukin-6; HOMA-IR index: Homeostasis Model Assessment insulin resistance index; TNF- α : tumor necrosis factor-alpha.

We further applied a multivariate hurdle algorithm for those variables that were significant in the pre-analysis. In total we had $n=1,704$ subjects included and BMI remained positively associated with agmatine ($1.16e^{-2}$, $p = 1.84e^{-4}$) (fig. 17) in the first part of the model (count model). Confounders such as gender, age, metformin and BMI were added to the model. Table 27 shows associations of agmatine with the particular phenotypical parameter.

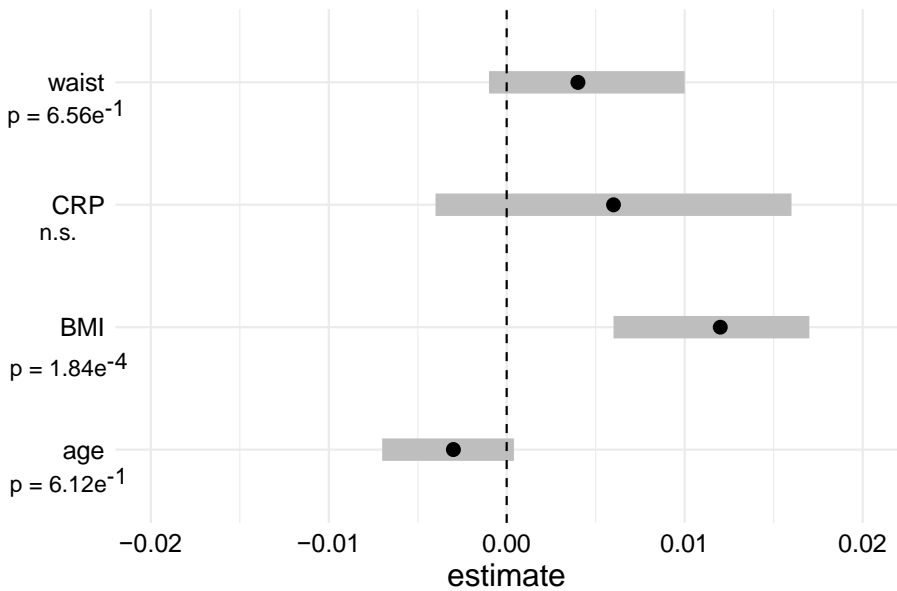


Figure 17: Association of agmatine with the particular phenotypical parameter (count model)

Association of phenotypical parameter and agmatine tested with a two-part hurdle model displaying only the count part here. Confounder such as gender, age, metformin and BMI were included. Results were reported through estimate and p -adjusted according to FDR-correction. Statistical significance was set at $p < 0.05$. Abbreviations: BMI: body mass index; CRP: C-reactive protein.

Table 27: Association of agmatine with the particular phenotypical parameter (hurdle model)

parameter	confounder	model	estimate	p	significance	p-adjusted
BMI	gender, age, metformin	count	1.16e ⁻²	2.63e ⁻⁵	***	1.84e ⁻⁴
		zero	1.19e ⁻²	3.13e ⁻²	*	2.19e ⁻¹
Waist	gender, age, metformin	count	4.42e ⁻³	9.37e ⁻²		6.56e ⁻¹
		zero	1.66e ⁻²	1.85e ⁻²	*	1.3e ⁻¹
Age	gender, metformin, BMI	count	-3.08e ⁻³	8.74e ⁻²		6.12e ⁻¹
		zero	-4.06e ⁻³	3.0e ⁻¹		1
CRP	gender, age, metformin, BMI	count	6.0e ⁻³	2.52e ⁻¹	.	1
		zero	-2.18e ⁻²	5.36e ⁻²		3.75e ⁻¹

Association of phenotypical parameter and agmatine tested with a two-part hurdle model consisting of count and zero part. Confounder such as gender, age, metformin and BMI were included. Results were reported through estimate, p-value, significance level and p-adjusted according to FDR-correction in the respective part. Statistical significance was set at $p < 0.05$. Abbreviations: BMI: body mass index; CRP: c-reactive protein.

When we analyzed various metabolic and inflammatory diseases we looked at different distributions in either absence or presence of the disease concerning agmatine absence or agmatine presence (χ^2 -test). Table 28 summarizes analyses whereby no disease was significantly prevalent in subjects of agmatine groups after p-adjusted values.

Table 28: Differences in prevalence of the particular disease between agmatine absence and agmatine presence

parameter	Cramers V	p	p-adjusted
IBD	$5.0e^{-2}$	$3.81e^{-2}$	$2.28e^{-1}$
Parodontitis	$2.0e^{-2}$	$3.1e^{-1}$	1
Rheumatoid Arthr.	$1.0e^{-2}$	$4.9e^{-1}$	1
Skin disease	$6.0e^{-3}$	$8.0e^{-1}$	1
Diabetes	$1.0e^{-2}$	$4.6e^{-1}$	1
Neuropathy	$3.0e^{-2}$	$1.2e^{-1}$	$7.2e^{-1}$

χ^2 -test was used to determine group differences for categorical parameter. Results were reported through cramers V, p-value and p-adjusted according to FDR-correction. Statistical significance was set at $p < 0.05$. Abbreviations: IBD: inflammatory bowel disease, Rheumatoid Arthr.: Rheumatoid Arthritis.

Additionally, we tested for differences in absence or presence of the disease concerning agmatine intensities (Wilcoxon-rank sum test). Figure 18A shows an elevated agmatine level in subjects of IBD absence ($p = 5.1e^{-2}$).

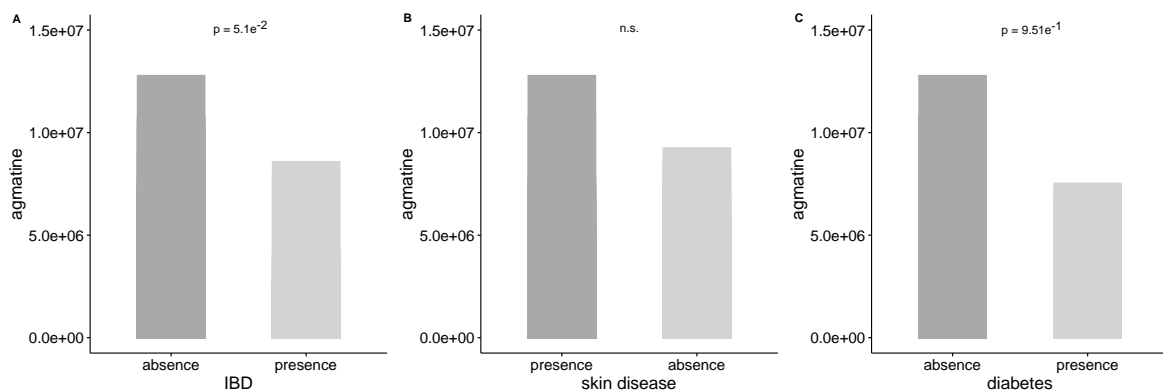


Figure 18: Differences in absence or presence of IBD (A), skin disease (B) or diabetes (C) regarding agmatine.

Wilcoxon-rank sum test was used to determine between group differences for continuous parameter. P-adjusted according to FDR-correction was displayed. Statistical significance was set at $p < 0.05$. Abbreviations: IBD: inflammatory bowel disease.

As well for diseases, we used the hurdle algorithm to calculate associations and found that IBD was nominally positively associated with agmatine in the second part of the model (zero part) ($p = 1.3e^{-2}$), whereas skin disease was nominally positively associated with agmatine in the count part ($p = 2.4e^{-2}$) (tab. 29). Figure 19 shows associations of agmatine with skin disease and IBD only in the count model.

Table 29: Association of agmatine with the particular disease (hurdle model)

parameter	confounder	model	estimate	p	significance	p-adjusted
IBD	gender, age, metformin, BMI	count	$7.88e^{-2}$	$4.17e^{-1}$		1
		zero	$5.41e^{-1}$	$1.3e^{-2}$	*	$8.9e^{-2}$
Skin disease	gender, age, metformin, BMI	count	$1.41e^{-1}$	$2.4e^{-2}$	*	$1.66e^{-1}$
		zero	$-5.39e^{-2}$	$6.84e^{-1}$		1

Association of diseases and agmatine tested with a two-part hurdle model consisting of count and zero part. Confounder such as gender, age, metformin and BMI were included. Results were reported through estimate, p-value, significance level and p-adjusted according to FDR-correction in the respective part. Statistical significance was set at $p < 0.05$. Abbreviations: IBD: inflammatory bowel disease.

Results

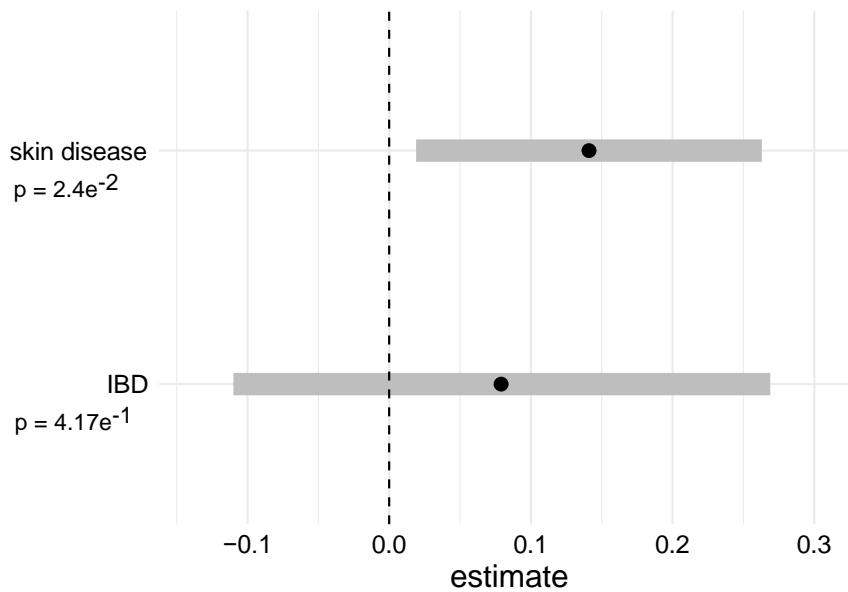


Figure 19: Association of agmatine with the particular disease (count model)

Association of diseases and agmatine tested with a two-part hurdle model displaying only the count part here. Confounder such as gender, age, metformin and BMI were included. Results were reported through estimate and nominal p-value. Statistical significance was set at $p < 0.05$. Abbreviations: IBD: inflammatory bowel disease.

4.3.2 Agmatine and dietary intake including medication (metformin)

Regarding univariate analysis, we tested for associations of agmatine with $n=134$ nutrients originated from the dietary intake records of the FFQ. For this analysis we used $n=1,193$ subjects due to previous data set adjustments. Data revealed that eight nutrients were nominally significant (tab. 30). All other nutrients showed no significant association.

Table 30: Associations of agmatine with the particular parameter

parameter	r	p	p-adjusted
Alcohol	-7.39×10^{-2}	1.06×10^{-2}	4.3×10^{-1}
Serine	6.56×10^{-2}	2.35×10^{-2}	4.3×10^{-1}
Phenylalanine	6.2×10^{-2}	3.22×10^{-2}	4.3×10^{-1}
Non-essential amino acids	6.13×10^{-2}	3.43×10^{-2}	4.3×10^{-1}
Valine	6.1×10^{-2}	3.52×10^{-2}	4.3×10^{-1}
Linoleic acid	5.98×10^{-2}	3.91×10^{-2}	4.3×10^{-1}

Proline	5.93e ⁻²	4.06e ⁻²	4.3e ⁻¹
Protein	5.87e ⁻²	4.25e ⁻²	4.3e ⁻¹

Spearman correlation test was used to determine associations between two continuous parameters. Results were reported through r , p -value and p -adjusted according to FDR-correction. Statistical significance was set at $p < 0.05$.

For dietary intake, we also tested associations of agmatine and $n=134$ nutrients with a hurdle algorithm and found 23 nutrients to be nominally associated with agmatine in the count model ($n=1,570$). Further, we used these 23 nutrients for a hurdle algorithm including the following confounder: gender, age, metformin, cut-off, maltose and plant protein. Table 31 shows nominal significantly associations of amgatine with maltose (negatively) ($-2.47e^{-2}$, $p = 8.28e^{-3}$), plant protein (positively) ($7.77e^{-3}$, $p = 4.79e^{-3}$) and lactose (negatively) ($1.77e^{-2}$, $p = 1.77e^{-2}$) in the count model. All other nutrients were not significant.

Table 31: Association of agmatine with the particular nutrient (hurdle model)

variable	confounder	mode I	estimate	p	signific ance	p- adjusted
Maltose (KDM)	gender, age, metformin, cut- off, maltose, plant protein	count	$-2.47e^{-2}$	$8.28e^{-3}$	**	$1.90e^{-1}$
		zero	$-2.96e^{-2}$	$1.44e^{-1}$		1
Plant protein (EPF)	gender, age, metformin, cut- off, maltose, plant protein	count	$7.77e^{-3}$	$4.79e^{-3}$	**	$1.11e^{-1}$
		zero	$-5.57e^{-5}$	$9.92e^{-1}$		1
Vitamin B2 (VB2)	gender, age, metformin, cut- off, maltose, plant protein	count	$-1.36e^{-1}$	$7.80e^{-2}$		1
		zero	$1.56e^{-1}$	$3.06e^{-1}$		1
Vitamin	gender, age,	count	-24.9	$8.18e^{-2}$		1

Results

B12 (VB12)	metformin, cut-off, maltose, plant protein	zero	30.92	2.92e ⁻¹	1
Lactose (KDL)	gender, age, metformin, cut-off, maltose, plant protein	count	-9.41e ⁻³	1.77e ⁻² *	4.08e ⁻¹
		zero	5.32e ⁻³	5.24e ⁻¹	1
Organic acids (ZO)	gender, age, metformin, cut-off, maltose, plant protein	count	3.17e ⁻⁴	9.71e ⁻¹	1
		zero	1.48e ⁻²	4.13e ⁻¹	1
Vitamin B5 (VB5)	gender, age, metformin, cut-off, maltose, plant protein	count	-1.58e ⁻²	5.62e ⁻¹	1
		zero	4.45e ⁻²	4.14e ⁻¹	1
Oligosaccharides (KPOR)	gender, age, metformin, cut-off, maltose, plant protein	count	-4.75e ⁻³	4.99e ⁻¹	1
		zero	2.67e ⁻³	8.06e ⁻¹	1
Phosphor (MP)	gender, age, metformin, cut-off, maltose, plant protein	count	-7.49e ⁻²	4.85e ⁻¹	1
		zero	1.15e ⁻¹	5.97e ⁻¹	1
Vitamin B3A (VB3A)	gender, age, metformin, cut-off, maltose, plant protein	count	-4.33e ⁻³	3.21e ⁻¹	1
		zero	4.27e ⁻³	6.19e ⁻¹	1
Magnesium (M)	gender, age, metformin, cut-	count	-7.29e ⁻²	8.58e ⁻¹	1

(MMG)	off, maltose, plant protein				
		zero	$3.42e^{-1}$	$6.93e^{-1}$	1
Glucose (KMT)	gender, age, metformin, cut-off, maltose, plant protein	count	$-1.76e^{-3}$	$4.65e^{-1}$	1
		zero	$2.04e^{-3}$	$6.75e^{-1}$	1
Monosaccharide (KM)	gender, age, metformin, cut-off, maltose, plant protein	count	$-6.14e^{-4}$	$6.02e^{-1}$	1
		zero	$6.11e^{-4}$	$7.97e^{-1}$	1
Vitamin B6 (VB6)	gender, age, metformin, cut-off, maltose, plant protein	count	$-2.20e^{-2}$	$7.66e^{-1}$	1
		zero	$7.85e^{-2}$	$6.1e^{-1}$	1
Vitamin B3 (VB3)	gender, age, metformin, cut-off, maltose, plant protein	count	$-3.81e^{-3}$	$5.64e^{-1}$	1
		zero	$4.29e^{-3}$	$7.48e^{-1}$	1
Fructose (KMF)	gender, age, metformin, cut-off, maltose, plant protein	count	$-7.90e^{-7}$	$7.22e^{-1}$	1
		zero	$3.38e^{-4}$	$9.4e^{-1}$	1
Zinc (MZN)	gender, age, metformin, cut-off, maltose, plant protein	count	$-1.06e^{-2}$	$3.73e^{-1}$	1
		zero	$4.55e^{-3}$	$8.49e^{-1}$	1
Sulphur (MS)	gender, age, metformin, cut-off, maltose, plant	count	$-1.97e^{-1}$	$3.05e^{-1}$	1

Results

protein					
		zero	2.25e ⁻¹	5.48e ⁻¹	1
Nonadecatrienic acid (F193)	gender, age,	count	10.95	1.75e ⁻¹	1
	metformin, cut-off, maltose, plant				
	protein				
		zero	4.93	7.73e ⁻¹	1
Vitamin B7 (VB7)	gender, age,	count	-5.42e ⁻¹	8.32e ⁻¹	1
	metformin, cut-off, maltose, plant				
	protein				
		zero	4.76	3.63e ⁻¹	1
Tryptophan (ETRP)	gender, age,	count	-2.14e ⁻¹	1.8e ⁻¹	1
	metformin, cut-off, maltose, plant				
	protein				
		zero	1.94e ⁻¹	5.3e ⁻¹	1
Octadecanoic/Steatric acid (F180)	gender, age,	count	-8.05e ⁻³	5.46e ⁻¹	1
	metformin, cut-off, maltose, plant				
	protein				
		zero	-6.78e ⁻³	7.95e ⁻¹	1
Vitamin B1 (VB1)	gender, age,	count	-3.68e ⁻²	6.89e ⁻¹	1
	metformin, cut-off, maltose, plant				
	protein				
		zero	-1.99e ⁻²	9.16e ⁻¹	1

Association of dietary parameter and agmatine tested with a two-part hurdle model consisting of count and zero part. Confounder such as gender, age, metformin, cut-off, maltose and plant protein were included. Results were reported through estimate, p-value, significance level and p-adjusted according to FDR-correction in the respective part. Statistical significance was set at $p < 0.05$. Abbreviations: vitamin B3A: niacin equivalent.

Figure 20 shows the five highest negative estimates and the three highest positive estimates and additionally maltose and lactose regardless of the significance level.

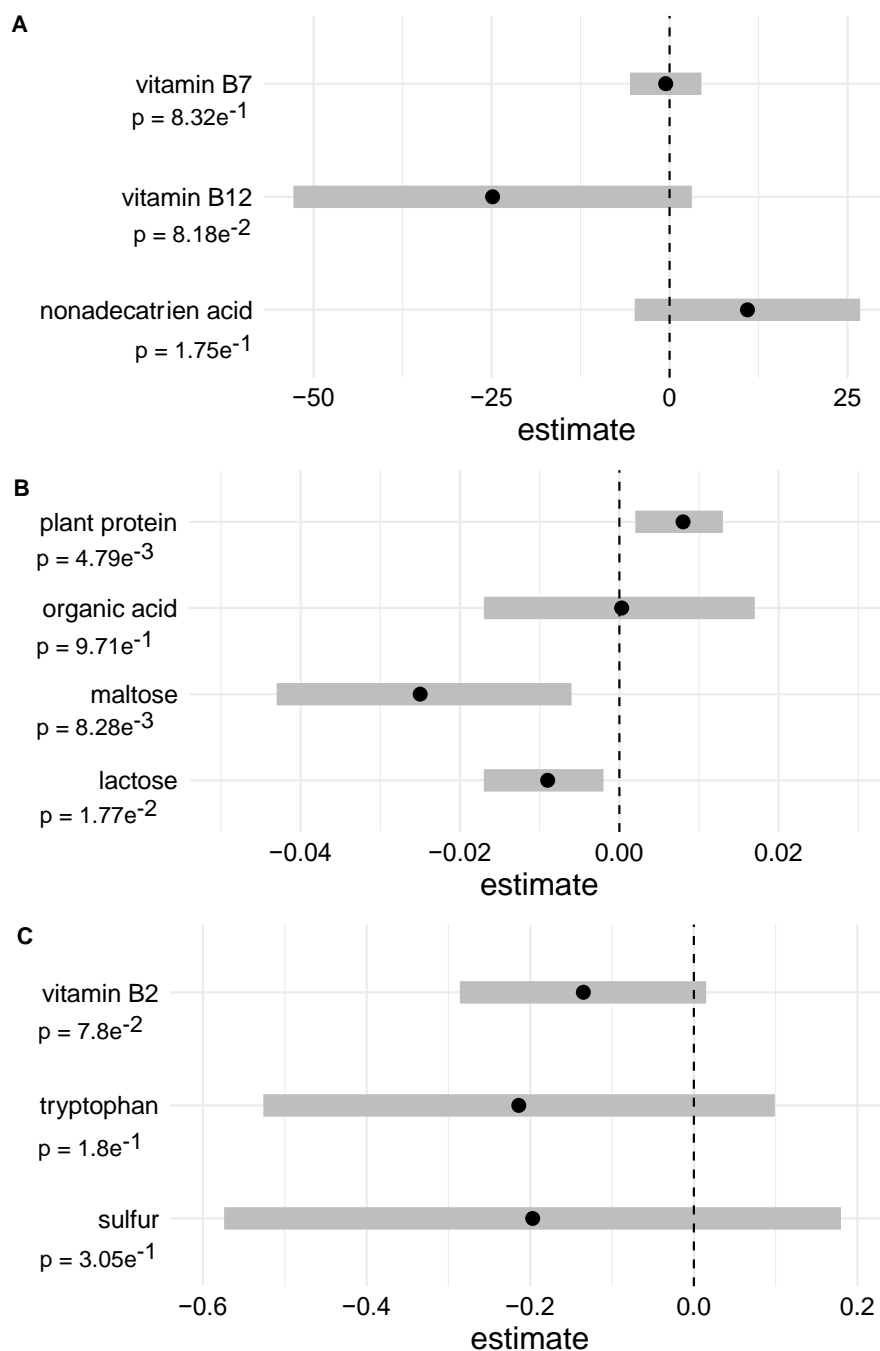


Figure 20: Association of agmatine with the particular dietary parameter (count model)

Association of dietary parameter and agmatine tested with a two-part hurdle model displaying only the count part here. Confounder such as gender, age, metformin, cut-off, maltose and plant protein were included. Dietary parameter were shown and separated according to resembling estimates (A,B,C). Results were reported through estimate and nominal p-values. Statistical significance was set at $p < 0.05$.

Results

Since previous published data revealed an association of the drug metformin and agmatine (62), we figured that in our data ($n=1,704$) there is no difference of the distribution in metformin presence or metformin absence concerning agmatine absence or agmatine presence (χ^2 -test) ($p = 2.37e^{-1}$) (fig. 21A). We further looked at subjects with agmatine presence ($n=473$) and there was no difference in metformin presence and metformin absence regarding agmatine intensity ($p = 5.96e^{-1}$) (fig. 21B). In a sub analysis we used subjects with a BMI greater than 25 kg/m^2 and type 2 diabetes ($n=69$) and there was no difference in metformin presence and metformin absence regarding agmatine intensity either ($p = 3.61e^{-1}$) (fig. 21C).

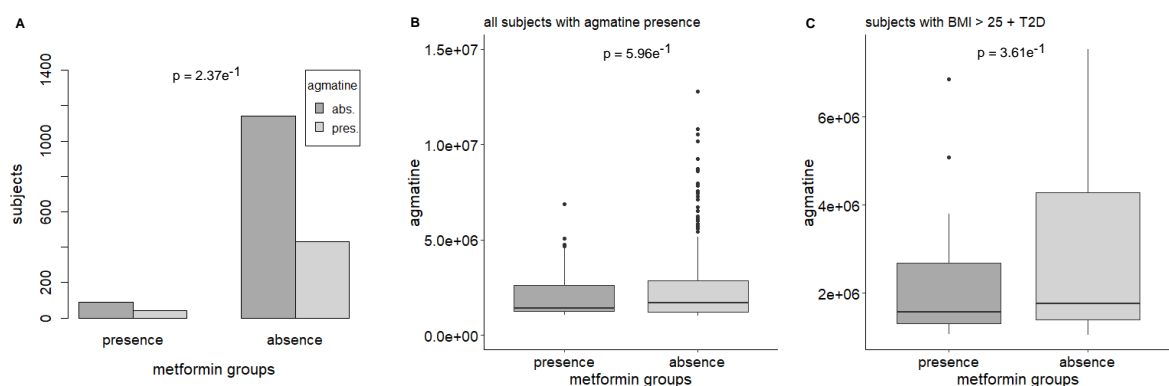


Figure 21: (A) Differences in prevalence of agmatine absence and agmatine presence in metformin presence and metformin absence, (B) Differences in metformin presence and metformin absence regarding agmatine intensity, (C) Differences in metformin presence and metformin absence regarding agmatine intensity in subjects with BMI > 25 kg/m^2 and type 2 diabetes

(A) χ^2 -test was used to determine group differences for categorical parameter. Nominal p-value was displayed. Statistical significance was set at $p < 0.05$. (B, C) Wilcoxon-rank sum test was used to determine between group differences for continuous parameter. Nominal p-value was displayed. Statistical significance was set at $p < 0.05$. (B) Statistical analysis included $n=473$ subjects. (C) Statistical analysis includes $n=69$ subjects.

4.3.3 Agmatine and gut microbiomics

For microbiome analysis we made use of ASV data from 16S rRNA gene sequencing of $n=1,335$ subjects. A comparison of agmatine groups with the general microbiome composition revealed significant differences in β -diversity measures (Permanova: Bray

Curtis distance: $p = 2.0e^{-3}$, Jaccard index: $p = 9.0e^{-4}$ (fig. 22A) (fig. 23A). P-values remained consistent although confounder such as gender, age, metformin and BMI were included in the model (fig. 22B, 23B).

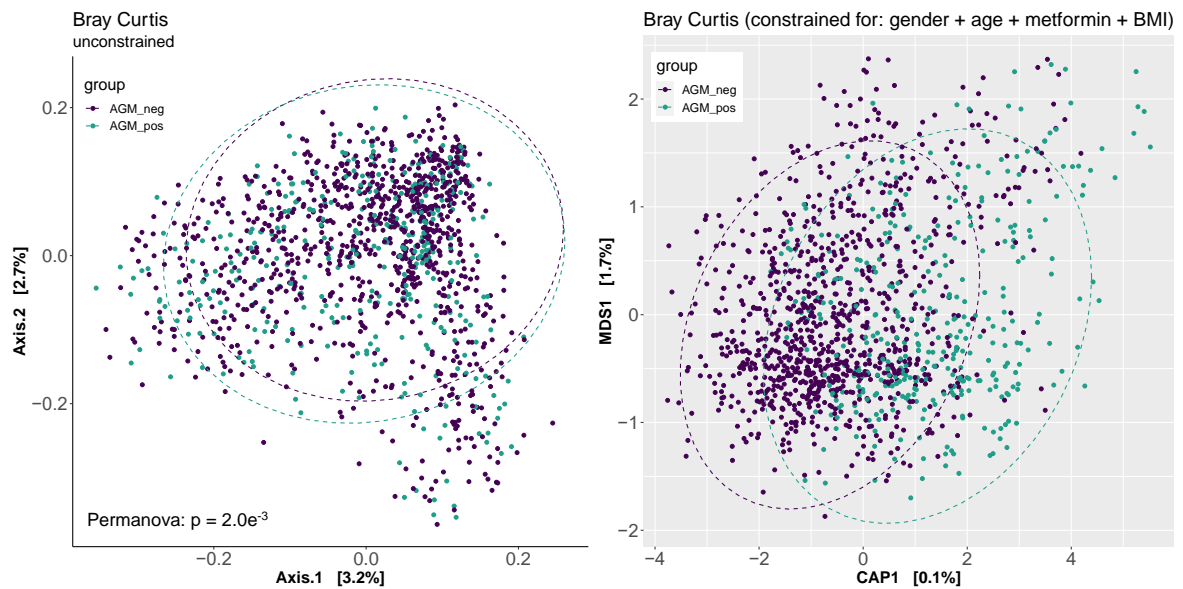


Figure 22: Bray Curtis distance of agmatine groups and general microbiome composition without confounders (A) and with confounders (B).

β -diversity in subjects with agmatine absence (AGM_neg) and agmatine presence (AGM_pos) without confounders (A) and with confounders (B) such as gender, age, metformin and BMI. Statistical significance was set at $p < 0.05$. Abbreviations: BMI: body mass index.

Results

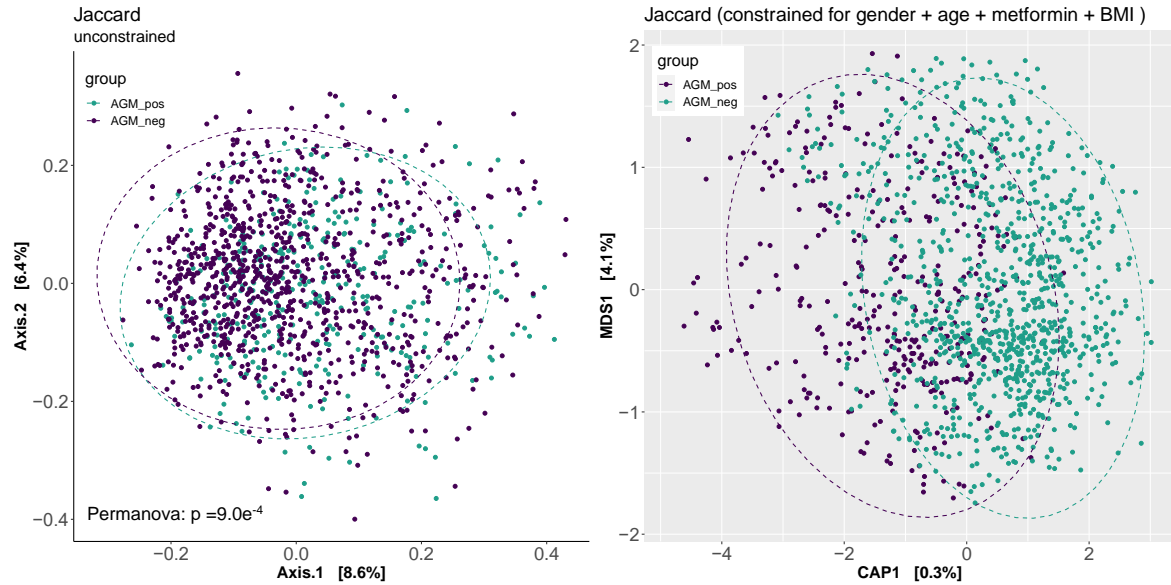


Figure 23: Jaccard index of agmatine groups and general microbiome composition without confounders (A) and with confounders (B).

β -diversity in subjects with agmatine absence (AGM_neg) and agmatine presence (AGM_pos) without confounders (A) and with confounders (B) such as gender, age, metformin and BMI. Statistical significance was set at $p < 0.05$. Abbreviations: BMI: body mass index.

Moreover, α -diversity was significantly reduced in subjects with agmatine presence (Wilcoxon-rank sum test, $p = 3.0e^{-3}$) solely according to the Shannon Index. No significant results were obtained for Chao1 or Species Richness ($p = 5.4e^{-1}$, $p = 5.4e^{-1}$) (fig. 24). The Shannon Index remained consistent if confounders such as gender, age, metformin and BMI were added to the model.

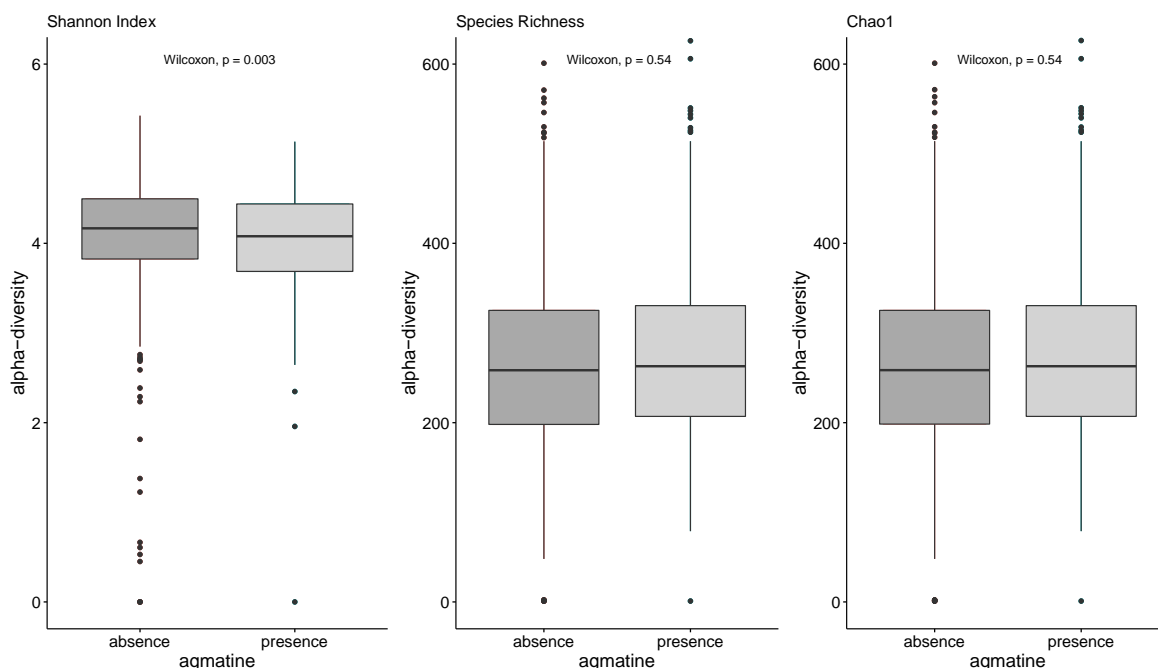


Figure 24: α -diversity in subjects with absence or presence of agmatine regarding Shannon Index (A), Species Richness (B) and Chao1 (C).

Wilcoxon signed-rank test was used to show differences in α -diversity through three indices in subjects with absence or presence of agmatine. Statistical significance was set at $p < 0.05$.

We then looked at the particular ASVs, which were part of the core measurable microbiome in order to investigate which ASVs are responsible for the difference in clustering of the two groups agmatine absence and agmatine presence (tab. 32). *Bacteroides* ($p = 3.17e^{-2}$) and *Bacteroides vulgatus* ($p = 5.1e^{-2}$) were appointed to make the difference. When confounders such as gender, age, metformin and BMI were added, the effect diminished.

Table 32: ASVs, which imply the most difference between clustering of the two groups agmatine absence and agmatine presence

ASV	p	p-adjusted
1 [<i>Bacteroides</i>]	$8.57e^{-4}$	$3.17e^{-2}$
14 [<i>Bacteroides vulgatus</i>]	$2.8e^{-3}$	$5.1e^{-2}$

Association of ASVs and agmatine absence and agmatine presence tested with a two-part hurdle model only displaying the count part here. Results were reported through p-value, and p-adjusted according to FDR-correction. Statistical significance was set at $p < 0.05$. Abbreviations: ASVs: amplicon sequence variants.

Results

We further specified the core measurable microbiome and found that it consists of 49 taxa for both groups (agmatine absence and agmatine presence). There were 44 taxa for subjects with agmatine absence and 44 taxa for subjects with agmatine presence. Figure 25 shows the distribution whereby both groups have 5 taxa individually.

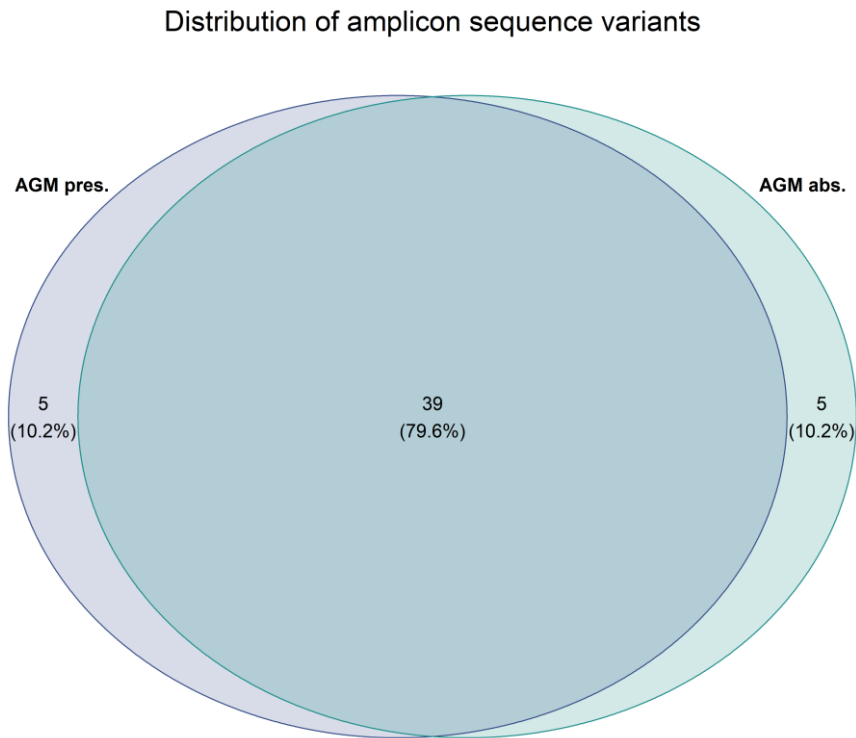


Figure 25: Venn diagram shows the distribution of taxa in agmatine absence and agmatine presence of the core measurable microbiome

Clustering of taxa in agmatine absence (AGM abs.) and agmatine presence (AGM pres.) as well as shared taxa in total numbers and percentages in brackets. Abbreviations: AGM pres.: agmatine presence; AGM abs.: agmatine absence.

Lastly, we calculated the relative distribution of bacterial families (fig. 26) as well as bacterial genus (fig. 27) for each group of agmatine absence and agmatine presence (composition plots). We observed that the most obvious difference between both groups was the family of Bacteroidaceae and the genus of *Bacteroides*.

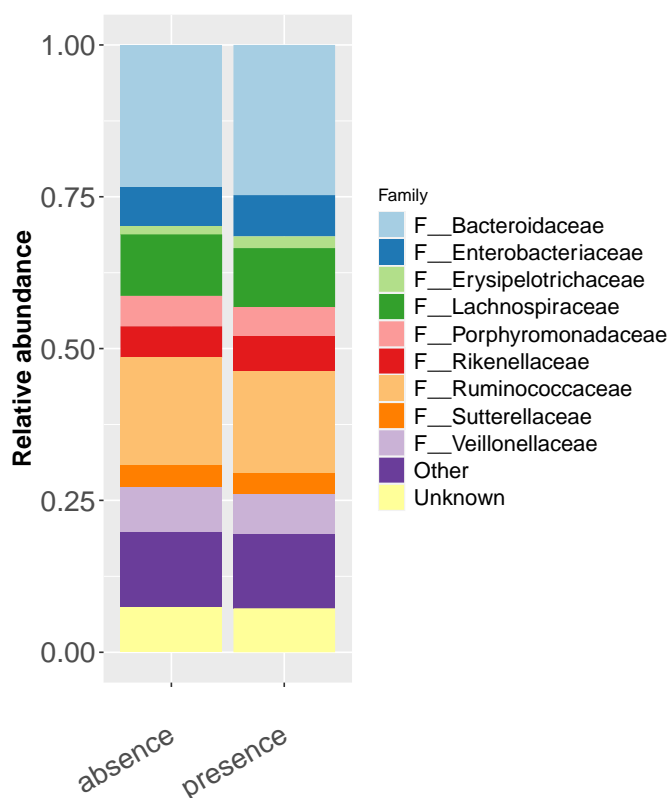


Figure 26: Distribution of bacterial families in groups of agmatine absence and agmatine presence

Clustering of the relative abundance of bacterial families in agmatine absence (AGM_neg) and agmatine presence (AGM_pos) to a sum of 1.

Results

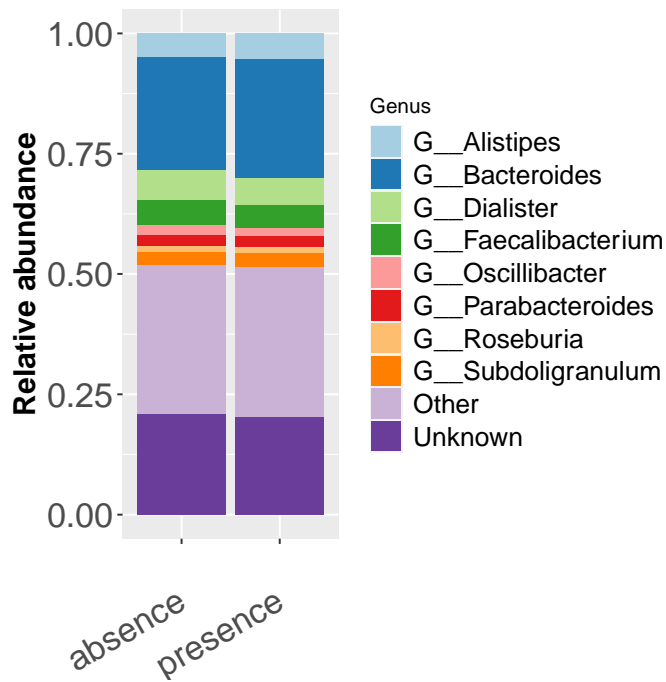


Figure 27: Distribution of bacterial genus in groups of agmatine absence and agmatine presence

Clustering of the relative abundance of bacterial genus in agmatine absence (AGM_neg) and agmatine presence (AGM_pos) to a sum of 1.

4.3.4 Agmatine and host genomics

Regarding genomic analysis, we performed a GWAS for $n=1,486$ subjects. In the logistic model, that included agmatine presence and agmatine absence in association to 937,641 SNPs, covariates such as BMI and age were also included. There was no SNP genome-wide significantly associated with agmatine absence/agmatine presence. A few SNPs were suggestively significant at a threshold of $p < 0.00001$ (chr18:61264298, chr10:99214761, chr18:61261540) (fig. 28). Q-Q-plot displayed p-values included in the analysis (suppl. fig. 5).

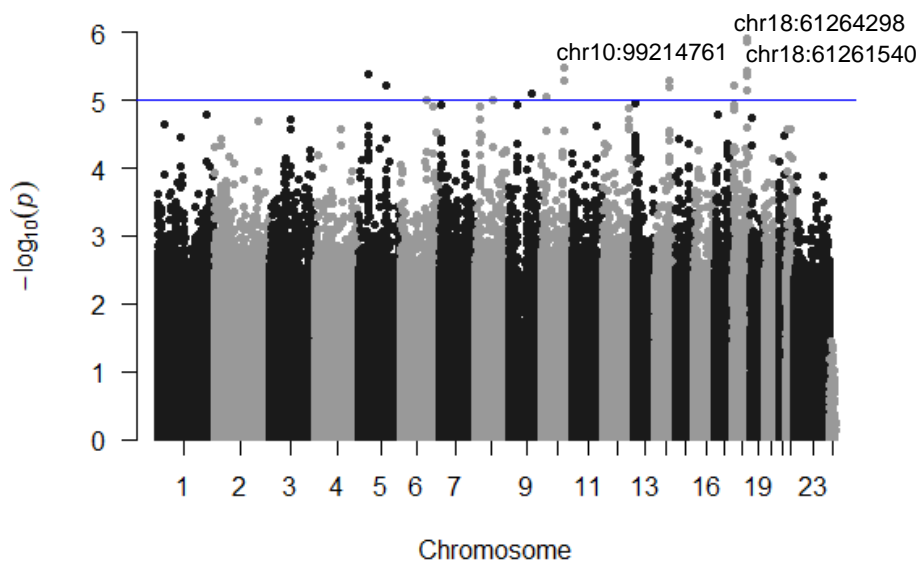


Figure 28: Association of agmatine and SNPs (logistic model) of n=1,486 subjects

Manhattan plot showed no genome wide association of SNPs with agmatine absence/agmatine presence. A logistic regression model including n=1,486 subjects and 937,641 SNPs as well as BMI and age as covariates was used. The blue line typifies a suggestive threshold of $p < 1 \times 10^{-5}$. The x-axis shows autosomal chromosomes. The y-axis shows negative logarithm of p-values ($-\log_{10}(p)$).

Further, we associated the continuous variable of agmatine (n=410), that was previously log-transformed, with SNPs (covariates BMI and age). Also, we found no SNP genome-wide significant. A few SNPs were suggestively significant at a threshold of $p < 0.00001$ (chr13:107486592, chr14:39818591, chr14:92974354) (fig. 29).

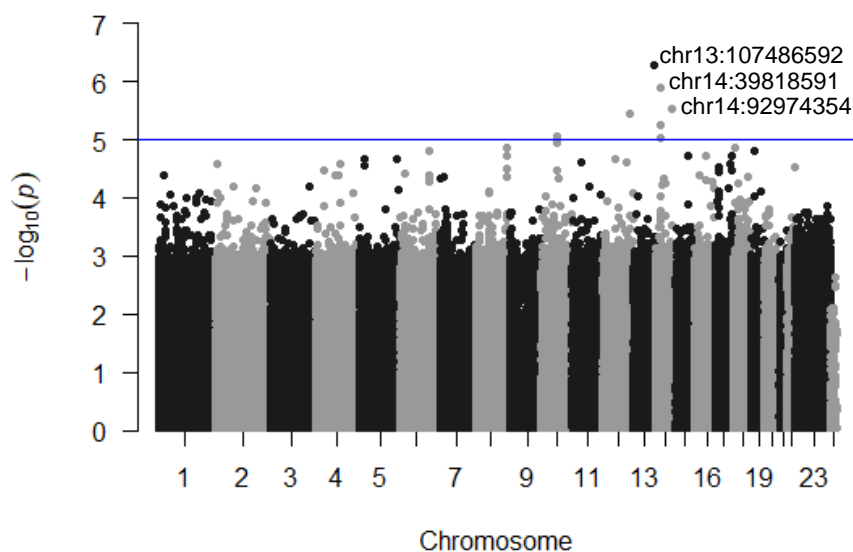


Figure 29: Association of agmatine and SNPs (log-transformed, linear model) of n=410 subjects

Manhattan plot showed no genome wide association of SNPs with agmatine absence/agmatine presence. A linear regression model including n=410 subjects as well as BMI and age as covariates was used. The blue line typifies a suggestive threshold of $p < 1 \times 10^{-5}$. The x-axis shows autosomal chromosomes. The y-axis shows negative logarithm of p-values ($-\log_{10}(p)$).

4.3.5 Agmatine and host urine metabolomics

Urine metabolomics data were available of n=973 subjects of the FoCus cohort, consisting of n=12 detectable positively ionized metabolites. In a first hurdle model, where we tested continuous agmatine with positively ionized metabolites, we found pyrroline carboxylate significantly associated with agmatine (-2.82×10^{-2} , $p = 7.19 \times 10^{-3}$) (tab. 33) in the zero part. In a second hurdle model, where we additionally included gender, age and BMI as covariates, we were able to determine proline (-3.61×10^{-2} , $p = 5.0 \times 10^{-4}$), arginine (-4.04×10^{-2} , $p = 6.0 \times 10^{-4}$) and again pyrroline carboxylate (-2.76×10^{-2} , $p = 1.01 \times 10^{-2}$) as significantly associated with agmatine (tab. 33) in the zero part. For n=3 detectable negatively ionized metabolites of n=973 subjects we found no significant associations with continuous agmatine.

Table 33: Association of agmatine and positively ionized urine metabolites

parameter	confounder	model	estimate	p	significance	p-adjusted
Agm ~ X1.Pyrroline.5. carboxylate	-	count	-8.81e ⁻⁵	9.64e ⁻¹		9.8e ⁻¹
		zero	-2.82e ⁻²	1.79e ⁻³	**	7.19e ⁻³
Agm ~ Proline	gender, age, BMI	count	4.5e ⁻⁴	8.15e ⁻¹		9.92e ⁻¹
		zero	-3.61e ⁻²	4.0e ⁻⁵	***	5.0e ⁻⁴
Agm ~ Arginine	gender, age, BMI	count	3.0e ⁻⁴	8.73e ⁻¹		
		zero	-4.04e ⁻²	1.0e ⁻⁴	***	6.0e ⁻⁴
Agm ~ X1.Pyrroline.5.c arboxylate	gender, age, BMI	count	-1.0e ⁻⁵	9.92e ⁻¹		9.92e ⁻¹
		zero	-2.76e ⁻²	2.53e ⁻³	**	1.01e ⁻²

Association of positive urine metabolites and agmatine tested with a two-part hurdle model consisting of count and zero part. Confounder such as gender, age and BMI were included. Results were reported through estimate, p-value, significance level and p-adjusted according to FDR-correction in the respective part. Statistical significance was set at $p < 0.05$. Abbreviations: BMI: body mass index; Agm: agmatine.

We then investigated if there is an association of agmatine absence or agmatine presence regarding n=12 detectable positively ionized metabolites in a binomial logistic regression model. It turned out that agmatine absence/agmatine presence was associated with arginine ($-4.04e^{-2}$, $p = 1.15e^{-3}$), proline ($-3.74e^{-2}$, $p = 1.99e^{-4}$) and pyrroline carboxylate ($-2.8e^{-2}$, $p = 2.16e^{-2}$) (tab. 34). After adding gender, age and BMI as covariates to the model the three metabolites remained significant ($p = 1.3e^{-3}$, $p = 5.02e^{-4}$, $p = 3.04e^{-2}$). For n=3 detectable negative metabolites of n=973 subjects we found no significant associations with agmatine absence/agmatine presence.

Results

Table 34: Association of agmatine absence/agmatine presence and positively ionized urine metabolites

parameter	confounder	model	coefficient	p	significance	p-adjusted
Agm group ~ Arginine	-	glm	-4.04e ⁻²	9.57e ⁻⁵	***	1.15e ⁻³
Agm group ~ Proline	-	glm	-3.74e ⁻²	1.66e ⁻⁵	***	1.99e ⁻⁴
Agm group ~ X1.Pyrroline.5. carboxylate	-	glm	-2.82e ⁻²	1.8e ⁻³	***	2.16e ⁻²
Agm group ~ N1_Acetylspermidine__N8_Acetylspermidine	-	glm	-3.81e ⁻²	2.07e ⁻²	*	2.48e ⁻¹
Agm group ~ Creatinine	-	glm	-1.85e ⁻¹	3.76e ⁻²	*	4.51e ⁻¹
Agm group ~ L.Glutamate.5. semialdehyde	-	glm	-1.97e ⁻²	4.6e ⁻²	*	5.52e ⁻¹
Agm group ~ Arginine	gender, age, BMI	glm	-4.04e ⁻²	1.1e ⁻⁴	***	1.32e ⁻³
Agm group ~ Proline	gender, age, BMI	glm	-3.61e ⁻²	4.18e ⁻⁵	***	5.02e ⁻⁴
Agm group ~ X1.Pyrroline.5. carboxylate	gender, age, BMI	glm	-2.76e ⁻²	2.53e ⁻³	**	3.04e ⁻²
Agm group ~ N1_Acetylspermidine__N8_Acetylspermidine	gender, age, BMI	glm	-3.65e ⁻²	2.79e ⁻²	*	3.35e ⁻¹
Agm group ~ L.Glutamate.5. semialdehyde	gender, age, BMI	glm	-2.24e ⁻²	2.72e ⁻²	*	3.26e ⁻¹

Association of positive urine metabolites and agmatine absence/agmatine presence tested with a binomial logistic regression model. Confounder such as gender, age and BMI were included. Results were reported through coefficient, p-value, significance level and p-adjusted according to FDR-correction in the respective part. Statistical significance was set at $p < 0.05$. Abbreviations: BMI: body mass index; Agm group: agmatine group; glm: general logistic model.

4.3.6 Agmatine and functional effects on mouse adipocytes

In a viability assay (n=3) we investigated if 1mM agmatine might have apoptotic effects on mouse pre-adipocytes. We showed that 1mM agmatine has positive effects on cell viability in comparison to PBS-control and was significantly elevated in comparison to EtOH ($p = 1.0e^{-3}$) (overall test: Kruskal-Wallis, $p = 6.09e^{-3}$) (fig. 30). Therefore, we used a concentration of agmatine up to 1mM in the following experiments.

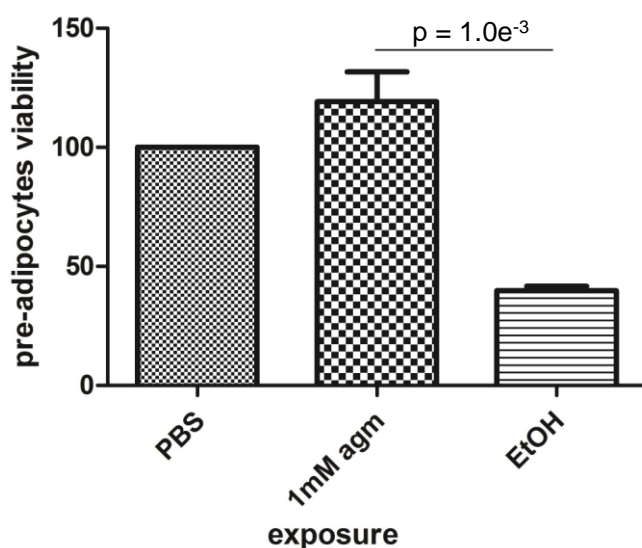


Figure 30: Viability of mouse pre-adipocytes with exposure of agmatine

Viability assay in undifferentiated 3T3-L1 cells treated with either PBS (negative control), 1mM agmatine or EtOH (positive control) with an incubation period of 24h. Kruskal-Wallis test and Dunn's Post-hoc test were used to determine differences between groups. Abbreviations: PBS: phosphate buffered saline; agm: agmatine; EtOH: ethanol.

In differentiated 3T3-L1 cells (adipocytes), we found with addition of either 100μM or 500μM agmatine that ppar-γ was decreased in both stimulations compared to PBS-control

Results

($p = 3.23e^{-2}$, $p = 2.5e^{-3}$) (overall test: ANOVA, $p = 9.45e^{-4}$). Undifferentiated cells were included to prove that the three weeks differentiation protocol succeeded for all stimulations (fig. 31).

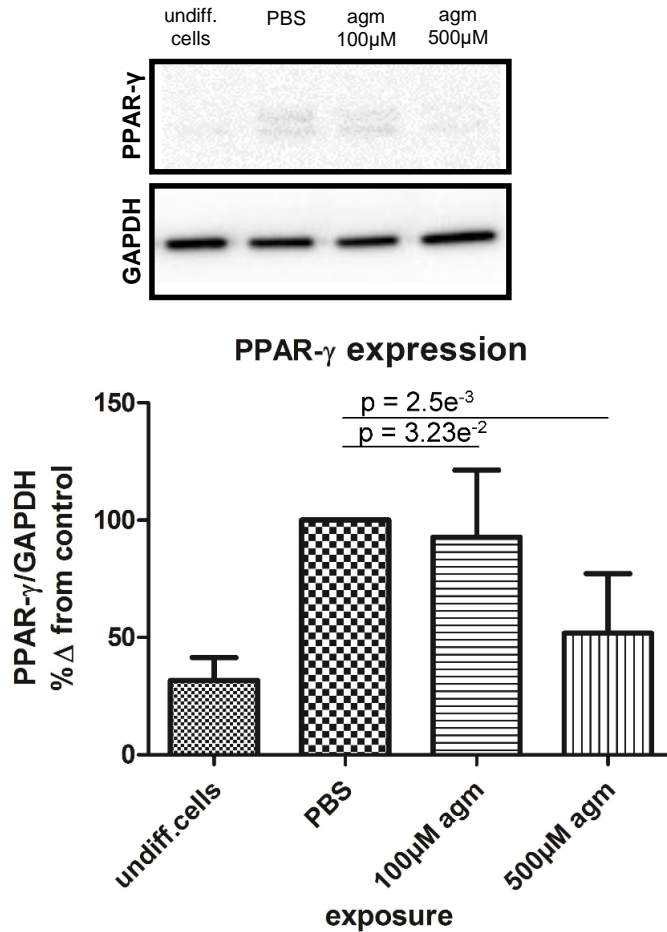


Figure 31: Expression of PPAR- γ in mouse adipocytes

Western blot of PPAR- γ expression in undifferentiated 3T3-L1 cells, differentiated 3T3-L1 cells treated with PBS or 100 μ M agm or 500 μ M agm with an incubation period of eight days. One-way ANOVA and Dunnett's Post-hoc test were used to determine differences between groups. Abbreviations: PBS: phosphate buffered saline; agm: agmatine; undiff. cells: undifferentiated cells; PPAR- γ : peroxisome-proliferator-activated receptor gamma; GAPDH: glyceraldehyd-3-phosphat-dehydrogenase.

We also investigated the expression of FABP4 when exposing adipocytes to either 100 μ M or 500 μ M agmatine. We calculated increased FABP4 expression in 500 μ M agmatine stimulation in comparison to PBS-control ($p = 2.48e^{-2}$), (overall test: Kruskal-Wallis, $p = 3.41e^{-2}$) (fig. 32).

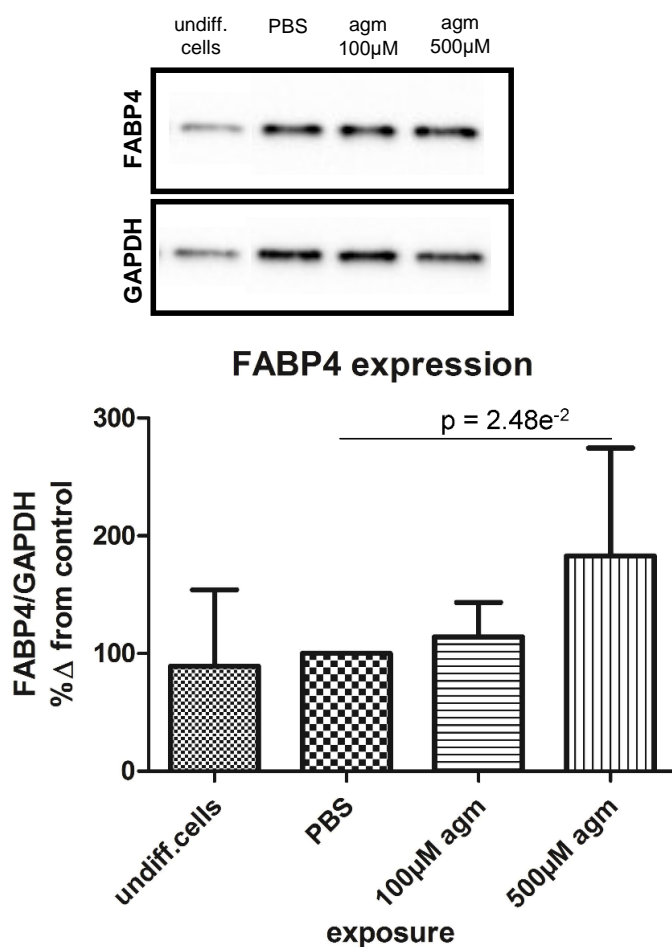


Figure 32: Expression of FABP4 in mouse adipocytes

Western blot of FABP4 expression in undifferentiated 3T3-L1 cells, differentiated 3T3-L1 cells treated with PBS or 100µM agm or 500µM agm with an incubation period of eight days. Kruskal-Wallis test and Dunn's Post-hoc test were used to determine differences between groups. Abbreviations: PBS: phosphate buffered saline; agm: agmatine; undiff. cells: undifferentiated cells; FABP4: fatty acid-binding protein 4; GAPDH: glyceraldehyd-3-phosphat-dehydrogenase.

4.3.7 Agmatine and functional effects on human gut epithelial cells

Firstly, we did pre-experiments and cultured CaCo-2 cells for three days using a concentration of 1mM agmatine. For time-response experiments we used TNF- α stimulation and various incubations of agmatine ranging from 0.25h until 2h. There was no difference between groups in the expression of either zonula occludens 2 (ZO-2) (fig. 33A) or claudin 3 (fig. 33B) compared to control (+TNF- α) (overall test: ANOVA, $p = 3.12e^{-1}$, $p = 9.72e^{-1}$).

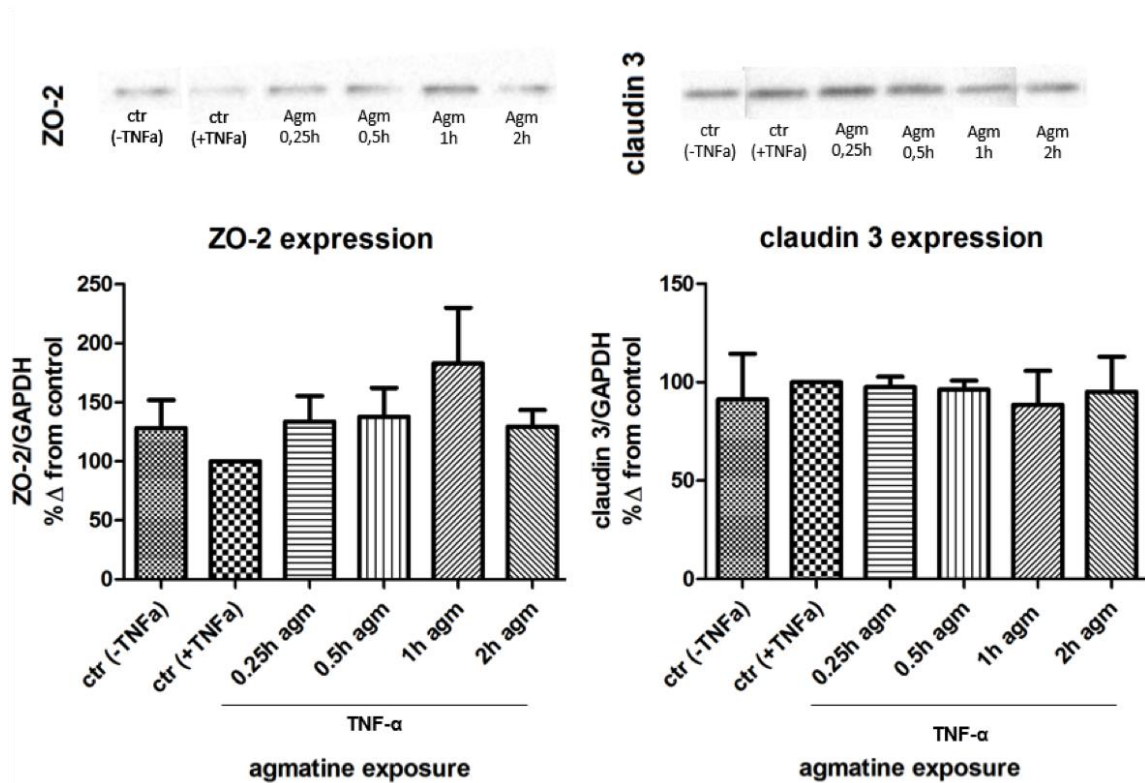


Figure 33: Expression of ZO-2 (A) and claudin 3 (B) with TNF- α stimulation in human gut epithelial cells

Western blot of (A) ZO-2 expression in three days cultured Caco-2 cells treated with ctr (PBS without TNF- α), ctr (PBS with TNF- α), or TNF- α and 1mM agmatine with varying incubation periods of 0.25h, 0.5h, 1h or 2h and (B) claudin 3 expression in three days cultured Caco-2 cells treated with ctr (PBS without TNF- α), ctr (PBS with TNF- α), or TNF- α and 1mM agmatine with varying incubation periods of 0.25h, 0.5h, 1h or 2h. One-way ANOVA and Dunnett's Post-hoc test were used to determine differences between groups. Abbreviations: ctr: control; agm: agmatine; ZO-2: zonula occludens-2; GAPDH: glycerinaldehyd-3-phosphat-dehydrogenase.

We then repeated the experiment without TNF- α stimulation but there was solely one difference between incubation of 0.5h of agmatine and PBS-control ($p = 3.93e^{-2}$). There was no difference between all other groups compared to control in the expression of ZO-2 and claudin 3 (overall test: ANOVA, $p = 3.31e^{-1}$, $p = 8.79e^{-1}$) (fig. 34).

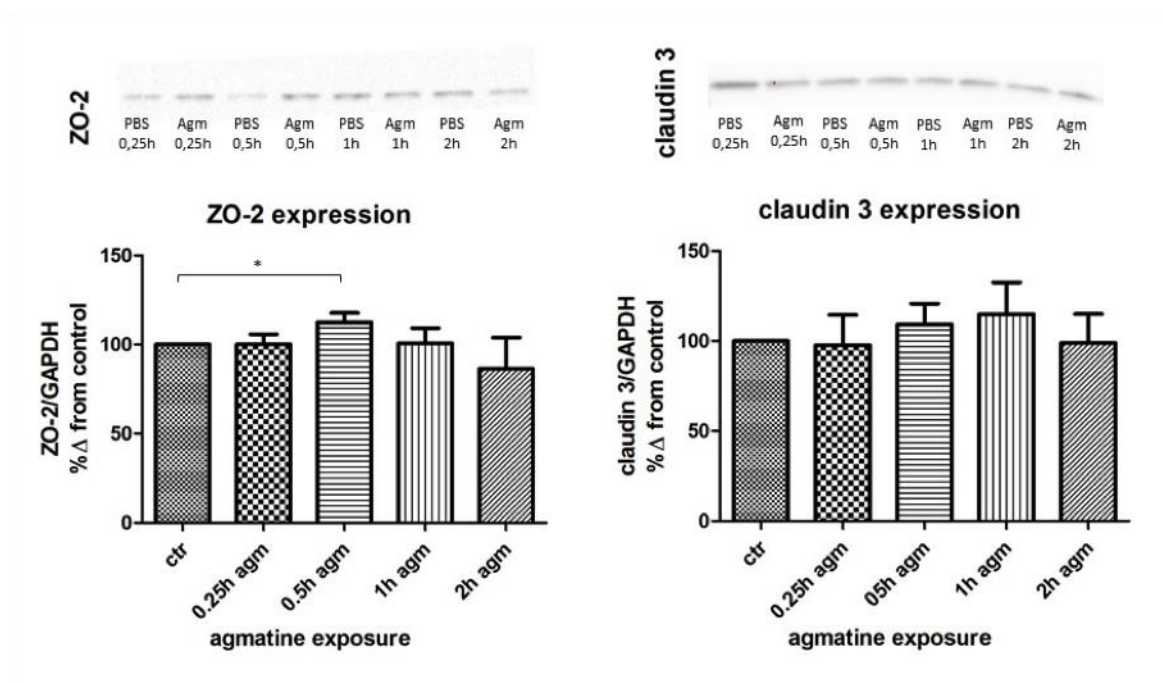


Figure 34: Expression of ZO-2 (A) and claudin 3 (B) without TNF- α stimulation in human gut epithelial cells

Western blot of (A) ZO-2 expression in three days cultured Caco-2 cells treated with ctr (PBS) or 1mM agmatine with varying incubation periods of 0.25h, 0.5h, 1h or 2h and (B) claudin 3 expression in three days cultured Caco-2 cells treated with ctr (PBS) or 1mM agmatine with varying incubation periods of 0.25h, 0.5h, 1h or 2h. One-way ANOVA and Dunnett's Post-hoc test were used to determine differences between groups. * $p < 0.05$. Abbreviations: ctr: control; agm: agmatine; ZO-2: zonula occludens-2; GAPDH: glyceraldehyd-3-phosphat-dehydrogenase.

Regarding the time-response and dose-response experiment with pNF κ B expression, we found that agmatine did not reduce TNF- α induced inflammation in comparison to controls. TNF- α treatment for 24h caused 50-150% increase in pNF κ B (p65) expression in both experiments ($p = 3.0e^{-7}$, $p = 1.0e^{-3}$) (fig. 35). The overall effect of agmatine in both experiments was not significant (overall test: ANOVA: $p = 4.59e^{-1}$, $p = 8.73e^{-1}$).

Results

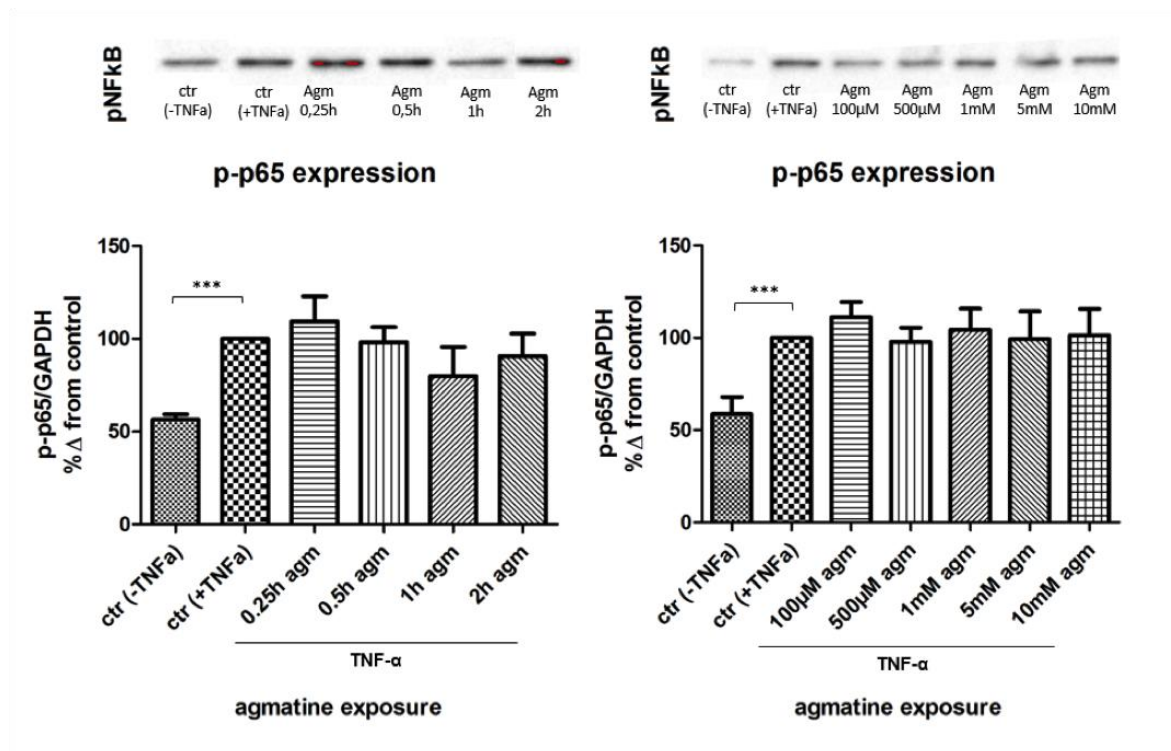


Figure 35: Expression of pNFκB with TNF-α stimulation in human gut epithelial cells

Western blot of (A) pNFκB (p-p65) expression in three days cultured Caco-2 cells treated with ctr (PBS without TNF-α), ctr (PBS with TNF-α), or TNF-α and 1mM agmatine with varying incubation periods of 0.25h, 0.5h, 1h or 2h and (B) pNFκB (p-p65) expression in three days cultured Caco-2 cells treated with ctr (PBS without TNF-α), ctr (PBS with TNF-α), or TNF-α with varying doses of 100μM, 500μM, 1mM, 5mM or 10mM agmatine for an incubation period of 1h. One-way ANOVA and Dunnett's Post-hoc test were used to determine differences between groups. *** $p < 0.001$ Abbreviations: ctr: control; agm: agmatine; pNFκB: phosphorylated NFκB; GAPDH: glyceraldehyde-3-phosphat-dehydrogenase.

Finally, we cultured CaCo-2 cells three weeks in order to obtain fully grown tight junction proteins. Still, we could not show a difference neither between 1mM agmatine stimulation compared with PBS-control ($p = 3.06e^{-1}$) nor between TNF-α and 1mM agmatine stimulated cells compared with TNF-α stimulation ($p = 4.19e^{-1}$). The overall effect of agmatine was not significant (overall test: Kruskal-Wallis, $p = 5.9e^{-1}$) (fig. 36).

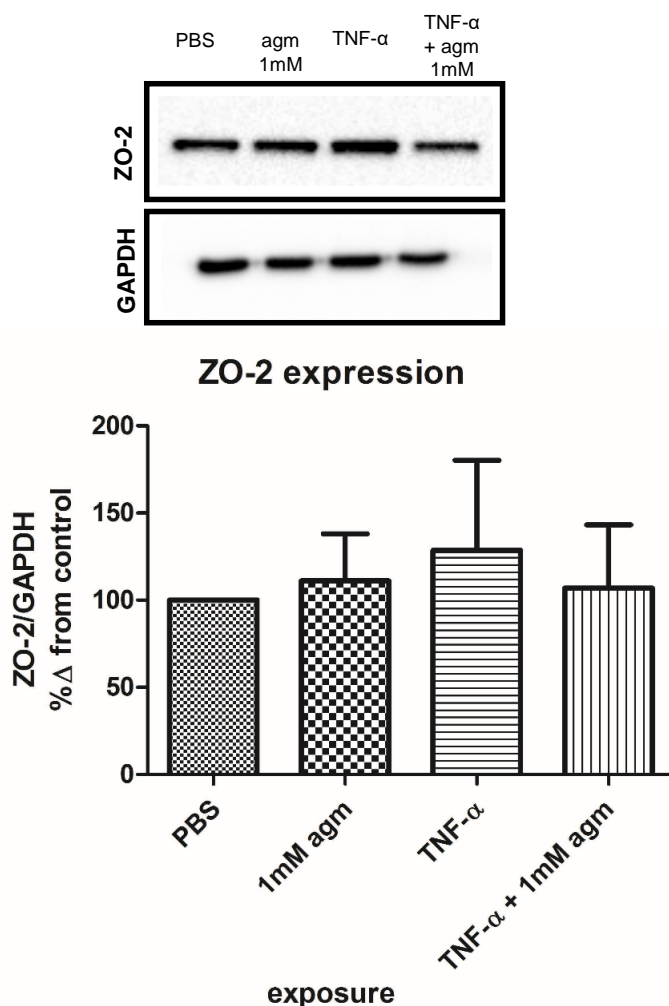


Figure 36: Expression of ZO-2 in human gut epithelial cells differentiated for three weeks

Western blot of ZO-2 expression in three weeks cultured Caco-2 cells treated with PBS, 1mM agmatine, TNF- α or TNF- α and 1mM agmatine with an incubation period of 14 days for agmatine stimulation. Cells were treated with TNF- α 24h before lysis. Kruskal-Wallis test and Wilcoxon-rank sum test were used to determine differences between groups. Abbreviations: PBS: phosphate buffered saline; agm: agmatine; ZO-2: zonula occludens-2; GAPDH: glycerinaldehyd-3-phosphat-dehydrogenase.

4.3.8 Agmatine and functional effects on human hepatocytes

In human hepatocytes, sterol regulatory element-binding protein-1 (SREBP1) expression revealed no significant differences in groups exposed with 500 μ M agmatine in comparison with PBS-control group in a time-response experiment for 0.5h, 1h and 2h incubation (overall test: Kruskal-Wallis, $p = 1.47e^{-1}$). Solely 1h of agmatine incubation in comparison to PBS-control was significant ($p = 2.11e^{-2}$) (fig. 37).

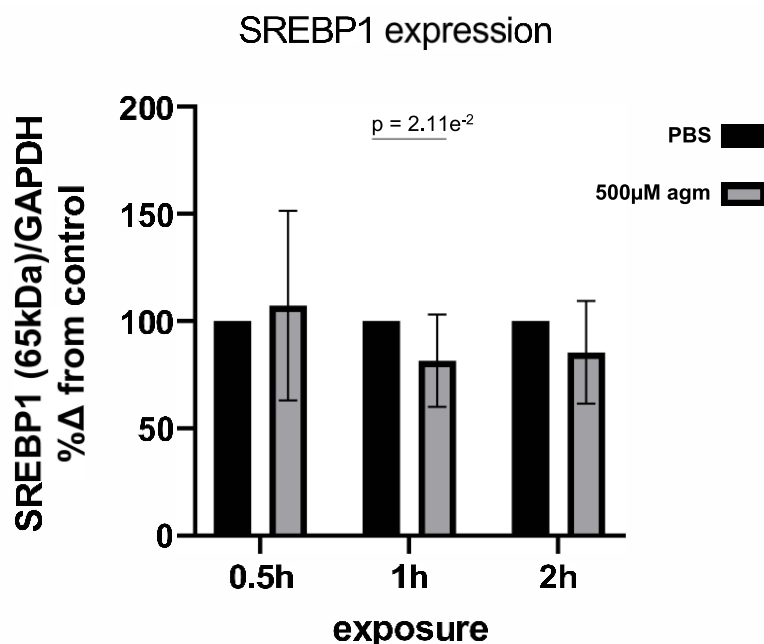


Figure 37: Expression of SREBP1 in human hepatocytes

Western blot of SREBP1 expression in three days cultured HEP-G2 cells treated with either PBS or 500μM agmatine with varying incubation periods of 0.5h, 1h or 2h. Kruskal-Wallis test and Wilcoxon-rank sum test were used to determine differences between groups. Abbreviations: PBS: phosphate buffered saline; SREBP1: sterol regulatory element-binding protein-1; GAPDH: glycerinaldehyd-3-phosphat-dehydrogenase.

4.3.9 Agmatine and functional effects on human macrophages

In a viability assay (n=4) we found that agmatine stimulation, ranging from 100μM to 10mM, had a positive effect on macrophages up to a concentration of 1mM (viability was nearly 100%) (overall test: Kruskal-Wallis, $p = 8.27e^{-3}$) (fig. 38). Whereby viability of macrophages decreased at a concentration of 5mM to 50% ($p = 4.8e^{-2}$) and at a concentration of 10mM to 25% ($p = 1.0e^{-2}$) in comparison to PBS-control.

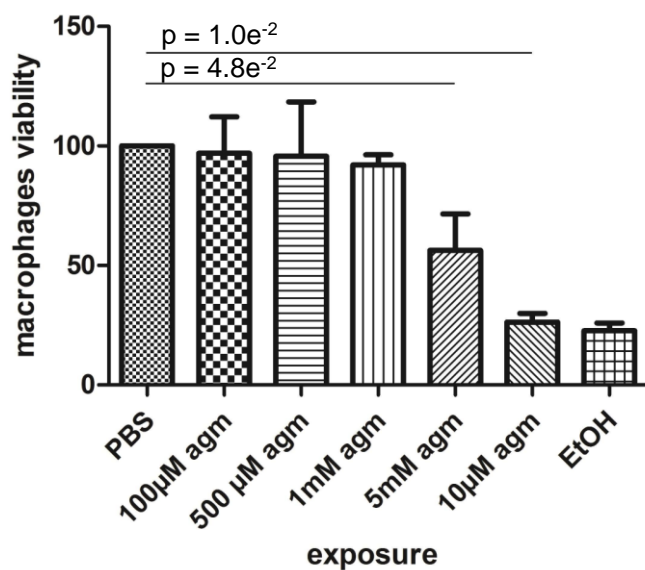


Figure 38: Viability of human macrophages exposed with agmatine

Viability assay in differentiated THP-1 cells treated with either PBS (negative control), varying doses of 100µM, 500µM, 1mM, 5mM, 10mM agmatine or EtOH (positive control) with an incubation period of 24h. Kruskal-Wallis test and Dunn's Post-hoc test were used to determine differences between groups. Abbreviations: PBS: phosphate buffered saline; agm: agmatine; EtOH: ethanol.

We continued to apply dose-response experiments (n=4) and used agmatine concentrations ranging from 100µM to 10mM and a 2h incubation period. There was no difference in the expression of NFκB (p105/p50) between groups and PBS-control (overall test: Kruskal-Wallis, $p = 9.13e^{-2}$) (fig. 39).

Results

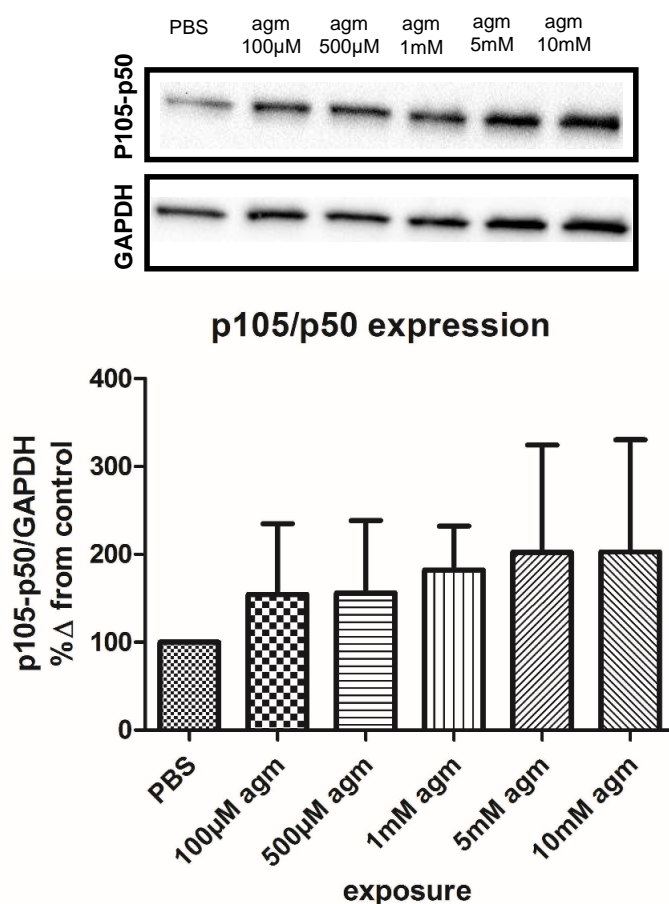


Figure 39: Expression of NFκB (p105/p50) in human macrophages exposed with agmatine for 2h in a dose-response experiment

Western blot of NFκB (p105/p50) expression in differentiated THP-1 cells treated with PBS or varying doses of 100μM, 500μM, 1mM, 5mM or 10mM agmatine for an incubation period of 2h. Kruskal-Wallis test was used to determine differences between groups. Abbreviations: PBS: phosphate buffered saline; agm: agmatine; GAPDH: glycerinaldehyd-3-phosphat-dehydrogenase.

Further, we repeated the same experimental setup (n=4) except of using an incubation period of 4h. We revealed a significant difference in the expression of NFκB (p105/p50) between groups and PBS-control (overall test: Kruskal-Wallis, $p = 2.28e^{-2}$) (fig. 40). Specifically, there was a difference between 1mM agmatine ($p = 2.2e^{-2}$), 5mM agmatine ($5.0e^{-3}$) and 10mM agmatine ($p = 1.5e^{-2}$) each with PBS-control.

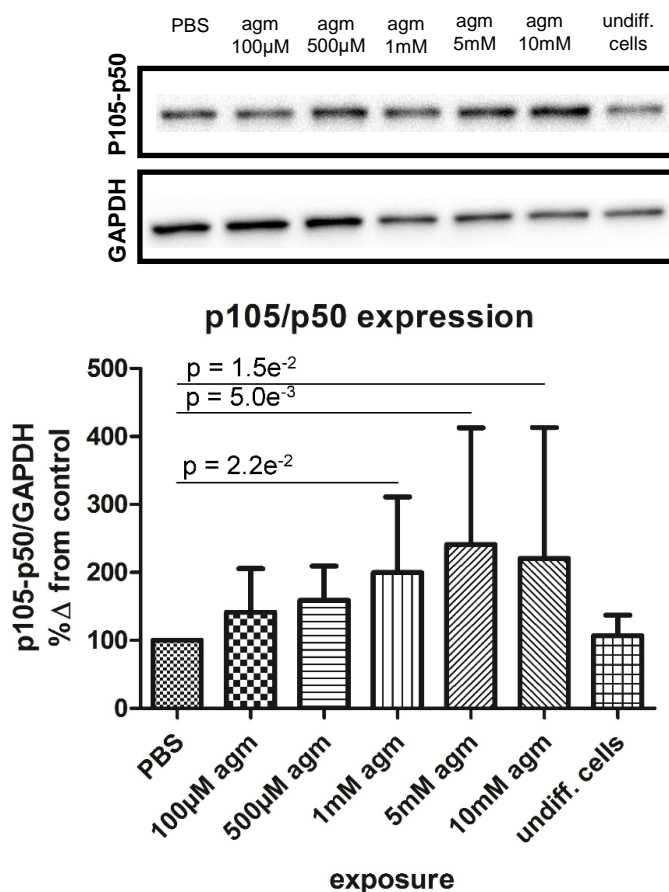


Figure 40: Expression of NF κ B (p105/p50) in human macrophages exposed with agmatine for 4h in a dose-response experiment

Western blot of NF κ B (p105/p50) expression in undifferentiated THP-1 cells, differentiated THP-1 cells treated with PBS or varying doses of 100μM, 500 μM, 1mM, 5mM, 10mM agmatine with an incubation period of 4h. Kruskal-Wallis test and Dunn's Post-hoc test were used to determine differences between groups. Abbreviations: PBS: phosphate buffered saline; agm: agmatine; undiff. cells: undifferentiated cells; GAPDH: glycerinaldehyd-3-phosphat-dehydrogenase.

In a time-response experiment (n=4), we used incubation periods ranging from 0.25h to 2h and a concentration of 1mM agmatine. We found no difference in the expression of NF κ B (p105/p50) between groups compared with PBS-control (overall test: Kruskal-Wallis, $p = 4.61e^{-1}$) (fig. 41).

Results

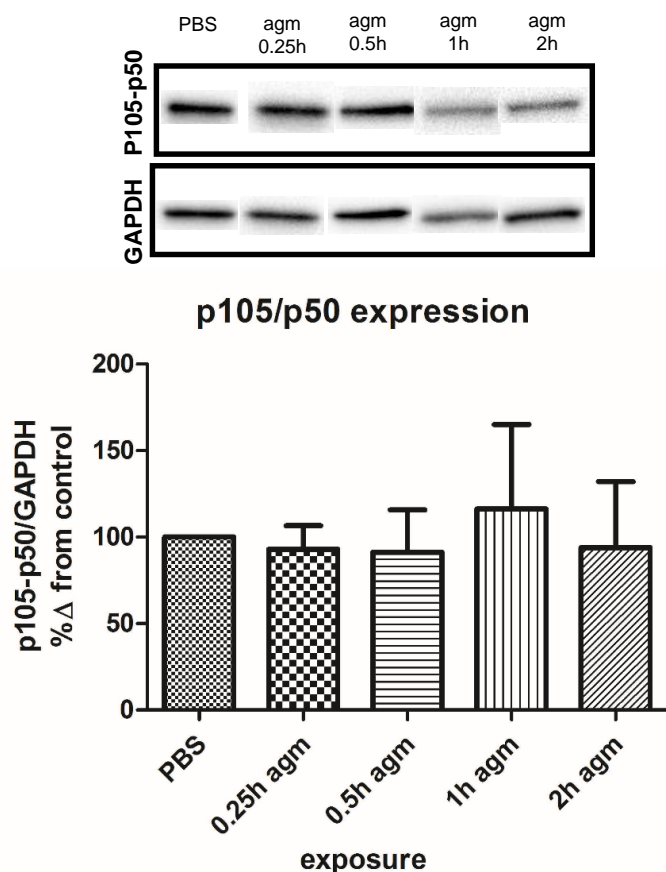


Figure 41: Expression of NFκB (p105/p50) in human macrophages exposed with 1mM agmatine in a time-response experiment

Western blot of NFκB (p105/p50) expression in differentiated THP-1 cells treated with PBS or 1mM agmatine with varying incubation periods of 0.25h, 0.5h, 1h or 2h. Kruskal-Wallis test was used to determine differences between groups. Abbreviations: PBS: phosphate buffered saline; agm: agmatine; GAPDH: glycerinaldehyd-3-phosphat-dehydrogenase.

4.3.10 Agmatine and functional effects on human embryonic kidney cells

Incubation of HEK293 cells with TNF-α for 1h showed a significant elevation of the relative NFκB-promoter activation ($p = 5.42e^{-2}$). While co-incubation of TNF-α and agmatine showed no significant difference to TNF-α stimulated HEK293 cells in the NFκB-promoter activation ($p = 7.34e^{-1}$) (fig. 42). Raw values of $n=3$ independent measurements were displayed in suppl. figure 6.

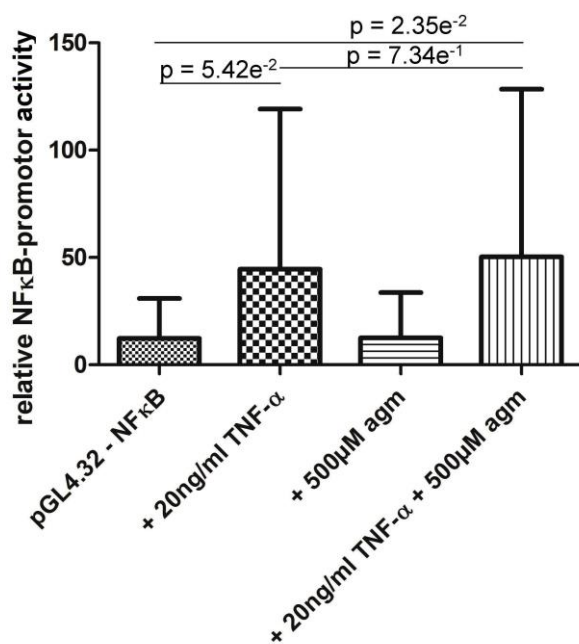


Figure 42: Relative NFκB-promoter activation after an incubation period of 1h with TNF-α, agmatine and TNF-α + agmatine

Kruskal-Wallis test and Dunn's Post-hoc test were used to determine differences between groups.

Abbreviations: agm: agmatine; NFκB: nuclear factor kappa B.

5 Discussion

In the following part, reported results concerning *Parasutterella* and agmatine are compared with and classified to recent findings in the literature. This research suggests a dietary carbohydrate – gut *Parasutterella* – human fatty acid biosynthesis metabolic axis in obesity and type 2 diabetes. Further, it shows potential benefits of agmatine in healthy human obese without low-grade inflammation present, but rather a negative, pro-inflammatory role in vitro.

5.1 *Parasutterella*

In recent years, several studies have investigated the relation of gut microbial composition at the phylum level to obesity and its metabolic co-morbidities. Due to previous findings in various rodent models, we further characterized a specific bacterium, *Parasutterella*, at the genus level using more than 1,500 subjects from the FoCus cohort in Kiel. We observed a positive association between *Parasutterella* abundance and obesity, as well as type 2 diabetes and carbohydrate-rich food intake. Additionally, *Parasutterella* was significantly reduced after a sustained weight loss intervention in subjects with obesity and associated with L-cysteine among other metabolites. Metabolite pathway analysis revealed an enrichment of the fatty acid biosynthesis pathway. For genetic measurements we found no associations of SNPs to *Parasutterella* sp., but in our weight loss intervention *Parasutterella excrementihominis* was reduced after 12 weeks. This indicates that the abundance of *Parasutterella* depends on changes in environmental factors rather than differences in genetic susceptibility loci.

5.1.1 Phenotypes

Our data indicate a positive association between *Parasutterella* and obesity, which we were able to validate in the independent Canadian ATP cohort. These results are in line with research of mechanistic studies in animal models from independent groups. For example, Gu et al. found that *Parasutterella* sp. was significantly enriched in obesity-prone mice in comparison to obesity-resistant mice both fed a HFD (44). Furthermore, bacteria of Proteobacteria phylum, to which *Parasutterella* sp. belongs, are known to be highly abundant in obesity and other metabolic diseases (112)(37). In addition, several authors

classify *Parasutterella* sp. as pro-diabetic in animal studies. For instance, in a study by Cheng et al. the authors reported that mice fed with galacto-oligosaccharides (GOS) exhibit a change in their microbiota with a significant enrichment in *Parasutterella* sp. and at the same time a significantly increased blood glucose level compared to control animals (45). This is in line with our finding that *Parasutterella* sp. is elevated in patients with type 2 diabetes.

Dietary patterns are a key factor in determining gut microbiota composition in humans as well as the pathogenesis of obesity (38). As such, we examined the role of diet in *Parasutterella* sp. abundance. Therefore, in the present analysis we made use of the detailed EPIC dietary data available for all FoCus subjects. Our data indicate that carbohydrate (especially monosaccharides) and ω 3-linolenic acid intake is associated with the abundance of our target bacterium. A higher intake of carbohydrates was associated with a higher abundance of *Parasutterella* sp., whereas a higher intake of linolenic acid was associated with a lower abundance of *Parasutterella* sp. In a previous study using the FoCus cohort, we found that polyunsaturated fatty acids are positively associated with the β -diversity of microbial composition (113). Hence, the negative association of *Parasutterella* with ω 3-linolenic acid fits into the concept that this bacterium is related to negative cardio-vascular effects (114), which are usually associated with a decreased diversity. Additionally, monosaccharides such as sugar, refined grains and corn-derived fructose are known to reduce microbial diversity and increase inflammation (115) which supports our findings that *Parasutterella* sp. was positively associated with the intake of monosaccharides.

In our previous project regarding hypothalamic inflammation we found an association of *Parasutterella* with the MRI density in the hypothalamus in severe obese subjects (30). This is of interest since in the present study *Parasutterella* was associated with obesity and type 2 diabetes, but not with systemic inflammatory markers like IL-6 and CRP in the periphery. As IL-6 and CRP reflect the degree of metabolic inflammation in obesity (116), our data might suggest that *Parasutterella* mediates its negative effects on host glucose metabolism - at least in the periphery - via direct metabolic effects rather by influencing the innate immune system.

5.1.2 Gut microbiomics and host metabolomics

Most research data regarding the role of the gut microbiome in the development of obesity and type 2 diabetes are on phylum level, showing that both diseases are associated with a reduced α - and/or β -diversity. It has to be mentioned that this reduction in diversity

measures is not specific for metabolic diseases but is also found in chronic inflammatory bowel disease (117), chronic heart failure (118) and diverse oncological diseases (119). Thus, from our point of view the present data and the published data on *Akkermansia* indicate that future research should also examine single bacterial genera derived from 16S gene sequencing data that can be used as potential indicators or even pathogenic factors of specific diseases rather than solely rely on phylum data. In addition, the finding of higher *Parasutterella* abundance in obese subjects known to have lower overall diversity might underline the specificity of the novel nutrition-*Parasutterella*-host metabolic axis. Nevertheless, our data shows as well, that subjects with increased *Parasutterella* sp. have higher α -diversity suggesting a diverse bacterial gut composition.

By using our untargeted mass spectrometry metabolomics data set, L-cysteine revealed an inverse association with *Parasutterella* sp. displaying a convincing estimate that underlines the fact that L-cysteine is linked to blood glucose control which was described in the literature (66). Intriguingly, metabolic network modeling revealed *Parasutterella* sp. as a potential top consumer of L-cysteine within the human gut microbiota. Furthermore, a study of Ju et al. investigated mice colonized with *Parasutterella* which had significantly reduced concentrations of taurine (degradation product of cysteine) and NMDA that implies *Parasutterella* to be able to reduce also cysteine associated metabolites (120). So far, it is known that supplementation of L-cysteine improves glycemia and also lowers vascular inflammation in diabetic rodents (66) meaning L-cysteine reveals anti-diabetic characteristics. In rats that were fed a high-sucrose diet and a whey concentrate rich in L-cysteine, data showed that an increase in L-cysteine limited the impairment of glucose homeostasis through lowering oxidative stress (121). As a matter of interest, it is known that pancreatic β -cells are vulnerable to oxidative stress because these cells produce high amounts of reactive oxygen species (ROS) and express low amounts of anti-oxidative enzymes (122). Since we found that *Parasutterella* is associated with type 2 diabetes but not with (BMI-independent) measures of insulin resistance, this finding might point towards abnormalities in insulin secretion due to *Parasutterella* promoting type 2 diabetes development.

The metabolite 19,20-DiHDPA was also inversely associated with *Parasutterella* sp. in our data. This metabolite originates of the polyunsaturated fatty acid docosahexaenoic acid, which is part of the ω -3 fatty acids (123). Studies postulate that elevated 19,20-DiHDPA is associated with inflammatory tissue as well as lipid peroxidation reduction. Since levels of 19,20-DiHDPA are reduced in obese subjects with increased *Parasutterella* sp., this would fit into the context while low-grade inflammation is commonly related to obesity.

In a second analysis we examined the enrichment of metabolic sets and found an association of *Parasutterella* sp. abundance with the fatty acid biosynthesis pathway. This

finding falls in line with the fact that elevated BMI and body weight linked to an obese phenotype has elevated fatty acid biosynthesis systemically. Of interest, it is known that *Parasutterella secunda* does not produce significant amounts of SCFA (46) and *Parasutterella excrementihominis* produces only traces of propionate (47). Since SCFA are known to inhibit human fatty acid biosynthesis and induce human fatty acid oxidation, this might suggest a mechanism on how *Parasutterella* induces human fatty acid biosynthesis as has been found in our analysis.

5.1.3 Genetics

Scientific studies postulate that the composition of the human gut microbiota is mostly influenced by environmental factors (12). However, studies showed variations in the vitamin D receptor locus (113) influencing the gut microbiome and in the pro-opiomelanocortin (POMC) locus (124) to be associated with weight dysregulation. In order to get a broader view, we also included a genetic analysis and decided to test all SNPs for associations with *Parasutterella* sp., but did not find any genome-wide significant SNPs. Taken into consideration as a whole, our data suggests that *Parasutterella* sp. abundance is rather related to environmental compared to host genetic factors and might be targeted through e.g. nutrition as a potential regulator.

5.1.4 Translation to a human intervention study

Biostatistical data revealed a multi-layer interpretation so far, but we also aimed to prove that *Parasutterella* can be measured experimentally via qPCR in the course of a dietary change in humans. We found a reduction of *Parasutterella excrementihominis* after 12 weeks of weight loss intervention accompanied by a drop in BMI. Whereas it was already published that during these 12 weeks the overall gut microbiome diversity has changed in comparison to baseline (125). The formula diet used has a low carbohydrate content, which might be highly relevant for the interpretation of the data, since a study found that the plasticity of the gut microbiota after 10 weeks of dietary low carb intervention was increased for very successful dieters (126). In this case, investigating kinetic trends in gut bacterial community showed enhanced variability after a low carb diet compared to our study, which shows one microbe to react significantly to variations in body weight as well. However, another study where obese patients underwent a low carb diet achieved significant weight loss but no effect on the overall microbial structure was investigated after 12 weeks (118). Nevertheless, the authors postulate that the microbiota (especially

increase of *Bacteroidaceae Bacteroides*) before the diet can predict outcomes of individualized weight loss through a prediction model. They specifically put the higher relative abundance of *Porphyromonadaceae Parabacteroides* and *Ruminococcaceae Oscillospira* after the diet into focus, which were positively associated with efficacy of weight loss. Both are known as butyrate producers in the gastrointestinal tract.

A study by Sanchez et al. investigated a specific bacterial family in human faeces before and after a randomised trial of 24 weeks. Subjects supplemented *Lactobacillus rhamnosus* and lost a significant amount of weight as well as fat mass in comparison to the placebo group. Interestingly, *Lachnospiraceae* was increased in faeces of successful subjects which was inversely associated with circulating leptin concentration also found in mice previously (128). This is another good example of integrating the analysis of a particular bacterial family being very specific into a human intervention study.

5.2 Agmatine

Host metabolites became one focus of gut microbiota research since high advanced mass spectrometry measures were improved to specify degradation products of bacteria. We focused on agmatine since a previous study showed promising life-extending effects of agmatine during metformin intake in type 2 diabetes patients bioinformatically (62). For this reason, we concentrated on agmatine intensities in human serum samples of the FoCus cohort in association to phenotypical, urine metabolomics, dietary, microbiomics and genomics data. To sum up, we found that increased agmatine was associated with elevated BMI in human subjects, whereby agmatine was inversely associated with pyrroline carboxylate, arginine and proline in urine. Additionally, the dietary parameter of plant protein was positively associated and maltose as well as lactose was negatively associated with agmatine. Microbiome analysis revealed a difference in agmatine absence and agmatine presence of microbial composition and α -diversity showed at least in the Shannon index a decreased microbial diversity in agmatine presence. *Bacteroides* made the most difference between the two groups, and also the family of *Bacteroidaceae* was enriched in the agmatine presence group. Agmatine in relation to genomic SNPs revealed no association. The second part experimentally elaborated the role of agmatine on different cell types, either mouse or human originated. In mouse adipocytes, the addition of agmatine showed decreased levels of ppar- γ . Whereby in human macrophages agmatine showed activating inflammatory characteristics. In the remaining cell types there was no major effect of agmatine and rather slightly significant differences between groups or small trends seen in the data.

5.2.1 Phenotypes, urine metabolomics and diet

Exploratory univariate analysis of evaluating differences in agmatine absence and presence groups showed that subjects with elevated BMI and waist measure are seen in the agmatine presence group independently of other metabolic and inflammatory parameters. Correlation analysis showed agmatine to be positively correlated to BMI and waist. And lastly, multivariate analysis confirmed agmatine to be robustly associated with BMI. So far, a study by Nissim et al. that included agmatine in drinking water of rats fed a high fat diet showed that metabolic changes, such as decreased fat mass, elevated synthesis and levels of cAMP and increased protein mass, concluded in overall reduced weight gain in comparison to rats without agmatine (129). Since this study reveals contradictory results to ours, it is also worth mentioning that we primarily found agmatine to be elevated in obese female subjects. Agmatine status in serum might also be influenced by hormones, namely leptin, adiponectin, cholesterol and triglycerides that were all decreased in the study mentioned (129). Differential results to ours could be explained by the fact that solely male rats were included in the study and human biostatistical cohort data could differ to rodent data.

For IBD subjects we found significantly less agmatine intensity in serum. In relation to this, a study found that putrescine (degradation product of agmatine) has symbiotic characteristics for the mouse metabolism, which results in reinforcing the mucosal homeostasis in the intestine and suppressing colitis (130). Therefore, this polyamine metabolism might be a promising approach in targeting diseases of the intestinal tract, especially in the colon.

For urine metabolomics, positively ionized metabolites such as pyrroline carboxylate, arginine and proline were inversely associated with agmatine in serum. This might be explained by arginine being a precursor of agmatine and if arginine is less available in the urine, higher levels of agmatine were metabolized beforehand. Agmatine synthesis might be influenced by multiple interactions and intracellular arginine pools (58).

For dietary parameters, agmatine was positively associated with plant protein, which is in accordance with the literature since agmatine can be exogenously attained from e.g. soybeans (131). Further, in concordance with previous results of Pryor et al., we found that elevated levels of maltose and lactose are associated with decreased serum agmatine levels. The authors have confirmed in an in vitro study that the bacterium *E. coli* (in combination with metformin) produces high amounts of agmatine but in case of high sugar levels (e.g. glucose), the association diminished (62). While in this study the intake

of metformin in type 2 diabetes patients revealed even higher levels of agmatine than in obese patients, our investigations showed no such association of metformin and agmatine. The main difference between both research approaches is that Pryor et al. used bioinformatical prediction models whereby agmatine concentration was predicted by the amount of dietary intake, whereas our research is based on agmatine intensity measured in human serum with mass spectrometry.

A long-term case study of the intake of dietary agmatine in humans evaluated the safety circumstances in oral administration of this dietary supplement over 4-5 years (132). Subjects took a relatively high daily dose of 2.67g of agmatine sulphate that was encapsulated in gelatine capsules. No abnormal laboratory blood and urine results have been reported.

5.2.2 Gut microbiomics

While we found an existing dissimilarity between agmatine absence and agmatine presence group in the number of bacterial species, we further looked at the α -diversity to evaluate the intra-individual diversity within each group. The intra-individual diversity was reduced in agmatine presence group, which fits to our phenotypical analysis whereby agmatine intensity was positively associated with increased BMI. Other studies also found slightly decreased intra-individual diversity in diabetes (133) and obesity (134) but authors remain cautious in evaluating results being biological and clinical relevant. *Bacteroides* made the most difference in agmatine absence and agmatine presence group in our data whereby increased *Bacteroides* was abundant in agmatine presence. This makes sense, since *Bacteroides* is a known genus that is able to produce agmatine (62), besides *E. coli*, *Enterobacter* and *Citrobacter* modeled by Pryor et al. Also, Xu et al. indicated that modified *E. coli* is able to produce high amounts of agmatine in fed-batch fermentation in vitro (135). Hence, we can conclude that serum concentration of agmatine in our research is not solely derived from diet but also from microbial bacteria.

Still, we have to admit that the core measurable microbiome consists of 39 common taxa whereby solely 5 taxa each group represents individually. Therefore, nearly 80% of taxa are present in both groups and solely a few taxa make differences. This is in line with the literature, since the gut microbiota consists of six phyla whereby a two phylum system of Firmicutes and Bacteroidetes exists that make up around 90% of the microbial mass (131)(29). Therefore, the first step would be to define those genus as well as species that differ between two habitats, and secondly, the effectiveness of the function of the bacteria e.g. in producing SCFA or other health promoting metabolites would be even more

important. While the shift in the Firmicutes/Bacteroidetes ratio in obesity-related diseases is discussed controversial (137), it should be brought forward to focus on species such as *Akkermansia* or *Lactobacillus* as diagnostic biomarkers in population-specific studies.

5.2.3 Genetics

In order to cover a multi-layer analysis such as in the previous *Parasutterella* topic, we included a genomic analysis of all SNPs in association to agmatine. We found none of the SNPs associated with agmatine. However, a study of Nag et al. identified specific genetic loci associated with metabolites (138). While that study focused on metabolites in saliva, it still proves the relevance of genetic loci in metabolite research. In this study, the *AGMAT* locus was associated with the 4-guandinobutanoate metabolite (part of the agmatine pathway) and was one of the biomarker identified with oral health. Moreover, the presence of other amino acids in serum such as phenylalanine, tyrosine, glutamine and valine have been previously associated with specific genetic loci (130). Metabolites e.g. phenylalanine, tyrosine and valine were associated with type 2 diabetes in a study of n=189 diabetic subjects. Authors suggest to include amino acid profiles in early diabetes development diagnosis (140).

5.2.4 Experimental cell culture models

Viability of macrophages and pre-adipocytes with addition of agmatine

Since the viability assay in THP-1 cells showed negative (toxic) effects of agmatine in concentrations of 5mM and 10mM, we mainly focused on concentrations at 1mM or lower for subsequent experiments. Also, a second viability assay in mouse pre-adipocytes confirmed that a concentration of 1mM agmatine has a positive effect on cell viability. As well we took into account previous experiments in the literature and adapted our concentrations of agmatine accordingly for other cell types used in this research (141)(142).

In vitro, we observed that ppar- γ as an adipogenesis regulator was down regulated in increasing exposure of agmatine. In the human body, ppar- γ is highest in adipocytes and it plays a key role in energy balance and lipid biosynthesis (143). A study in rodents applied a deficiency of the ppar- γ gene in mature adipocytes (144). It was shown that

brown and white adipose mass decreased in those mice. This would be contradicting to our bioinformatical data on phenotypes since agmatine was increased with elevated BMI in subjects. However, translation from rodent to human studies should be handled carefully. Coming back to the cell culture experiment, whereby ppar- γ decreased with addition of agmatine, it is important to mention that in vitro agmatine shows a decrease of the differentiation of pre-adipocytes to adipose cells. This means, that ppar- γ cannot maintain normal organ function in liver and skeletal muscle as well as cannot keep normal functioning of adipose tissue, which might also result in impaired systemic insulin sensitivity (145). Further, free fatty acids reach the blood system and trigger the development of diseases such as liver cirrhosis, type 2 diabetes and dyslipidemia (144). Additionally, normal function of ppar- γ is coupled with lowering fasting triglycerides and NF κ B (146) which will be addressed in one of the next sections. To conclude, regarding this particular cell culture experiment, agmatine shows rather negative metabolic effects in relation to adipose tissue cells.

In human gut epithelial cells we usually found no effect of agmatine on zonula occludens 2 (ZO-2) which is a cytoplasmic protein of tight junctions and is part of the epithelial wall (147). Solely one comparison of 0.5h incubation with agmatine and control showed a significant difference, which should be interpreted with care. It is common ground that when tight junctions are decreased, certain substances can easily enter blood circulation from the intestinal tract that can harm human health (148). We tried to imitate the effect of agmatine on the human intestinal barrier function through either inflamed (+TNF- α) or non-inflamed (-TNF- α) epithelial cells, but found no effect on ZO-2, claudin 3 or pNF κ B. TNF- α besides IL-1 is commonly used in the literature to imitate inflammation of the intestinal wall (149). A study that investigated cyaniding-3-glucoside (antioxidant) found positive and inhibitive effects of NF κ B in Caco-2 cells that were exposed to TNF- α . The nuclear factor erythroid 2-derived-like 2 (NRF2) in the nucleus was increased (150). Authors used the same method as in our research except for using a transwell inserts system, which forms monolayers and formation of tight junctions was evaluated with Trans-Epithelial Electrical Resistance (TEER). In retrospect, this would have been a possible adaption to our research, since after three days of culturing Caco-2, we cannot be sure that tight junctions are fully established. However, even though we added the three weeks differentiation experiment we could not find any effect of agmatine in Caco-2 cells. Hence, we assume that agmatine has rather an effect via the crosstalk of adipose tissue with the blood circulation than locally in the gut through the epithelial wall.

As results indicated, agmatine had no effect on seven days cultured Hep-G2 cells except for a difference in 1h incubation of agmatine compared to control. SREBP1 was

decreased in agmatine treated cells, which could be interpreted as restricted gene transcription. The membrane-bound precursor of 125 kDa SREBP1 is converted into the 65 kDa version which relocates to the nucleus (151). It activates the LDL receptor meaning transcription is decreased like in our results. In mice experiments, effects of agmatine were evaluated as protective and anti-inflammatory in liver injury (152). On the contrary, in rat hepatocytes authors found that agmatine promotes cell apoptosis (153). Since we solely found one effect in hepatocytes, results have to be interpreted with care and subsequent experiments with different doses should be carried out.

In human macrophages, we found no effect of agmatine in the 2h dose-response experiment, but instead there was an increase of NF κ B in 1mM, 5mM and 10mM agmatine in comparison to PBS-control in the 4h dose-response experiment. For the time-response experiment there was no effect of agmatine. Since the viability assay in macrophages showed a rather toxic effect of agmatine in 5mM and 10mM concentrations, we will not further elaborate on the effect of agmatine on NF κ B in these doses since concentrations were chosen too high, which might influence general cell processes enormously. Instead, 1mM agmatine activated NF κ B signalling in macrophages that can be classified as a pro-inflammatory effect. Conversely, in the literature, the agmatine stress response (ASR) is a commonly discussed topic. So far, it is known that agmatine is able to regulate inflammatory processes via iNOS. Inhibition of iNOS is initiated through the conversion of agmatine to an aldehyde by amine oxidase (154)(155). Authors postulate that iNOS is deactivated by agmatine in various tissues and cells in response to stress which was already published in rodent models (156)(75). A study of Chai et al. even found decreasing iNOS in macrophages treated with lipopolysaccharides and agmatine for 24h in vitro (157). Its antioxidant activity against ROS was initiated by the nuclear factor NRF2 activation. Since none of the known receptors that agmatine binds to, have been identified by the authors in the reduction of oxidative stress, there might be different, yet unknown receptors involved in particular in macrophages. Moreover, the precursor of agmatine, L-arginine is known to activate iNOS as showing counteractive effects (158). However, iNOS and NF κ B metabolisms are two biological events but closely related, so data should be interpreted with care, still contradictory to the literature, we found agmatine activating NF κ B in macrophages.

Macrophages are known to be increased in white adipose tissue of obese subjects and contribute to inflammation by expressing high levels of iNOS (159). Since our bioinformatical calculations showed an increase in BMI with elevated agmatine, we would also expect to see clinical inflammatory parameters such as CRP and IL-6 to be increased. Additionally, in a luciferase assay the relative NF κ B-promoter expression might

not be influenced by agmatine either (see following paragraph). Still, in macrophages agmatine had pro-inflammatory effects.

Stimulation of HEK293 cells with pro-inflammatory TNF- α showed an activation of the NF κ B promoter, whereby co-stimulation of TNF- α and agmatine showed no effect. Therefore, in our research, agmatine indicated no activating or inhibiting effect of NF κ B in human embryonic kidney cells. Human embryonic kidney cells are commonly used as a model for new drug discovery and are described as robust and reliable (160).

5.3 Strengths and limitations

Having included a cohort that has over 1,500 subjects incorporated is an enormous advantage. The large sample size is supported by information that enables a multi-layer approach for both research topics. Information on phenotypical as well as dietary data, 16S rRNA sequencing data, genome-wide SNPs and metabolomics in serum and urine was analysed. In addition, we were able to incorporate an international cohort (ATP cohort) to validate the main biostatistical findings of *Parasutterella*. Additionally, we made use of an intervention cohort of 55 subjects that added valuable clinical data while incorporating laboratory functional methods (qPCR). We further added experimental cell culture models as well as a luciferase assay construct in five different cell lines to investigate functional effects of agmatine in vitro. This highly supports the differential view on biological relevance facing bioinformatical cohort measurements.

A limiting factor of the serum metabolomics data of agmatine might be the instable amount of agmatine in human serum with a known half-time-period of less than 10 minutes in mice (161). In our case it represents a steady state but it might fluctuate during the day. Additionally, we cannot distinguish between the amount of agmatine derived from the diet or gut microbiota or specific organ metabolism. Since this is a known problem in human studies, it might be advantageous to investigate agmatine in a rodent model to determine agmatine in various tissues, cells, serum and urine. The half-time-period in tissue is more consistent being 12h available (161). Secondly, regarding dietary intake it has to be mentioned that data relies on a 12-month retrospective food questionnaire that is self-reported and might be underreported by the subjects. We therefore included a variable of either under-, average- or over- reporter as a confounding variable to circumvent this issue. Also, this is why we incorporated solely FoCus dietary intake that was adjusted for energy intake for further calculations. Specifically for the agmatine data, using plant protein and maltose as confounder in our model is controversial. For instance, even though diet is a source of agmatine and is found in plant protein, positive effects can be exerted by agmatine directly instead of total plant protein consumed.

Regarding microbiomics, the 16S rRNA gene sequencing region of the FoCus cohort samples was the V1 V2 region. In most studies, the V3 V4 region is used which is, firstly recommended (162) and, secondly, it might complicate the comparability of our research to other studies (*Parasutterella*). Depending on the sought bacterium, the percentage of the relative abundance of a bacterium can highly differ in V1 V2 compared to V3 V4 region.

There are limitations to the experimental cell culture model insofar that in pre-experiments of Caco-2 cells, tight junctions might not be mature enough in order to respond to agmatine treatment. However, a longer differentiation period was then solely applied in the final experiment when cells were cultured for 21 days. When investigating tight junctions in Caco-2, especially ZO-2 is a multifunctional protein that is also involved in gene regulation in the nucleus. ZO-2 expression might have been influenced by the overall amount of ZO-2 in the cell. For this reason, the expression of other tight junctions such as claudin 1 and occludin could have been included (163). Further, a detection assay of iNOS by enzyme-linked immunosorbent assay (ELISA) in relation to agmatine (in Caco-2 and THP-1 cells) could be included since it resembles the degree of inflammation focusing on another marker than pNF κ B.

Regarding the macrophages and agmatine experimental set up, it is important to mention that experiments would have been more precise regarding the investigation of NF κ B if an extended lysis procedure was incorporated. In this regard, nucleus and cytosol are lysed separately whereby each cell material is blotted on a membrane to focus on either the p105 or p50 form of NF κ B. Another possible improvement in regard to higher specificity, the amount of the antibody pNF κ B could have been measured in order to focus on the p50 form.

6 Conclusion and outlook

The aim of this research was to deeply characterize the gut bacterium *Parasutterella* and the metabolite agmatine in regard to human physiology, metabolism abnormalities and diseases such as obesity and type 2 diabetes.

Regarding *Parasutterella*, our data indicates that the genus is associated with human obesity and type 2 diabetes independent of metabolic inflammation and might be implicated in a novel dietary carbohydrate – microbiome – host metabolic axis. Thereby, the link to the fatty acid biosynthesis pathway might be important for body weight gain in obesity in response to a carbohydrate rich diet whereas the link to L-cysteine could be relevant for type 2 diabetes development. Furthermore, the abundance of *Parasutterella excrementihominis* decreased during a weight loss intervention in severely obese patients showing this bacterium reacts to varying environmental circumstances. The inverse association of *Parasutterella* with the intake of linolenic acid might be of interest for future intervention studies since ω -3 fatty acids could provide a potential to target human gut bacteria (suppl. fig. 7).

Agmatine, as a metabolite derived from human diet as well as gut microbiota, revealed increased levels in subjects with obesity independently of other metabolic diseases. The microbial intra-individual diversity in subjects with agmatine was decreased which is interesting in relation to resembling findings in microbiota composition of obese. For IBD patients who have a local gut inflammation, agmatine levels showed the opposite effect being decreased. Urine metabolites related to the arginine and proline metabolism (including pyrroline carboxylate) were reduced in subjects with elevated agmatine suggesting possible metabolizing effects of agmatine in precursors of human urine. On the one hand, a relation to dietary plant protein proved agmatine levels in serum to be directly influenced by food intake whereby metformin intake did not influence agmatine levels. On the other hand, *Bacteroides* seem to be the genus with the utmost capacity to produce agmatine. In vitro, we found rather negative metabolic effects of agmatine in adipocytes as well as activating inflammatory characteristics in human macrophages (suppl. fig. 8).

Finally, these findings contribute to the research design of future studies e.g. clinical interventions focusing [1] on L-cysteine as a possible anti-diabetic amino acid (in combination with linolenic acid) shaping the gut microbiota and [2] on agmatine as a potential beneficial metabolite in healthy human obese without low-grade inflammation present.

7 References

1. Karlsson F, Tremaroli V, Nielsen J, Bäckhed F. Assessing the Human Gut Microbiota in Metabolic Diseases. *Diabetes*. 2013 Oct;62(10):3341–9.
2. David LA, Maurice CF, Carmody RN, Gootenberg DB, Button JE, Wolfe BE, et al. Diet rapidly and reproducibly alters the human gut microbiome. *Nature*. 2014 Jan 23;505(7484):559–63.
3. Goodrich JK, Waters JL, Poole AC, Sutter JL, Koren O, Blekhman R, et al. Human genetics shape the gut microbiome. *Cell*. 2014 Nov 6;159(4):789–99.
4. Moreno-Indias I, Cardona F, Tinahones FJ, Queipo-Ortuño MI. Impact of the gut microbiota on the development of obesity and type 2 diabetes mellitus. *Front Microbiol*. 2014;5:190.
5. Lambeth SM, Carson T, Lowe J, Ramaraj T, Leff JW, Luo L, et al. Composition, Diversity and Abundance of Gut Microbiome in Prediabetes and Type 2 Diabetes. *J Diabetes Obes*. 2015 Dec 26;2(3):1–7.
6. Cani PD, Everard A. Talking microbes: When gut bacteria interact with diet and host organs. *Mol Nutr Food Res*. 2016 Jan;60(1):58–66.
7. Abdou RM, Zhu L, Baker RD, Baker SS. Gut Microbiota of Nonalcoholic Fatty Liver Disease. *Dig Dis Sci*. 2016 May;61(5):1268–81.
8. Hyland N, Stanton C, editors. *The gut-brain axis: dietary, probiotic, and prebiotic interventions on the microbiota*. Amsterdam: Elsevier/Academic Press; 2016. 486 p.
9. Hooper LV, Littman DR, Macpherson AJ. Interactions between the microbiota and the immune system. *Science*. 2012 Jun 8;336(6086):1268–73.
10. Pincus MR, Pei Z. Beyond infectious disease: welcome to the era of population microbiology. *Clin Lab Med*. 2014 Dec;34(4):xi–xiii.
11. Cox AJ, West NP, Cripps AW. Obesity, inflammation, and the gut microbiota. *The Lancet Diabetes & Endocrinology*. 2015 Mar;3(3):207–15.
12. Lloyd-Price J, Abu-Ali G, Huttenhower C. The healthy human microbiome. *Genome Med* [Internet]. 2016 Apr 27 [cited 2021 Mar 26];8. Available from: <https://www.ncbi.nlm.nih.gov/pmc/articles/PMC4848870/>
13. Etxeberria U, Fernández-Quintela A, Milagro FI, Aguirre L, Martínez JA,

References

- Portillo MP. Impact of polyphenols and polyphenol-rich dietary sources on gut microbiota composition. *J Agric Food Chem*. 2013 Oct 9;61(40):9517–33.
14. Caesar R, Reigstad CS, Bäckhed HK, Reinhardt C, Ketonen M, Lundén GÖ, et al. Gut-derived lipopolysaccharide augments adipose macrophage accumulation but is not essential for impaired glucose or insulin tolerance in mice. *Gut*. 2012 Dec;61(12):1701–7.
15. Wu H, Tremaroli V, Bäckhed F. Linking Microbiota to Human Diseases: A Systems Biology Perspective. *Trends Endocrinol Metab*. 2015 Dec;26(12):758–70.
16. Chassaing B, Koren O, Goodrich JK, Poole AC, Srinivasan S, Ley RE, et al. Dietary emulsifiers impact the mouse gut microbiota promoting colitis and metabolic syndrome. *Nature*. 2015 05;519(7541):92–6.
17. Dhurandhar EJ, Keith SW. The aetiology of obesity beyond eating more and exercising less. *Best Pract Res Clin Gastroenterol*. 2014 Aug;28(4):533–44.
18. Turnbaugh PJ, Ley RE, Mahowald MA, Magrini V, Mardis ER, Gordon JL. An obesity-associated gut microbiome with increased capacity for energy harvest. *Nature*. 2006 Dec;444(7122):1027–31.
19. Bäckhed F, Manchester JK, Semenkovich CF, Gordon JL. Mechanisms underlying the resistance to diet-induced obesity in germ-free mice. *Proc Natl Acad Sci USA*. 2007 Jan 16;104(3):979–84.
20. Hotamisligil GS. Inflammation and metabolic disorders. *Nature*. 2006 Dec 14;444(7121):860–7.
21. Kuwahara A. Contributions of colonic short-chain Fatty Acid receptors in energy homeostasis. *Front Endocrinol (Lausanne)*. 2014;5:144.
22. Rakoff-Nahoum S, Paglino J, Eslami-Varzaneh F, Edberg S, Medzhitov R. Recognition of commensal microflora by toll-like receptors is required for intestinal homeostasis. *Cell*. 2004 Jul 23;118(2):229–41.
23. Biesalski H-K, Bischoff SC, Pirlich M, Weimann A, Adolph M, Arends J, et al., editors. *Ernährungsmedizin: nach dem Curriculum Ernährungsmedizin der Bundesärztekammer*. 5., vollständig überarbeitete und erweiterte Auflage. Stuttgart New York: Georg Thieme Verlag; 2018. 1064 p.
24. Fei N, Zhao L. An opportunistic pathogen isolated from the gut of an obese human causes obesity in germfree mice. *ISME J*. 2013 Apr;7(4):880–4.
25. Shin N-R, Whon TW, Bae J-W. Proteobacteria: microbial signature of dysbiosis in gut microbiota. *Trends Biotechnol*. 2015 Sep;33(9):496–503.

26. Vrieze A, Van Nood E, Holleman F, Salojärvi J, Kootte RS, Bartelsman JFWM, et al. Transfer of Intestinal Microbiota From Lean Donors Increases Insulin Sensitivity in Individuals With Metabolic Syndrome. *Gastroenterology*. 2012 Oct 1;143(4):913-916.e7.
27. Rinninella E, Raoul P, Cintoni M, Franceschi F, Miggiaro GAD, Gasbarrini A, et al. What is the Healthy Gut Microbiota Composition? A Changing Ecosystem across Age, Environment, Diet, and Diseases. *Microorganisms*. 2019 Jan 10;7(1):14.
28. Eckburg PB, Bik EM, Bernstein CN, Purdom E, Dethlefsen L, Sargent M, et al. Diversity of the Human Intestinal Microbial Flora. *Science*. 2005 Jun 10;308(5728):1635–8.
29. Clemente JC, Ursell LK, Parfrey LW, Knight R. The Impact of the Gut Microbiota on Human Health: An Integrative View. *Cell*. 2012 Mar 16;148(6):1258–70.
30. Kreutzer C, Peters S, Schulte DM, Fangmann D, Türk K, Wolff S, et al. Hypothalamic Inflammation in Human Obesity Is Mediated by Environmental and Genetic Factors. *Diabetes*. 2017 Sep;66(9):2407–15.
31. Mandaşescu S, Mocanu V, Dăscălița A-M, Haliga R, Nestian I, Stitt PA, et al. Flaxseed supplementation in hyperlipidemic patients. *Rev Med Chir Soc Med Nat Iasi*. 2005 Sep;109(3):502–6.
32. Depommier C, Everard A, Druart C, Plovier H, Van Hul M, Vieira-Silva S, et al. Supplementation with *Akkermansia muciniphila* in overweight and obese human volunteers: a proof-of-concept exploratory study. *Nat Med*. 2019 Jul 1;25(7):1096–103.
33. Anhê FF, Schertzer JD, Marette A. Bacteria to alleviate metabolic syndrome. *Nature Medicine*. 2019 Jul 1;25(7):1031–3.
34. Basolo A, Hohenadel M, Ang QY, Piaggi P, Heinitz S, Walter M, et al. Effects of underfeeding and oral vancomycin on gut microbiome and nutrient absorption in humans. *Nature Medicine*. 2020 Apr 1;26(4):589–98.
35. Bergström A, Skov TH, Bahl MI, Roager HM, Christensen LB, Ejlerskov KT, et al. Establishment of intestinal microbiota during early life: a longitudinal, explorative study of a large cohort of Danish infants. *Appl Environ Microbiol*. 2014 May;80(9):2889–900.
36. Subramanian S, Blanton LV, Frese SA, Charbonneau M, Mills DA, Gordon

References

- Jl. Cultivating healthy growth and nutrition through the gut microbiota. *Cell*. 2015 Mar 26;161(1):36–48.
37. Cani PD, Neyrinck AM, Fava F, Knauf C, Burcelin RG, Tuohy KM, et al. Selective increases of bifidobacteria in gut microflora improve high-fat-diet-induced diabetes in mice through a mechanism associated with endotoxaemia. *Diabetologia*. 2007 Nov;50(11):2374–83.
38. Wu GD, Chen J, Hoffmann C, Bittinger K, Chen Y-Y, Keilbaugh SA, et al. Linking long-term dietary patterns with gut microbial enterotypes. *Science*. 2011 Oct 7;334(6052):105–8.
39. Murphy EF, Clarke SF, Marques TM, Hill C, Stanton C, Ross RP, et al. Antimicrobials: Strategies for targeting obesity and metabolic health? *Gut Microbes*. 2013 Feb;4(1):48–53.
40. Cani PD, Bibiloni R, Knauf C, Waget A, Neyrinck AM, Delzenne NM, et al. Changes in gut microbiota control metabolic endotoxemia-induced inflammation in high-fat diet-induced obesity and diabetes in mice. *Diabetes*. 2008 Jun;57(6):1470–81.
41. Cani PD, Possemiers S, Van de Wiele T, Guiot Y, Everard A, Rottier O, et al. Changes in gut microbiota control inflammation in obese mice through a mechanism involving GLP-2-driven improvement of gut permeability. *Gut*. 2009 Aug;58(8):1091–103.
42. Tripathi MK, Giri SK. Probiotic functional foods: Survival of probiotics during processing and storage. *Journal of Functional Foods*. 2014 Jul 1;9:225–41.
43. Fox MJ, Ahuja KDK, Robertson IK, Ball MJ, Eri RD. Can probiotic yogurt prevent diarrhoea in children on antibiotics? A double-blind, randomised, placebo-controlled study. *BMJ Open*. 2015 Jan 14;5(1):e006474.
44. Gu Y, Liu C, Zheng N, Jia W, Zhang W, Li H. Metabolic and Gut Microbial Characterization of Obesity-Prone Mice under a High-Fat Diet. *J Proteome Res*. 2019 Apr 5;18(4):1703–14.
45. Cheng W, Lu J, Lin W, Wei X, Li H, Zhao X, et al. Effects of a galacto-oligosaccharide-rich diet on fecal microbiota and metabolite profiles in mice. *Food Funct*. 2018;9(3):1612–20.
46. Morotomi M, Nagai F, Watanabe Y. *Parasutterella secunda* sp. nov., isolated from human faeces and proposal of Sutterellaceae fam. nov. in the order Burkholderiales. *INTERNATIONAL JOURNAL OF SYSTEMATIC AND*

EVOLUTIONARY MICROBIOLOGY. 2011 Mar 1;61(3):637–43.

47. Nagai F, Morotomi M, Sakon H, Tanaka R. *Parasutterella excrementihominis* gen. nov., sp. nov., a member of the family Alcaligenaceae isolated from human faeces. INTERNATIONAL JOURNAL OF SYSTEMATIC AND EVOLUTIONARY MICROBIOLOGY. 2009 Jul 1;59(7):1793–7.

48. Chiodini RJ, Dowd SE, Chamberlin WM, Galandiuk S, Davis B, Glassing A. Microbial Population Differentials between Mucosal and Submucosal Intestinal Tissues in Advanced Crohn's Disease of the Ileum. PLoS ONE. 2015;10(7):e0134382.

49. Xiao S, Liu C, Chen M, Zou J, Zhang Z, Cui X, et al. *Scutellariae radix* and *coptidis rhizoma* ameliorate glycolipid metabolism of type 2 diabetic rats by modulating gut microbiota and its metabolites. Appl Microbiol Biotechnol. 2020 Jan;104(1):303–17.

50. Krautkramer KA, Fan J, Bäckhed F. Gut microbial metabolites as multi-kingdom intermediates. Nat Rev Microbiol. 2021 Feb;19(2):77–94.

51. Ramos-Molina B, Queipo-Ortuño MI, Lambertos A, Tinahones FJ, Peñafiel R. Dietary and Gut Microbiota Polyamines in Obesity- and Age-Related Diseases. Front Nutr. 2019 Mar 14;6:24.

52. Alex S, Lange K, Amolo T, Grinstead JS, Haakonsson AK, Szalowska E, et al. Short-Chain Fatty Acids Stimulate Angiopoietin-Like 4 Synthesis in Human Colon Adenocarcinoma Cells by Activating Peroxisome Proliferator-Activated Receptor γ . Mol Cell Biol. 2013 Apr;33(7):1303–16.

53. Latour YL, Gobert AP, Wilson KT. The Role of Polyamines in the Regulation of Macrophage Polarization and Function. Amino Acids. 2020 Feb;52(2):151–60.

54. Levy M, Thaïss CA, Elinav E. Metabolites: messengers between the microbiota and the immune system. Genes Dev. 2016 Jul 15;30(14):1589–97.

55. Crous-Bou M, Fung TT, Prescott J, Julin B, Du M, Sun Q, et al. Mediterranean diet and telomere length in Nurses' Health Study: population based cohort study. BMJ. 2014 Dec 2;349:g6674.

56. Kosonen R, Barua S, Kim JY, Lee JE. Role of agmatine in the application of neural progenitor cell in central nervous system diseases: therapeutic potentials and effects. Anat Cell Biol. 2021 Jun 30;54(2):143–51.

57. Xu W, Gao L, Li T, Shao A, Zhang J. Neuroprotective Role of Agmatine in Neurological Diseases. Curr Neuropharmacol. 2018 Nov;16(9):1296–305.

References

58. Laube G, Bernstein H-G. Agmatine: multifunctional arginine metabolite and magic bullet in clinical neuroscience? *Biochemical Journal*. 2017 Jul 26;474(15):2619–40.
59. Tofalo R, Perpetuini G, Schirone M, Suzzi G. Biogenic Amines: Toxicology and Health Effect. In: *Encyclopedia of Food and Health* [Internet]. Elsevier; 2016 [cited 2021 Sep 7]. p. 424–9. Available from: <https://linkinghub.elsevier.com/retrieve/pii/B9780123849472000714>
60. Akasaka N, Fujiwara S. The therapeutic and nutraceutical potential of agmatine, and its enhanced production using *Aspergillus oryzae*. *Amino Acids*. 2020 Feb 1;52(2):181–97.
61. Kitada Y, Muramatsu K, Toju H, Kibe R, Benno Y, Kurihara S, et al. Bioactive polyamine production by a novel hybrid system comprising multiple indigenous gut bacterial strategies. *Sci Adv*. 2018 Jun 27;4(6):eaat0062.
62. Pryor R, Norvaisas P, Marinos G, Best L, Thingholm LB, Quintaneiro LM, et al. Host-Microbe-Drug-Nutrient Screen Identifies Bacterial Effectors of Metformin Therapy. *Cell*. 2019 Sep 5;178(6):1299-1312.e29.
63. Satriano J. Agmatine: At the Crossroads of the Arginine Pathways. *Annals of the New York Academy of Sciences*. 2003 Dec 1;1009(1):34–43.
64. Mardinoglu A, Shoaie S, Bergentall M, Ghaffari P, Zhang C, Larsson E, et al. The gut microbiota modulates host amino acid and glutathione metabolism in mice. *Mol Syst Biol*. 2015 Oct 16;11(10):834.
65. J Y, W R, G Y, J D, X H, R F, et al. L-Cysteine metabolism and its nutritional implications. *Molecular nutrition & food research* [Internet]. 2016 Jan [cited 2022 Jan 3];60(1). Available from: <https://pubmed.ncbi.nlm.nih.gov/25929483/>
66. Jain SK. L-cysteine supplementation as an adjuvant therapy for type-2 diabetes. *Can J Physiol Pharmacol*. 2012 Aug;90(8):1061–4.
67. McGavigan AK, O'Hara HC, Amin A, Kinsey-Jones J, Spreckley E, Alamshah A, et al. L-cysteine suppresses ghrelin and reduces appetite in rodents and humans. *Int J Obes (Lond)*. 2015 Mar;39(3):447–55.
68. Wada M, Takagi H. Metabolic pathways and biotechnological production of L-cysteine. *Appl Microbiol Biotechnol*. 2006 Nov;73(1):48–54.
69. Piletz JE, Aricioglu F, Cheng J-T, Fairbanks CA, Gilad VH, Haenisch B, et al. Agmatine: clinical applications after 100 years in translation. *Drug Discovery*

Today. 2013 Sep 1;18(17):880–93.

70. Halaris A, Plietz J. Agmatine: Metabolic Pathway and Spectrum of Activity in Brain. *CNS Drugs*. 2007;21(11):885–900.

71. Su C-H, Liu I-M, Chung H-H, Cheng J-T. Activation of I2-imidazoline receptors by agmatine improved insulin sensitivity through two mechanisms in type-2 diabetic rats. *Neurosci Lett*. 2009 Jul 3;457(3):125–8.

72. Sener A, Lebrun P, Blachier F, Malaisse WJ. Stimulus-secretion coupling of arginine-induced insulin release. Insulinotropic action of agmatine. *Biochem Pharmacol*. 1989 Jan 15;38(2):327–30.

73. Velasco M, Díaz-García CM, Larqué C, Hiriart M. Modulation of Ionic Channels and Insulin Secretion by Drugs and Hormones in Pancreatic Beta Cells. *Mol Pharmacol*. 2016 Sep 1;90(3):341–57.

74. Mónica FZ, Bian K, Murad F. The Endothelium-Dependent Nitric Oxide–cGMP Pathway. In: *Advances in Pharmacology* [Internet]. Elsevier; 2016 [cited 2021 Dec 30]. p. 1–27. Available from: <https://linkinghub.elsevier.com/retrieve/pii/S1054358916300321>

75. Bila I, Dzydzan O, Brodyak I, Sybirna N. Agmatine Prevents Oxidative-nitrative Stress in Blood Leukocytes Under Streptozotocin-induced Diabetes Mellitus. *Open Life Sci*. 2019 Jul 23;14:299–310.

76. Rashidian A, Keshavarz-Bahaghighat H, Abdollahi A, Chamanara M, Faghir-Ghanesefat H, Hoseini-Ahmadabadi M, et al. Agmatine ameliorates acetic acid-induced colitis in rats: involvement of nitrergic system. *Immunopharmacology and Immunotoxicology*. 2019 Mar 4;41(2):242–9.

77. Halaris A, Plietz J. Agmatine : metabolic pathway and spectrum of activity in brain. *CNS Drugs*. 2007;21(11):885–900.

78. Kim DJ, Kim DI, Lee SK, Suh SH, Lee YJ, Kim J, et al. Protective Effect of Agmatine on a Reperfusion Model After Transient Cerebral Ischemia: Temporal Evolution on Perfusion MR Imaging and Histopathologic Findings. *AJNR Am J Neuroradiol*. 2006 Apr;27(4):780–5.

79. Sastre M, Regunathan S, Galea E, Reis DJ. Agmatinase Activity in Rat Brain: A Metabolic Pathway for the Degradation of Agmatine. *Journal of Neurochemistry*. 2002 Nov 23;67(4):1761–5.

80. Tune JD, Goodwill AG, Sassoon DJ, Mather KJ. Cardiovascular consequences of metabolic syndrome. *Transl Res*. 2017 May;183:57–70.

References

81. Ouchi N, Parker JL, Lugus JJ, Walsh K. Adipokines in inflammation and metabolic disease. *Nat Rev Immunol*. 2011 Feb;11(2):85–97.
82. Ouchi N, Higuchi A, Ohashi K, Oshima Y, Gokce N, Shibata R, et al. Sfrp5 Is an Anti-Inflammatory Adipokine That Modulates Metabolic Dysfunction in Obesity. *Science*. 2010 Jul 23;329(5990):454–7.
83. Furman D, Campisi J, Verdin E, Carrera-Bastos P, Targ S, Franceschi C, et al. Chronic inflammation in the etiology of disease across the life span. *Nat Med*. 2019 Dec;25(12):1822–32.
84. Elisia I, Lam V, Hofs E, Li MY, Hay M, Cho B, et al. Effect of age on chronic inflammation and responsiveness to bacterial and viral challenges. *PLoS One*. 2017 Nov 29;12(11):e0188881.
85. Zhang X, Wang H, Yin P, Fan H, Sun L, Liu Y. Flaxseed oil ameliorates alcoholic liver disease via anti-inflammation and modulating gut microbiota in mice. *Lipids in Health and Disease* [Internet]. 2017 Dec [cited 2019 Jan 2];16(1). Available from: <http://lipidworld.biomedcentral.com/articles/10.1186/s12944-017-0431-8>
86. Thingholm LB, Rühlemann MC, Koch M, Fuqua B, Laucke G, Boehm R, et al. Obese Individuals with and without Type 2 Diabetes Show Different Gut Microbial Functional Capacity and Composition. *Cell Host Microbe*. 2019 Aug 14;26(2):252-264.e10.
87. Ye M, Robson PJ, Eurich DT, Vena JE, Xu J-Y, Johnson JA. Cohort Profile: Alberta's Tomorrow Project. *International Journal of Epidemiology*. 2017 Aug 1;46(4):1097–1098l.
88. Kroke A, Klipstein-Grobusch K, Voss S, Möseneder J, Thielecke F, Noack R, et al. Validation of a self-administered food-frequency questionnaire administered in the European Prospective Investigation into Cancer and Nutrition (EPIC) Study: comparison of energy, protein, and macronutrient intakes estimated with the doubly labeled water, urinary nitrogen, and repeated 24-h dietary recall methods. *The American Journal of Clinical Nutrition*. 1999 Oct 1;70(4):439–47.
89. Fangmann D, Theismann E-M, Türk K, Schulte DM, Relling I, Hartmann K, et al. Targeted Microbiome Intervention by Microencapsulated Delayed-Release Niacin Beneficially Affects Insulin Sensitivity in Humans. *Diabetes Care*. 2018;41(3):398–405.
90. Rohmann N, Schlicht K, Geisler C, Hollstein T, Knappe C, Krause L, et al.

Circulating sDPP-4 is Increased in Obesity and Insulin Resistance but Is Not Related to Systemic Metabolic Inflammation. *The Journal of Clinical Endocrinology & Metabolism*. 2020 Oct 21;dgaa758.

91. Heinsen F-A, Fangmann D, Müller N, Schulte DM, Rühlemann MC, Türk K, et al. Beneficial Effects of a Dietary Weight Loss Intervention on Human Gut Microbiome Diversity and Metabolism Are Not Sustained during Weight Maintenance. *Obes Facts*. 2016;9(6):379–91.

92. Callahan BJ, McMurdie PJ, Holmes SP. Exact sequence variants should replace operational taxonomic units in marker-gene data analysis. *ISME J*. 2017 Dec;11(12):2639–43.

93. Matyash V, Liebisch G, Kurzchalia TV, Shevchenko A, Schwudke D. Lipid extraction by methyl-tert-butyl ether for high-throughput lipidomics. *J Lipid Res*. 2008 May;49(5):1137–46.

94. Kind T, Fiehn O. Seven Golden Rules for heuristic filtering of molecular formulas obtained by accurate mass spectrometry. *BMC Bioinformatics*. 2007 Mar 27;8:105.

95. R Core Team. A language and environment for statistical computing. R Foundation for Statistical Computing, Vienna, Austria; 2018.

96. Zeileis A, Kleiber C, Jackman S. Regression Models for Count Data in R. *J Stat Soft*. 2008 Jul 29;27:1–25.

97. Delday M, Mulder I, Logan ET, Grant G. *Bacteroides thetaiotaomicron* Ameliorates Colon Inflammation in Preclinical Models of Crohn's Disease. *Inflamm Bowel Dis*. 2019 Jan;25(1):85–96.

98. Chen L, Li J, Zhu W, Kuang Y, Liu T, Zhang W, et al. Skin and Gut Microbiome in Psoriasis: Gaining Insight Into the Pathophysiology of It and Finding Novel Therapeutic Strategies. *Front Microbiol* [Internet]. 2020 Dec 15 [cited 2021 Mar 23];11. Available from: <https://www.ncbi.nlm.nih.gov/pmc/articles/PMC7769758/>

99. Black A. Critical evaluation of energy intake using the Goldberg cut-off for energy intake:basal metabolic rate. A practical guide to its calculation, use and limitations. *Int J Obes*. 2000 Sep;24(9):1119–30.

100. Schofield WN. Predicting basal metabolic rate, new standards and review of previous work. *Hum Nutr Clin Nutr*. 1985;39 Suppl 1:5–41.

101. Willett WC, Howe GR, Kushi LH. Adjustment for total energy intake in

References

- epidemiologic studies. The American Journal of Clinical Nutrition. 1997 Apr 1;65(4):1220S-1228S.
102. Marker-based metagenomic tutorial. alpha-diversity metrics [Internet]. 2015. Available from: <https://evolution.unibas.ch>
103. Bray JR, Curtis JT. An Ordination of the Upland Forest Communities of Southern Wisconsin. Ecological Monographs. 1957 Oct;27(4):325–49.
104. Jaccard P. The Distribution of the Flora in the Alpine Zone.1. New Phytologist. 1912;11(2):37–50.
105. Anderson MJ. A new method for non-parametric multivariate analysis of variance. Austral Ecology. 2001;26(1):32–46.
106. Zimmermann J, Kaleta C, Waschina S. gapseq: informed prediction of bacterial metabolic pathways and reconstruction of accurate metabolic models. Genome Biol. 2021 Mar 10;22:81.
107. Orth JD, Thiele I, Palsson BØ. What is flux balance analysis? Nat Biotechnol. 2010 Mar;28(3):245–8.
108. Gelius-Dietrich G, Desouki AA, Fritzemeier CJ, Lercher MJ. sybil – Efficient constraint-based modelling in R. BMC Syst Biol. 2013 Nov 13;7:125.
109. Marees AT, de Kluiver H, Stringer S, Vorspan F, Curis E, Marie-Claire C, et al. A tutorial on conducting genome-wide association studies: Quality control and statistical analysis. Int J Methods Psychiatr Res. 2018 Feb 27;27(2):e1608.
110. Chen Y-J, Wu H, Wu S-D, Lu N, Wang Y-T, Liu H-N, et al. *Parasutterella* , in association with irritable bowel syndrome and intestinal chronic inflammation: *Parasutterella* may be related with IBS. Journal of Gastroenterology and Hepatology. 2018 Nov;33(11):1844–52.
111. Kristina Sengebusch. Untersuchungen von small dense Low Density Lipoprotein-Serumkonzentrationen und deren Beeinflussung durch Biologika bei Patienten mit chronisch-entzündlichen Erkrankungen. 2018.
112. Zhang X, Zhao Y, Zhang M, Pang X, Xu J, Kang C, et al. Structural Changes of Gut Microbiota during Berberine-Mediated Prevention of Obesity and Insulin Resistance in High-Fat Diet-Fed Rats. PLoS One [Internet]. 2012 Aug 3 [cited 2020 Dec 16];7(8). Available from: <https://www.ncbi.nlm.nih.gov/pmc/articles/PMC3411811/>
113. Wang J, Thingholm LB, Skiecevičienė J, Rausch P, Kummén M, Hov JR, et

- al. Genome-wide association analysis identifies variation in vitamin D receptor and other host factors influencing the gut microbiota. *Nat Genet.* 2016 Nov;48(11):1396–406.
114. Yamada T, Takahashi D, Hase K. The diet-microbiota-metabolite axis regulates the host physiology. *J Biochem.* 2016 Jul;160(1):1–10.
115. Mills S, Stanton C, Lane JA, Smith GJ, Ross RP. Precision Nutrition and the Microbiome, Part I: Current State of the Science. *Nutrients.* 2019 Apr 24;11(4):923.
116. Park HS, Park JY, Yu R. Relationship of obesity and visceral adiposity with serum concentrations of CRP, TNF- α and IL-6. *Diabetes Research and Clinical Practice.* 2005 Jul 1;69(1):29–35.
117. Matsuoka K, Kanai T. The gut microbiota and inflammatory bowel disease. *Semin Immunopathol.* 2015;37:47–55.
118. Kitai T, Tang WHW. GUT MICROBIOTA IN CARDIOVASCULAR DISEASE AND HEART FAILURE. *Clin Sci (Lond).* 2018 Jan 16;132(1):85–91.
119. Lauka L, Reitano E, Carra MC, Gaiani F, Gavrilidis P, Brunetti F, et al. Role of the intestinal microbiome in colorectal cancer surgery outcomes. *World J Surg Oncol [Internet].* 2019 Dec 2 [cited 2021 Mar 26];17. Available from: <https://www.ncbi.nlm.nih.gov/pmc/articles/PMC6889350/>
120. Ju T, Kong JY, Stothard P, Willing BP. Defining the role of *Parasutterella*, a previously uncharacterized member of the core gut microbiota. *ISME J.* 2019 Jun;13(6):1520–34.
121. Blouet C, Mariotti F, Azzout-Marniche D, Mathé V, Mikogami T, Tomé D, et al. Dietary cysteine alleviates sucrose-induced oxidative stress and insulin resistance. *Free Radical Biology and Medicine.* 2007 Apr 1;42(7):1089–97.
122. Wang J, Wang H. Oxidative Stress in Pancreatic Beta Cell Regeneration. *Oxid Med Cell Longev.* 2017;2017:1930261.
123. Kuda O. Bioactive metabolites of docosahexaenoic acid. *Biochimie.* 2017 May;136:12–20.
124. Farooqi IS, Drop S, Clements A, Keogh JM, Biernacka J, Lowenbein S, et al. Heterozygosity for a POMC-Null Mutation and Increased Obesity Risk in Humans. *Diabetes.* 2006 Sep 1;55(9):2549–53.
125. Heinsen F-A, Fangmann D, Müller N, Schulte DM, Rühlemann MC, Türk K, et al. Beneficial Effects of a Dietary Weight Loss Intervention on Human Gut

References

Microbiome Diversity and Metabolism Are Not Sustained during Weight Maintenance. *Obes Facts*. 2016;9(6):379–91.

126. Grembi JA, Nguyen LH, Haggerty TD, Gardner CD, Holmes SP, Parsonnet J. Gut microbiota plasticity is correlated with sustained weight loss on a low-carb or low-fat dietary intervention. *Sci Rep*. 2020 Jan 29;10:1405.

127. Zhang S, Wu P, Tian Y, Liu B, Huang L, Liu Z, et al. Gut Microbiota Serves a Predictable Outcome of Short-Term Low-Carbohydrate Diet (LCD) Intervention for Patients with Obesity. *Microbiol Spectr*. 9(2):e00223-21.

128. Sanchez M, Darimont C, Drapeau V, Emady-Azar S, Lepage M, Rezzonico E, et al. Effect of *Lactobacillus rhamnosus* CGMCC1.3724 supplementation on weight loss and maintenance in obese men and women. *British Journal of Nutrition*. 2014 Apr;111(8):1507–19.

129. Nissim I, Horyn O, Daikhin Y, Chen P, Li C, Wehrli SL, et al. The Molecular and Metabolic Influence of Long Term Agmatine Consumption. *J Biol Chem*. 2014 Apr 4;289(14):9710–29.

130. Nakamura A, Kurihara S, Takahashi D, Ohashi W, Nakamura Y, Kimura S, et al. Symbiotic polyamine metabolism regulates epithelial proliferation and macrophage differentiation in the colon. *Nat Commun*. 2021 Apr 8;12:2105.

131. Kwon E-J, Kim M-M. Agmatine modulates melanogenesis via MITF signaling pathway. *Environmental Toxicology and Pharmacology*. 2017 Jan;49:124–30.

132. Gilad GM, Gilad VH. Long-Term (5 Years), High Daily Dosage of Dietary Agmatine—Evidence of Safety: A Case Report. *Journal of Medicinal Food*. 2014 Nov;17(11):1256–9.

133. Wilmanski T, Rappaport N, Earls JC, Magis AT, Manor O, Lovejoy J, et al. Blood metabolome predicts gut microbiome α -diversity in humans. *Nat Biotechnol*. 2019 Oct;37(10):1217–28.

134. Sze MA, Schloss PD. Looking for a Signal in the Noise: Revisiting Obesity and the Microbiome. *mBio*. 2016 Aug 23;7(4):e01018-16.

135. Xu D, Zhang L. Increasing Agmatine Production in *Escherichia coli* through Metabolic Engineering. *J Agric Food Chem*. 2019 Jul 17;67(28):7908–15.

136. Marchesi JR, Adams DH, Fava F, Hermes GDA, Hirschfield GM, Hold G, et al. The gut microbiota and host health: a new clinical frontier. *Gut*. 2016 Feb;65(2):330–9.

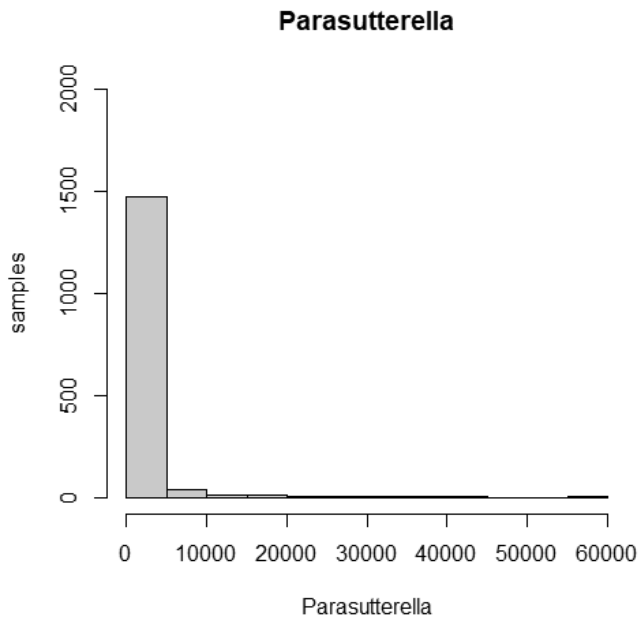
137. Duncan SH, Lopley GE, Holtrop G, Ince J, Johnstone AM, Louis P, et al. Human colonic microbiota associated with diet, obesity and weight loss. *Int J Obes.* 2008 Nov;32(11):1720–4.
138. Nag A, Kurushima Y, Bowyer RCE, Wells PM, Weiss S, Pietzner M, et al. Genome-wide scan identifies novel genetic loci regulating salivary metabolite levels. *Hum Mol Genet.* 2020 Mar 27;29(5):864–75.
139. Kettunen J, Tukiainen T, Sarin A-P, Ortega-Alonso A, Tikkanen E, Lyytikäinen L-P, et al. Genome-wide association study identifies multiple loci influencing human serum metabolite levels. *Nat Genet.* 2012 Jan 29;44(3):269–76.
140. Wang TJ, Larson MG, Vasan RS, Cheng S, Rhee EP, McCabe E, et al. Metabolite Profiles and the Risk of Developing Diabetes. *Nat Med.* 2011 Apr;17(4):448–53.
141. Hong S, Kim CY, Lee JE, Seong GJ. Agmatine protects cultured retinal ganglion cells from tumor necrosis factor- α -induced apoptosis. *Life Sciences.* 2009 Jan;84(1–2):28–32.
142. Hooshmandi E, Ghasemi R, Iloun P, Moosavi M. The neuroprotective effect of agmatine against amyloid β -induced apoptosis in primary cultured hippocampal cells involving ERK, Akt/GSK-3 β , and TNF- α . *Mol Biol Rep.* 2019 Feb 1;46(1):489–96.
143. Kliewer SA, Sundseth SS, Jones SA, Brown PJ, Wisely GB, Koble CS, et al. Fatty acids and eicosanoids regulate gene expression through direct interactions with peroxisome proliferator-activated receptors α and γ . *Proc Natl Acad Sci U S A.* 1997 Apr 29;94(9):4318–23.
144. He W, Barak Y, Hevener A, Olson P, Liao D, Le J, et al. Adipose-specific peroxisome proliferator-activated receptor γ knockout causes insulin resistance in fat and liver but not in muscle. *Proc Natl Acad Sci U S A.* 2003 Dec 23;100(26):15712–7.
145. Kintscher U, Law RE. PPAR γ -mediated insulin sensitization: the importance of fat versus muscle. *American Journal of Physiology-Endocrinology and Metabolism.* 2005 Feb;288(2):E287–91.
146. Tummala R, Ghosh RK, Jain V, Devanabanda AR, Bandyopadhyay D, Deedwania P, et al. Fish Oil and Cardiometabolic Diseases: Recent Updates and Controversies. *The American Journal of Medicine.* 2019 Oct;132(10):1153–9.
147. Nakahara T, Nishitani Y, Nishiumi S, Yoshida M, Azuma T. Astilbin from

References

- Engelhardtia chrysolepis enhances intestinal barrier functions in Caco-2 cell monolayers. *European Journal of Pharmacology*. 2017 Jun 5;804:46–51.
148. Suzuki T. Regulation of intestinal epithelial permeability by tight junctions. *Cell Mol Life Sci*. 2013 Feb;70(4):631–59.
149. Nie N, Bai C, Song S, Zhang Y, Wang B, Li Z. Bifidobacterium plays a protective role in TNF- α -induced inflammatory response in Caco-2 cell through NF- κ B and p38MAPK pathways. *Mol Cell Biochem*. 2020 Jan;464(1–2):83–91.
150. Ferrari D, Cimino F, Fratanzio D, Molonia MS, Bashllari R, Busà R, et al. Cyanidin-3-O-Glucoside Modulates the In Vitro Inflammatory Crosstalk between Intestinal Epithelial and Endothelial Cells. *Mediators Inflamm*. 2017;2017:3454023.
151. Wang X, Sato R, Brown MS, Hua X, Goldstein JL. SREBP-1, a membrane-bound transcription factor released by sterol-regulated proteolysis. *Cell*. 1994 Apr;77(1):53–62.
152. Han Z, Li Y, Yang B, Tan R, Wang M, Zhang B, et al. Agmatine Attenuates Liver Ischemia Reperfusion Injury by Activating Wnt/ β -catenin Signaling in Mice. *Transplantation*. 2020 Sep;104(9):1906–16.
153. Gardini G, Cabella C, Cravanzola C, Vargiu C, Belliardo S, Testore G, et al. Agmatine induces apoptosis in rat hepatocyte cultures. *Journal of Hepatology*. 2001 Oct;35(4):482–9.
154. Satriano J, Schwartz D, Ishizuka S, Lortie MJ, Thomson SC, Gabbai F, et al. Suppression of inducible nitric oxide generation by agmatine aldehyde: Beneficial effects in sepsis. *J Cell Physiol*. 2001 Sep;188(3):313–20.
155. Auguet M, Viossat I, Marin J-G, Chabrier P-E. Selective Inhibition of Inducible Nitric Oxide Synthase by Agmatine. *Japanese Journal of Pharmacology*. 1995;69(3):285–7.
156. Aricioglu F, Regunathan S. Agmatine attenuates stress- and lipopolysaccharide-induced fever in rats. *Physiol Behav*. 2005 Jun 30;85(3):370–5.
157. Chai J, Luo L, Hou F, Fan X, Yu J, Ma W, et al. Agmatine Reduces Lipopolysaccharide-Mediated Oxidant Response via Activating PI3K/Akt Pathway and Up-Regulating Nrf2 and HO-1 Expression in Macrophages. *PLoS One*. 2016 Sep 29;11(9):e0163634.
158. Robinson EK, Kelly DP, Mercer DW, Kozar RA. Differential Effects of Luminal Arginine and Glutamine on Metalloproteinase Production in the Postischemic Gut. *JPEN J Parenter Enteral Nutr*. 2008;32(4):433–8.

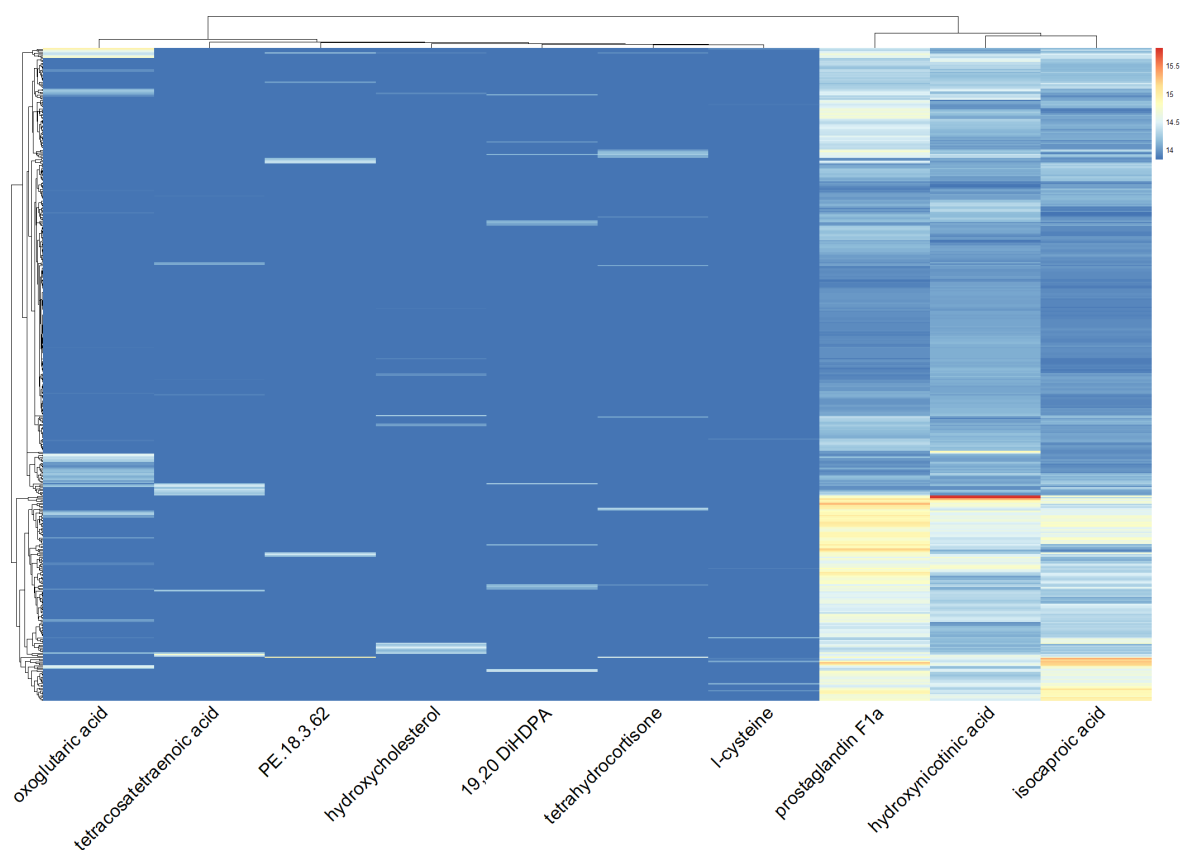
159. Zhao H, Shang Q, Pan Z, Bai Y, Li Z, Zhang H, et al. Exosomes From Adipose-Derived Stem Cells Attenuate Adipose Inflammation and Obesity Through Polarizing M2 Macrophages and Beiging in White Adipose Tissue. *Diabetes*. 2018 Feb;67(2):235–47.
160. Hu J, Han J, Li H, Zhang X, Liu L, Chen F, et al. Human Embryonic Kidney 293 Cells: A Vehicle for Biopharmaceutical Manufacturing, Structural Biology, and Electrophysiology. *Cells Tissues Organs*. 2018;205(1):1–8.
161. Roberts JC, Grocholski BM, Kitto KF, Fairbanks CA. Pharmacodynamic and Pharmacokinetic Studies of Agmatine after Spinal Administration in the Mouse. *J Pharmacol Exp Ther*. 2005 Sep 1;314(3):1226–33.
162. Rausch P, Rühlemann M, Hermes BM, Doms S, Dagan T, Dierking K, et al. Comparative analysis of amplicon and metagenomic sequencing methods reveals key features in the evolution of animal metaorganisms. *Microbiome*. 2019 Sep 14;7:133.
163. Suzuki T, Hara H. Quercetin Enhances Intestinal Barrier Function through the Assembly of Zonula Occludens-2, Occludin, and Claudin-1 and the Expression of Claudin-4 in Caco-2 Cells. *The Journal of Nutrition*. 2009 May 1;139(5):965–74.

8 Appendix



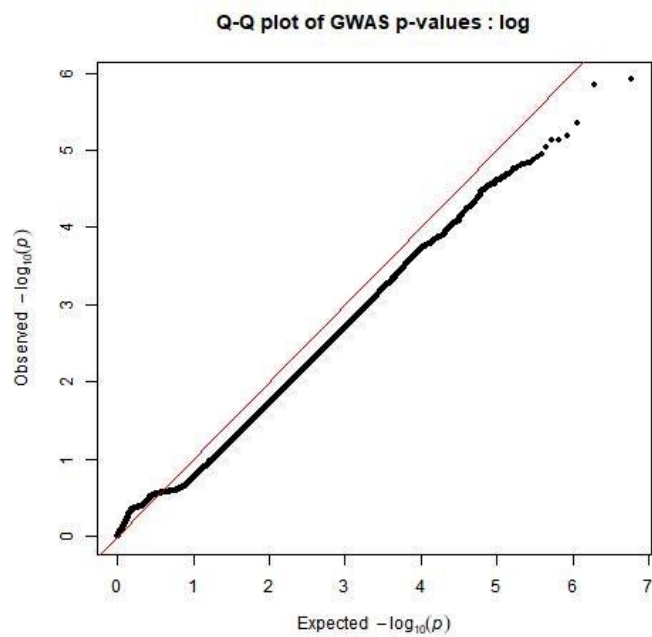
Supplementary figure 1

Distribution of Parasutterella sp. variable in the FoCus cohort. n=1544.



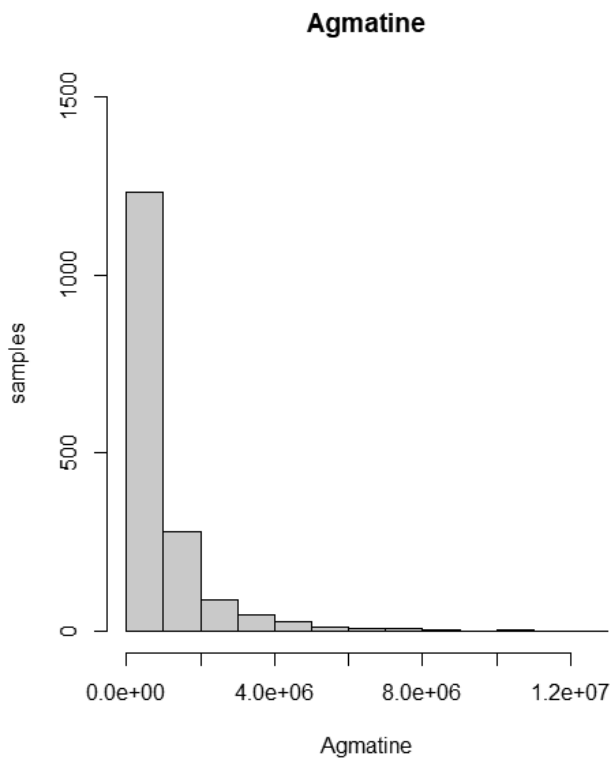
Supplementary figure 2

Ranges of raw values of the top ten metabolites associated with *Parasutterella* sp. n=470.



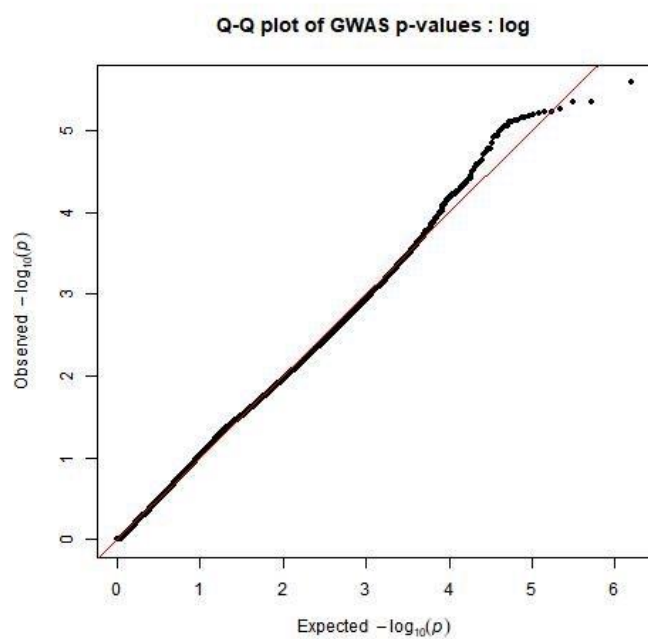
Supplementary figure 3

Expected vs. observed p-values of logistic analysis of *Parasutterella* sp. and SNPs.



Supplementary figure 4

Distribution of agmatine variable in the FoCus cohort. $n=1704$.



Supplementary figure 5

Expected vs. observed p-values of logistic analysis of agamnine and SNPs.

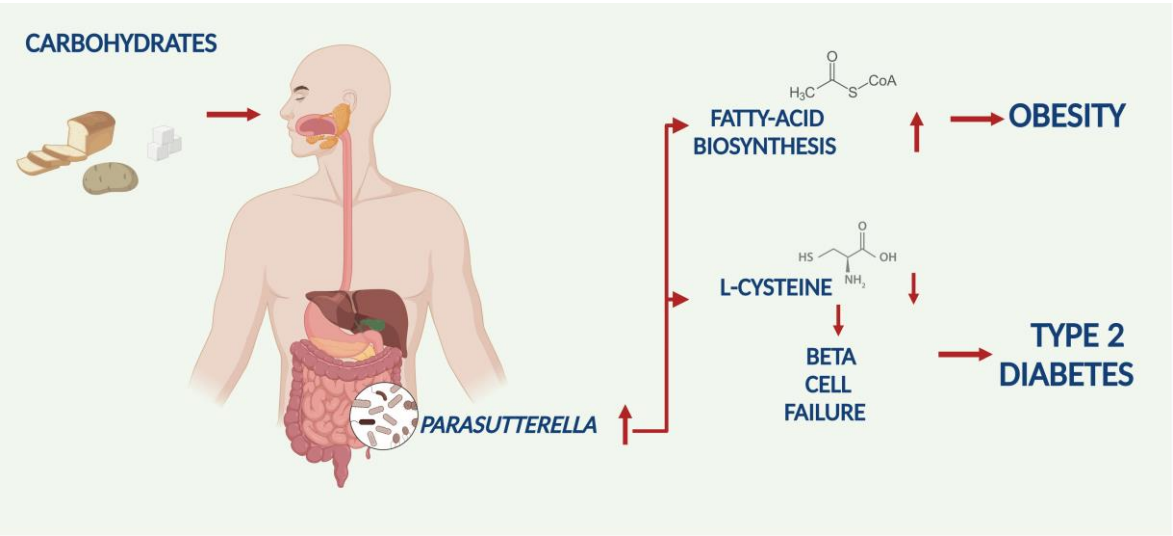
Appendix

Firefly, Label No.1, [RLU]		Renilla, Label No.2, [Units]	
Time/Pos	00:00:00	Time/Pos	00:00:00
A01	923500	A01	2724650
B01	7802780	B01	327260
A02	895250	A02	2871440
B02	7813490	B02	330270
A03	939020	A03	3267320
B03	3268530	B03	423230
A04	935420	A04	3195400
B04	3248390	B04	428510
A05	1145430	A05	3662590
A06	1145590	A06	3617590
A07	1144970	A07	4574850
A08	1150790	A08	4773880
A09	2808570	A09	407680
A10	2815000	A10	415430
A11	9717610	A11	429990
A12	9524260	A12	425740

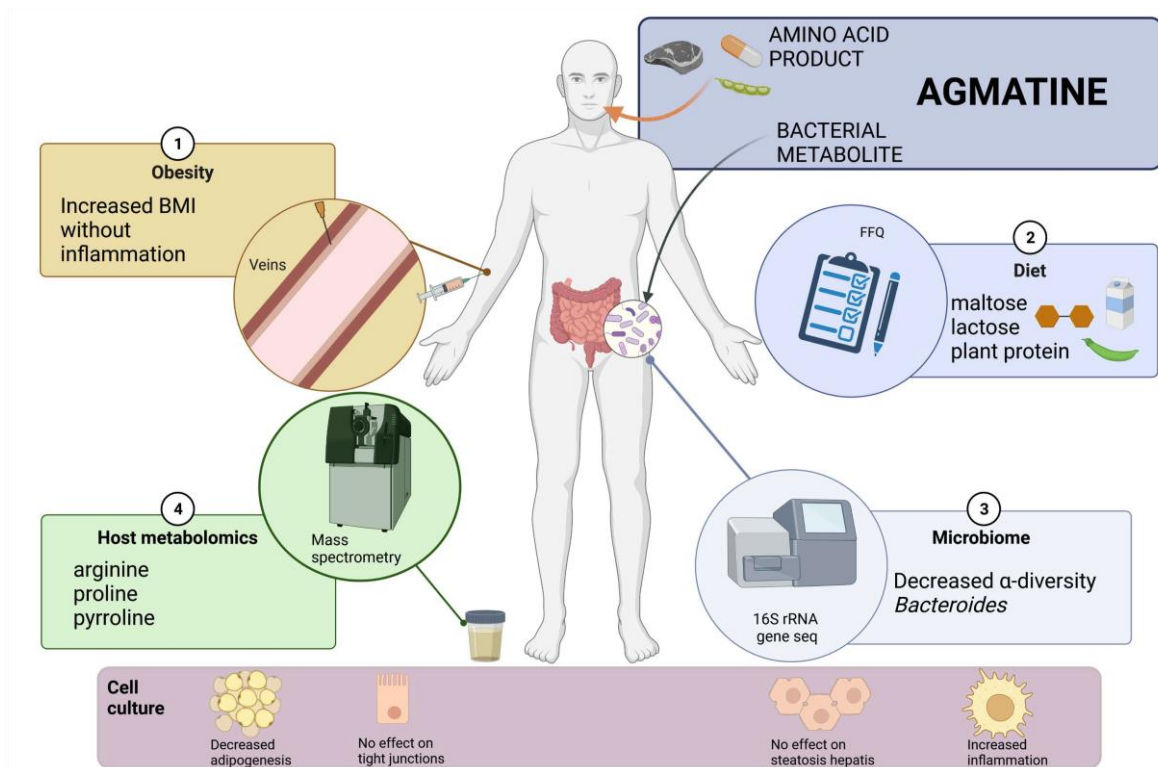
Firefly, Label No.1, [RLU]		Renilla, Label No.2, [Units]	
Time/Pos	00:00:00	Time/Pos	00:00:00
A01	1878270	A01	1638060
B01	14695110	B01	180780
A02	1834340	A02	1612490
B02	10668900	B02	117420
A03	2486720	A03	1193870
B03	1079590	B03	143690
A04	1253270	A04	903690
B04	1034450	B04	128650
A05	175030	A05	245750
A06	489440	A06	466620
A07	845230	A07	637570
A08	158510	A08	350660
A09	1614800	A09	179360
A10	1587710	A10	168000
A11	14058980	A11	173740
A12	14133240	A12	184170

Supplementary figure 6

Raw values of three independent measurements of either Firefly or Renilla luciferase using a luminometer with the Dual-Luciferase Reporter® Assay



Supplementary figure 7



Supplementary figure 8

Supplementary table 1

Metabolite	p-value	p-adjusted
PI.16.0.18.2.9Z.12Z...C43H79O13P	0.000000184036	0.000127066
DG.15.0.18.2.9Z.12Z..0.0..C36H66O5	0.000000266108	0.000127066
PE.16.0.22.6.4Z.7Z.10Z.13Z.16Z.19Z...C43H74NO8P	0.000000593232	0.000141634
PE.18.3.6Z.9Z.12Z..22.6.4Z.7Z.10Z.13Z.16Z.19Z...C45H72NO8P	0.000000593232	0.000141634
Prolylhydroxyproline.C10H16N2O4	0.000000765093	0.000146133
Prostaglandin.F1a.C20H36O5	0.000000988236	0.000157294
TG.8.0.8.0.8.0..C27H50O6	0.00000999466	0.001363557
L.Cysteine.C3H7NO2S	0.0000149757	0.00178772
PE.22.6.4Z.7Z.10Z.13Z.16Z.19Z..P.18.1.11Z...C45H76NO7P	0.0000212585	0.002255758
Galactosylhydroxylysine.C12H24N2O8	0.0000290202	0.002771424
Palmitoyl.glucuronide.C22H42O7	0.0000322228	0.002797527
Tetracosatetraenoic.acid..24.4n.6..C24H40O2	0.0000383026	0.003048246
Arachidonic.acid.C20H32O2	0.000060842	0.004145222
Pantothenol.C9H19NO4	0.0000617105	0.004145222
DHAP.6.0..C9H17O7P	0.0000651082	0.004145222
Octadecanedioic.acid.C18H34O4	0.0000698676	0.004170221
TG.18.3.9Z.12Z.15Z..20.4.5Z.8Z.11Z.14Z..22.6.4Z.7Z.10Z.13Z.16Z.19Z...C63H96O6	0.000105386	0.005518143
Eicosadienoic.acid.C20H36O2	0.000107086	0.005518143
PC.14.0.P.18.0..C40H80NO7P	0.000111069	0.005518143
Isocaproic.acid.C6H12O2	0.000118574	0.005518143
cis.4.Decenoic.acid.C10H18O2	0.000125151	0.005518143
PC.14.0.18.1.11Z...C40H78NO8P	0.00012712	0.005518143
X1.11.Undecanedicarboxylic.acid.C13H24O4	0.000138851	0.005681304
Trihydroxycoprostanic.acid.C28H48O5	0.000142776	0.005681304
Oenanthic.ether.C9H18O2	0.000237603	0.008488412
Adrenic.acid.C22H36O2	0.000245545	0.008488412
PC.15.0.22.6.4Z.7Z.10Z.13Z.16Z.19Z...C45H78NO8P	0.000246254	0.008488412
PC.16.1.9Z..22.6.4Z.7Z.10Z.13Z.16Z.19Z...C46H78NO8P	0.000253392	0.008488412
dUDP.C9H14N2O11P2	0.000257763	0.008488412
X12a.Hydroxy.3.oxocholadienic.acid.C24H34O4	0.000284734	0.008860663
X3.Oxo.4.6.choladienoic.acid.C24H34O3	0.000287624	0.008860663
X19.20.DiHDPa.C22H34O4	0.000379782	0.011071
MG.P.18.0e.0.0.0.0..C21H42O3	0.000382558	0.011071
Propionic.acid.C3H6O2	0.000424473	0.011697642
DHAP.10.0..C13H25O7P	0.000428709	0.011697642
Caprylic.acid.C8H16O2	0.000463028	0.011791271

Sebacic.acid.C10H18O4	0.000492333	0.011791271
MG.0.0.24.1.15Z..0.0..C27H52O4	0.00050084	0.011791271
PG.16.1.9Z..18.3.6Z.9Z.12Z...C40H71O10P	0.000503673	0.011791271
Cortol.C21H36O5	0.000512153	0.011791271
Alpha.ketoisovaleric.acid.C5H8O3	0.000525957	0.011791271
PC.14.0.14.1.9Z...C36H70NO8P	0.000527341	0.011791271
X3.Oxododecanoic.acid.C12H22O3	0.000533458	0.011791271
X16.Oxoestrone.C18H20O3	0.000543263	0.011791271
X6.Hydroxynicotinic.acid.C6H5NO3	0.00057415	0.012184739
Hypogeic.acid.C16H30O2	0.000597757	0.012409965
X3.Hydroxysebacic.acid.C10H18O5	0.000616407	0.012412846
Docosapentaenoic.acid..22n.6..C22H34O2	0.000623892	0.012412846
PC.15.0.20.2.11Z.14Z...C43H82NO8P	0.000644226	0.012555842
X13.14.Dihydro.PGF.1a.C20H38O5	0.000707084	0.013505313
Postin.C22H40N8O5	0.000729048	0.01365179
Capryloylglycine.C10H19NO3	0.000811073	0.014895661
X2.Methylbutyrylglycine.C7H13NO3	0.000839578	0.015128243
Alpha.Tocotrienol.C29H44O2	0.000900372	0.015923238
X3.Hydroxy.2.methyl..R..R.S...butanoic.acid.C5H10O3	0.000999178	0.01711694
X3a.16b.Dihydroxyandrosthenone.C19H28O3	0.001004029	0.01711694
X7.a.25.Dihydroxycholesterol.C27H46O3	0.001021639	0.01711694
X7Z.10Z.Hexadecadienoic.acid.C16H28O2	0.001080739	0.017794935
MG.0.0.22.0.0.0..C25H50O4	0.001139009	0.018383041
X2.Methyl.3.ketovaleric.acid.C6H10O3	0.001173343	0.018383041
Nonate.C9H16O4	0.001204752	0.018383041
Leukotriene.B4.C20H32O4	0.001204775	0.018383041
X13S.hydroxyoctadecadienoic.acid.C18H32O3	0.001215445	0.018383041
X17.HDoHE.C22H32O3	0.001246331	0.018383041
Homophytanic.acid.C21H42O2	0.001251202	0.018383041
X.S..Hydroxyoctanoyl.CoA.C29H50N7O18P3S	0.001322316	0.019133518
X3.Hydroxycapric.acid.C10H20O3	0.00139191	0.019839906
X24.Hydroxycholesterol.C27H46O2	0.001412688	0.01983995
Coenzyme.Q9.C54H82O4	0.001469432	0.020337794
N1.Acetylspermine.C12H28N4O	0.001542181	0.021039755
Acetic.acid.C2H4O2	0.001577161	0.02121392
Eicosenoic.acid.C20H38O2	0.001721334	0.022831579
Tetrahydrodeoxycorticosterone.C21H34O3	0.001746172	0.022843761
X2.Hydroxybutyric.acid.C4H8O3	0.001822079	0.023333574
Androsterone.C19H30O2	0.00183248	0.023333574

Appendix

Undecanoic.acid.C11H22O2	0.001868323	0.023476955
Capric.acid.C10H20O2	0.001977618	0.024141316
UDP.D.Xylose.C14H22N2O16P2	0.001981099	0.024141316
N.Acetylcystathionine.C9H16N2O5S	0.00199703	0.024141316
cis.4.Decenedioic.acid.C10H16O4	0.002167104	0.02586981
X16.a.Hydroxypregnenolone.C21H32O3	0.002222234	0.025994428
X9.12.13.TriHOME.C18H34O5	0.002231982	0.025994428
L.Lactic.acid.C3H6O3	0.002285968	0.026302399
X4.Hydroxybenzoic.acid.C7H6O3	0.00243704	0.027706822
CE.16.0..C43H76O2	0.002495647	0.028039332
PE.14.0.20.4.5Z.8Z.11Z.14Z...C39H70NO8P	0.00253724	0.028175167
X3.Oxodecanoic.acid.C10H18O3	0.002576866	0.028262573
PC.15.0.18.1.11Z...C41H80NO8P	0.0026043	0.028262573
X3.Oxotetradecanoic.acid.C14H26O3	0.002734031	0.029337073
X3.Hydroxydodecanoic.acid.C12H24O3	0.002832626	0.030057305
Hexanoylglycine.C8H15NO3	0.003026141	0.031757851
Inositol.cyclic.phosphate.C6H11O8P	0.003087	0.032044399
N1.N12.Diacetylspermine.C14H30N4O2	0.00316037	0.032453264
X3.Oxohexadecanoic.acid.C16H30O3	0.003294507	0.033470784
X2.Methylcitric.acid.C7H10O7	0.003410841	0.034287923
Pentadecanoic.acid.C15H30O2	0.003631527	0.036126129
Thiocysteine.C3H7NO2S2	0.003865086	0.03805317
Ganglioside.GD3..d18.0.20.0..C72H131N3O29	0.004036608	0.039336334
PC.14.1.9Z..22.2.13Z.16Z...C44H82NO8P	0.004092143	0.039417305
Tetrahydrocortisone.C21H32O5	0.004142328	0.039417305
PC.16.0.P.18.1.11Z...C42H82NO7P	0.004168741	0.039417305
PE.18.3.6Z.9Z.12Z..P.18.1.11Z...C41H74NO7P	0.004256468	0.039852227
Hexacosanoyl.carnitine.C33H65NO4	0.004315377	0.039863789
Hexanoylcarnitine.C13H25NO4	0.004341187	0.039863789
PE.22.2.13Z.16Z..24.1.15Z...C51H96NO8P	0.004609532	0.041573576
PE.20.3.5Z.8Z.11Z..22.6.4Z.7Z.10Z.13Z.16Z.19Z...C47H76NO8P	0.004641889	0.041573576
PE.22.1.13Z..24.1.15Z...C51H98NO8P	0.004657982	0.041573576
MG.0.0.14.1.9Z..0.0..C17H32O4	0.004807362	0.042232239
X3.Amino.2.piperidone.C5H10N2O	0.004820224	0.042232239
Undecanedioic.acid.C11H20O4	0.004947718	0.042955186
Hyaluronic.acid.C16H27NO12	0.005122845	0.044074926
Galabiosylceramide..d18.1.26.0..C56H107NO13	0.005290616	0.044893904
X19.Hydroxy.PGE2.C20H32O6	0.005312054	0.044893904
X2.Hydroxy.3.methylpentanoic.acid.C6H12O3	0.005370347	0.044988435

X5.8.Tetradecadienoic.acid.C14H24O2	0.005424717	0.045048741
PC.18.1.11Z..P.18.1.11Z...C44H84NO7P	0.005673832	0.04671129
PC.14.1.9Z..15.0..C37H72NO8P	0.006157696	0.050261532
TG.16.0.18.2.9Z.12Z..20.4.5Z.8Z.11Z.14Z...C57H98O6	0.006388152	0.051700723
Lithocholate.3.O.glucuronide.C30H48O9	0.006454349	0.051797504
Trihexosylceramide..d18.1.26.1.17Z...C62H117NO18	0.006529851	0.051939301
cis.4.Hydroxycyclohexylacetic.acid.C8H14O3	0.006580791	0.051939301
X4.Hydroxycyclohexylcarboxylic.acid.C7H12O3	0.006642267	0.051994794
Myristic.acid.C14H28O2	0.006785906	0.052687321
Oxoglutaric.acid.C5H6O5	0.006979016	0.053627472
PIP2.16.0.16.1.9Z...C41H79O19P3	0.007019303	0.053627472
PC.15.0.22.1.13Z...C45H88NO8P	0.007170502	0.054347852
Hexacosanoic.acid.C26H52O2	0.007422459	0.055814554
L.Aspartic.acid.C4H7NO4	0.008043171	0.059539154
Phenylpyruvic.acid.C9H8O3	0.008057446	0.059539154
Neuroprotectin.D1.C22H32O4	0.008104806	0.059539154
X3.Hydroxyisheptanoic.acid.C7H14O3	0.008209431	0.059847376
PC.20.2.11Z.14Z..22.6.4Z.7Z.10Z.13Z.16Z.19Z...C50H84NO8P	0.0084049	0.060808178
PC.16.0.P.18.0..C42H84NO7P	0.008488537	0.060951523
Isobutyrylglycine.C6H11NO3	0.008848575	0.063018179
Heptadecanoic.acid.C17H34O2	0.008908329	0.063018179
Tricosanoic.acid.C23H46O2	0.00926013	0.065025181
Dodecanoic.acid.C12H24O2	0.009344498	0.065138652
Glucosylsphingosine.C24H47NO7	0.009418143	0.065176277
PC.18.0.22.5.4Z.7Z.10Z.13Z.16Z...C48H86NO8P	0.009629152	0.06583975
DG.18.2.9Z.12Z..22.6.4Z.7Z.10Z.13Z.16Z.19Z..0.0..C43H68O5	0.009709998	0.06583975
Ceramide..d18.1.22.0..C40H79NO3	0.009720843	0.06583975
X2.Hydroxymyristic.acid.C14H28O3	0.009991511	0.067196431
O..N.acetyl.alpha.neuraminosyl...2..3..O.beta.D.galactopyranosyl..	0.010290376	0.068547777
1..4..O.2..acetylamino..2.deoxy.beta.D.glucopyranosyl..1..3..O.		
beta.D.galactopyranosyl..1..4..O.2..acetylamino..2.deoxy.beta.D.		
glucopyranosyl..1..3..O.beta.D.galactopyranosyl..1..4...D.Gluc.C51H85N3O39		
DG.18.4.6Z.9Z.12Z.15Z..18.4.6Z.9Z.12Z.15Z..0.0..C39H60O5	0.010336	0.068547777
PC.20.0.P.18.0..C46H92NO7P	0.010427107	0.068675086
Glucosylceramide..d18.1.26.1.17Z...C50H95NO8	0.010737174	0.070232887
Prostaglandin.E2.C20H32O5	0.010819127	0.070287526
Octacosanoic.acid.C28H56O2	0.010990072	0.070915665
Tridecanoic.acid.C13H26O2	0.011204034	0.071811091
PC.15.0.20.0..C43H86NO8P	0.011877065	0.075617312
X4.Coumaryl.alcohol.C9H10O2	0.012224794	0.077315751

Appendix

Presqualene.diphosphate.C30H52O7P2	0.012776399	0.080272768
Vanylglycol.C9H12O4	0.012950486	0.080834736
PC.14.0.22.6.4Z.7Z.10Z.13Z.16Z.19Z...C44H76NO8P	0.013554689	0.084056674
X5.Phenylvaleric.acid.C11H14O2	0.014158783	0.08723637
N.Acetylgalactosamine.C8H15NO6	0.014505601	0.088404023
X3.Hydroxysuberic.acid.C8H14O5	0.014651863	0.088404023
Cytidine.triphosphate.C9H16N3O14P3	0.014755928	0.088404023
Dimethylglycine.C4H9NO2	0.014763094	0.088404023
CDP.DG.18.0.18.0..C48H89N3O15P2	0.014871225	0.088404023
CE.12.0..C39H68O2	0.014937963	0.088404023
L.Cystine.C6H12N2O4S2	0.014996285	0.088404023
LysoPE.0.0.22.0..C27H56NO7P	0.015296903	0.089622959
Dehydroepiandrosterone.sulfate.C19H28O5S	0.015563585	0.090629414
Homoveratric.acid.C10H12O4	0.015815983	0.090811101
X2.3.Dinor.6.keto.prostaglandin.F1.a.C18H30O6	0.01585713	0.090811101
PC.22.1.13Z..22.6.4Z.7Z.10Z.13Z.16Z.19Z...C52H90NO8P	0.015880056	0.090811101
MG.0.0.18.1.11Z..0.0..C21H40O4	0.01638969	0.093167584
X3.Hydroxytetradecanedioic.acid.C14H26O5	0.016733959	0.094313678
S..Hydroxymethyl.glutathione.C11H19N3O7S	0.016788822	0.094313678
Tetradecanoylcarnitine.C21H41NO4	0.017464709	0.096742134
Glucosylceramide..d18.1.16.0..C40H77NO8	0.017519804	0.096742134
Uric.acid.C5H4N4O3	0.017525015	0.096742134
PC.15.0.18.2.9Z.12Z...C41H78NO8P	0.017647274	0.096857166
PC.22.5.4Z.7Z.10Z.13Z.16Z..P.18.1.11Z...C48H84NO7P	0.017829739	0.097185821
X3.Methylcrotonyl.CoA.C26H42N7O17P3S	0.017910685	0.097185821
PC.20.3.5Z.8Z.11Z..22.6.4Z.7Z.10Z.13Z.16Z.19Z...C50H82NO8P	0.019308513	0.104178701
Protoporphyrin.IX.C34H34N4O4	0.019509781	0.104673262
PG.18.3.6Z.9Z.12Z..18.3.6Z.9Z.12Z...C42H71O10P	0.020068032	0.107066876
Mevalonic.acid.C6H12O4	0.020347851	0.107956656
PC.15.0.16.0..C39H78NO8P	0.020773723	0.109607211
N.6..Methyllysine.C7H16N2O2	0.021529123	0.112968752
Glycerol.C3H8O3	0.021839281	0.113970018
cis.Aconitic.acid.C6H6O6	0.022451706	0.116529233
CE.18.3.6Z.9Z.12Z...C45H74O2	0.022720379	0.117227893
PE.22.0.P.18.1.11Z...C45H88NO7P	0.022900572	0.117227893
Galactonic.acid.C6H12O7	0.023053933	0.117227893
Leukotriene.C4.C30H47N3O9S	0.023203958	0.117227893
Suberic.acid.C8H14O4	0.023361451	0.117227893
PC.18.0.22.4.7Z.10Z.13Z.16Z...C48H88NO8P	0.023467348	0.117227893

Benzoic.acid.C7H6O2	0.023522886	0.117227893
Docosahexaenoic.acid.C22H32O2	0.02356833	0.117227893
PE.14.0.P.18.1.11Z...C37H72NO7P	0.023752753	0.117533055
PC.18.1.11Z..24.1.15Z...C50H96NO8P	0.024482682	0.119955159
X10.Nitrolinoleic.acid.C18H31NO4	0.024493462	0.119955159
Deoxycholic.acid.glycine.conjugate.C26H43NO5	0.025206036	0.122287005
PI.16.0.18.0..C43H83O13P	0.025319686	0.122287005
Hexadecanedioic.acid.C16H30O4	0.025353746	0.122287005
TG.20.0.20.0.20.4.5Z.8Z.11Z.14Z...C63H114O6	0.025963467	0.124598547
X2.Decaprenyl.3.methyl.6.methoxy.1.4.benzoquinone.C58H88O4	0.026281389	0.124720032
Citric.acid.C6H8O7	0.026304522	0.124720032
X5.Androstene.3b.16b.17a.triol.C19H30O3	0.026380572	0.124720032
Taurine.C2H7NO3S	0.027340338	0.128090121
TG.18.3.9Z.12Z.15Z..18.2.9Z.12Z..22.6.4Z.7Z.10Z.13Z.16Z.19Z...C61H96O6	0.027361659	0.128090121
MG.0.0.16.1.9Z..0.0..C19H36O4	0.028058557	0.130711815
LysoPC.22.6.4Z.7Z.10Z.13Z.16Z.19Z...C30H50NO7P	0.028618692	0.132468265
X13.L.Hydroperoxylinoleic.acid.C18H32O4	0.02883795	0.132468265
Behenic.acid.C22H44O2	0.028851727	0.132468265
PIP2.16.0.22.5.4Z.7Z.10Z.13Z.16Z...C47H83O19P3	0.029146893	0.133183173
PE.14.0.20.5.5Z.8Z.11Z.14Z.17Z...C39H68NO8P	0.030173735	0.137218651
X.R..3.Hydroxy.hexadecanoic.acid.C16H32O3	0.030517961	0.138126315
Tauroursodeoxycholic.acid.C26H45NO6S	0.030884916	0.138514856
Pyridinoline.C18H28N4O8	0.030893889	0.138514856
Heptadecanoyl.carnitine.C24H47NO4	0.031095169	0.138765826
PG.16.0.16.0..C38H75O10P	0.031546933	0.140047703
Oxidized.glutathione.C20H32N6O12S2	0.031675711	0.140047703
DG.20.3.5Z.8Z.11Z..24.1.15Z..0.0..C47H84O5	0.031874605	0.140277641
Cer.d18.1.14.0..C32H63NO3	0.032842162	0.143872776
cis.5.Tetradecenoylcarnitine.C21H39NO4	0.033512629	0.146139547
Vanillylmandelic.acid.C9H10O5	0.034102363	0.148035256
X7.Dehydrocholesterol.C27H44O	0.034418249	0.148730444
X1.2.Di..9Z.12Z.15Z.octadecatrienoyl..3..Galactosyl.alpha.	0.035093398	0.150489179
1.6.Galactosyl.beta.1..glycerol.C51H84O15		
LysoPC.18.4.6Z.9Z.12Z.15Z...C26H46NO7P	0.035140405	0.150489179
PI.16.0.16.2.9Z.12Z...C41H75O13P	0.035578437	0.151684853
Monoethyl.malonic.acid.C5H8O4	0.035948545	0.152581604
Ganglioside.GA1..d18.1.12.0..C56H102N2O23	0.036967898	0.156213904
X4.Aminobutyraldehyde.C4H9NO	0.03783029	0.158764494
X3.Deoxy.D.glycero.D.galacto.2.nonulosonic.acid.C9H16O9	0.03802328	0.158764494
PE.18.2.9Z.12Z..24.1.15Z...C47H88NO8P	0.038070229	0.158764494

Appendix

Deoxyuridine.triphosphate.C9H15N2O14P3	0.038277322	0.15880775
N.Acetyl.L.phenylalanine.C11H13NO3	0.038413184	0.15880775
PC.18.0.P.18.0..C44H88NO7P	0.039888504	0.164018625
X3.Hydroxyphenylacetic.acid.C8H8O3	0.04001711	0.164018625
Ganglioside.GM3..d18.0.20.0..C61H114N2O21	0.040535137	0.165431863
Erythronic.acid.C4H8O5	0.041231059	0.167556006
Mevalonic.acid.5P.C6H13O7P	0.041514897	0.167994605
PE.20.1.11Z..22.6.4Z.7Z.10Z.13Z.16Z.19Z...C47H80NO8P	0.041799866	0.168434061
Ganglioside.GM1..d18.1.26.1.17Z....C81H145N3O31	0.04373267	0.175051942
PC.14.0.18.2.9Z.12Z...C40H76NO8P	0.043808811	0.175051942
X3.Hexaprenyl.4.hydroxybenzoic.acid.C37H54O3	0.044465289	0.176934795
Bilirubin.C33H36N4O6	0.044962081	0.178169244
X14.15.DiHETrE.C20H34O4	0.045468523	0.179431567
PS.18.0.18.1.9Z...C42H80NO10P	0.045694984	0.179583169
TG.22.6.4Z.7Z.10Z.13Z.16Z.19Z..22.6.4Z.7Z. 10Z.13Z.16Z.19Z..22.6.4Z.7Z.10Z.13Z.16Z.19Z...C69H98O6	0.046593076	0.181736054
X8.11.14.Eicosatrienoic.acid.C20H34O2	0.0471321	0.181736054
Isovalerylglutamic.acid.C10H17NO5	0.047150707	0.181736054
MG.0.0.22.2.13Z.16Z..0.0..C25H46O4	0.047308595	0.181736054
Dodecanedioic.acid.C12H22O4	0.047537584	0.181736054
PI.16.0.16.0..C41H79O13P	0.047669337	0.181736054
Imidazoleacetic.acid.ribotide.C10H15N2O9P	0.047786751	0.181736054
Melanostatin.C13H24N4O3	0.047978949	0.181736054
X7.Methylguanosine.C11H16N5O5	0.048110174	0.181736054
N1.Methyl.2.pyridone.5.carboxamide.C7H8N2O2	0.048174057	0.181736054
PC.16.0.22.5.4Z.7Z.10Z.13Z.16Z...C46H82NO8P	0.048381374	0.181736054
Glycerophosphocholine.C8H20NO6P	0.048705317	0.181736054
MG.18.0.0.0.0.0..C21H42O4	0.04871668	0.181736054
DG.22.2.13Z.16Z..22.6.4Z.7Z.10Z.13Z.16Z.19Z...0.0..C47H76O5	0.0505952	0.188009401
L.Tyrosine.C9H11NO3	0.051365774	0.189261883
Asymmetric.dimethylarginine.C8H18N4O2	0.051691382	0.189261883
Tetradecanedioic.acid.C14H26O4	0.052040195	0.189261883
Glycocholic.acid.C26H43NO6	0.052056715	0.189261883
X3D.7D.11D.Phytanic.acid.C20H40O2	0.052137527	0.189261883
Lactosylceramide..d18.1.12.0..C42H79NO13	0.052245024	0.189261883
X5.6.Dihydro.5.6.dihydroxy.y.y.carotene.C40H60O2	0.052319515	0.189261883
PE.15.0.18.4.6Z.9Z.12Z.15Z...C38H68NO8P	0.052698298	0.189864847
DG.15.0.20.3.5Z.8Z.11Z..0.0..C38H68O5	0.052883821	0.189864847
X3.Phenylbutyric.acid.C10H12O2	0.053598501	0.191238133
Pantothenic.acid.C9H17NO5	0.053666827	0.191238133

L.Aspartyl.L.phenylalanine.C13H16N2O5	0.054049744	0.191886638
---------------------------------------	-------------	-------------

Complete results of the hurdle model association tests between Parasutterella sp. abundance and serum metabolites

Supplementary table 2

	total	hits	Raw p	Holm p	FDR
Fatty Acid Biosynthesis	35	7	1.16E-02	1.00E+00	1.00E+00
Alpha Linolenic Acid and Linoleic Acid	19	4	4.62E-02	1.00E+00	1.00E+00
Metabolism					
Beta Oxidation of Very Long Chain Fatty	17	2	3.64E-01	1.00E+00	1.00E+00
Acids					
Pantothenate and CoA Biosynthesis	21	2	4.70E-01	1.00E+00	1.00E+00
Gluconeogenesis	35	3	4.89E-01	1.00E+00	1.00E+00
Homocysteine Degradation	9	1	5.02E-01	1.00E+00	1.00E+00
De Novo Triacylglycerol Biosynthesis	9	1	5.02E-01	1.00E+00	1.00E+00
Malate-Aspartate Shuttle	10	1	5.39E-01	1.00E+00	1.00E+00
Glycerol Phosphate Shuttle	11	1	5.74E-01	1.00E+00	1.00E+00
Cardiolipin Biosynthesis	11	1	5.74E-01	1.00E+00	1.00E+00
Cysteine Metabolism	26	2	5.88E-01	1.00E+00	1.00E+00
Taurine and Hypotaurine Metabolism	12	1	6.06E-01	1.00E+00	1.00E+00
Propanoate Metabolism	42	3	6.17E-01	1.00E+00	1.00E+00
Glucose-Alanine Cycle	13	1	6.35E-01	1.00E+00	1.00E+00
Vitamin K Metabolism	14	1	6.63E-01	1.00E+00	1.00E+00
Alanine Metabolism	17	1	7.33E-01	1.00E+00	1.00E+00
Aspartate Metabolism	35	2	7.49E-01	1.00E+00	1.00E+00
Mitochondrial Electron Transport Chain	19	1	7.72E-01	1.00E+00	1.00E+00
Ethanol Degradation	19	1	7.72E-01	1.00E+00	1.00E+00
Nucleotide Sugars Metabolism	20	1	7.89E-01	1.00E+00	1.00E+00
Ubiquinone Biosynthesis	20	1	7.89E-01	1.00E+00	1.00E+00
Glutathione Metabolism	21	1	8.05E-01	1.00E+00	1.00E+00
Carnitine Synthesis	22	1	8.20E-01	1.00E+00	1.00E+00
Warburg Effect	58	3	8.22E-01	1.00E+00	1.00E+00
Valine, Leucine and Isoleucine Degradation	60	3	8.40E-01	1.00E+00	1.00E+00
Androstenedione Metabolism	24	1	8.46E-01	1.00E+00	1.00E+00
Glycerolipid Metabolism	25	1	8.58E-01	1.00E+00	1.00E+00

Appendix

Glycolysis	25	1	8.58E-01	1.00E+00	1.00E+00
Oxidation of Branched Chain Fatty Acids	26	1	8.69E-01	1.00E+00	1.00E+00
Phytanic Acid Peroxisomal Oxidation	26	1	8.69E-01	1.00E+00	1.00E+00
Plasmalogen Synthesis	26	1	8.69E-01	1.00E+00	1.00E+00
Mitochondrial Beta-Oxidation of Short Chain Saturated Fatty Acids	27	1	8.79E-01	1.00E+00	1.00E+00
Pyruvate Metabolism	48	2	8.86E-01	1.00E+00	1.00E+00
Phenylalanine and Tyrosine Metabolism	28	1	8.88E-01	1.00E+00	1.00E+00
Glutamate Metabolism	49	2	8.93E-01	1.00E+00	1.00E+00
Phospholipid Biosynthesis	29	1	8.97E-01	1.00E+00	1.00E+00
Pentose Phosphate Pathway	29	1	8.97E-01	1.00E+00	1.00E+00
Urea Cycle	29	1	8.97E-01	1.00E+00	1.00E+00
Lysine Degradation	30	1	9.04E-01	1.00E+00	1.00E+00
Ammonia Recycling	32	1	9.19E-01	1.00E+00	1.00E+00
Citric Acid Cycle	32	1	9.19E-01	1.00E+00	1.00E+00
Fructose and Mannose Degradation	32	1	9.19E-01	1.00E+00	1.00E+00
Amino Sugar Metabolism	33	1	9.25E-01	1.00E+00	1.00E+00
Beta-Alanine Metabolism	34	1	9.31E-01	1.00E+00	1.00E+00
Glycine and Serine Metabolism	59	2	9.44E-01	1.00E+00	1.00E+00
Methionine Metabolism	43	1	9.66E-01	1.00E+00	1.00E+00
Steroidogenesis	43	1	9.66E-01	1.00E+00	1.00E+00
Arachidonic Acid Metabolism	69	2	9.72E-01	1.00E+00	1.00E+00
Arginine and Proline Metabolism	53	1	9.85E-01	1.00E+00	1.00E+00
Pyrimidine Metabolism	59	1	9.91E-01	1.00E+00	1.00E+00
Tryptophan Metabolism	60	1	9.92E-01	1.00E+00	1.00E+00
Bile Acid Biosynthesis	65	1	9.94E-01	1.00E+00	1.00E+00
Tyrosine Metabolism	72	1	9.97E-01	1.00E+00	1.00E+00

Complete results from pathway overrepresentation analysis using metaboanalyst

9 Danksagung

Zuerst möchte ich mich bei Herrn Prof. Matthias Laudes für die Übernahme der Betreuung und die Bereitstellung meiner Forschungsprojekte bedanken. Besonders bedanke ich mich für das Ermöglichen meines forschungsorientierten Auslandsaufenthaltes am Wallenberg Laboratory in Göteborg, Schweden.

Ein besonderer Dank gilt Dr. Kristina Schlicht, die durch ihre bioinformatische Expertise zum Gelingen meiner Forschung beigetragen hat und stets ein offenes Ohr für alle Anliegen hatte. Des Weiteren bedanke ich mich bei Katharina Hartmann für die Hilfsbereitschaft in der praktischen Laborarbeit. In diesem Zuge möchte ich meinen Dank auch Dr. Andrea A. Andreani, Prof. Hila Emmert und Priv.-Doz. Dr. Claudia Geismann aussprechen, die mir bei der Planung von umfangreichen Laborexperimenten sehr geholfen haben. Der gesamten Arbeitsgruppe des Institutes für Diabetologie und klinische Stoffwechselforschung danke ich für die anregenden Diskussionen, die Unterstützung in organisatorischen Belangen und eine nette Arbeitsatmosphäre.

Ein ganz besonderer Dank gilt meinem Freund Jan für die unterstützenden Worte und meiner Familie für den emotionalen und finanziellen Rückhalt zu jeder Zeit meines akademischen Werdegangs.

Anlage 3

C A U	Christian-Albrechts-Universität zu Kiel	Agrar- und Ernährungs- wissenschaftliche Fakultät
------------------	---	--

Declaration of co-authorship

If a dissertation is based on already published or submitted co-authored articles, a declaration from each of the authors regarding the part of the work done by the doctoral candidate must be enclosed when submitting the dissertation.

1. Doctoral candidate

Name: Lea Henneke

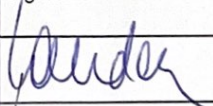

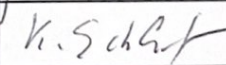
2. This co-author declaration applies to the following article:

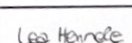
A Dietary Carbohydrate - Gut Parasutterella - Human Fatty Acid Biosynthesis metabolic axis in obesity and type 2 diabetes

The extent of the doctoral candidate's contribution to the article is assessed on the following scale:

- A. Has contributed to the work (0-33%)
- B. Has made a substantial contribution (34-66%)
- C. Did the majority of the work independently (67-100%)

3. Declaration on the individual phases of the scientific work (A,B,C)	Extent
Concept: Formulation of the basic scientific problem based on theoretical questions which require clarification, including a summary of the general questions which, it is assumed, will be answerable via analyses or concrete experiments/investigations	B
Planning: Planning of experiments/analyses and formulation of investigative methodology, including choice of method and independent methodological development, in such a way that the scientific questions asked can be expected to be answered	B
Execution: Involvement in the analysis or the concrete experiments/investigation	C
Manuscript preparation: Presentation, interpretation and discussion of the results obtained in article form	C

4. Signature of all co-authors		
Date	Name	Signature
12.01.2022	Matthias Laudes	
12.01.2022	Dominik Schulte	
12.01.2022	Kristina Schlicht	

5. Signature of doctoral candidate		
Date	Name	Signature
12.01.2022	Lea Henneke	

Anlage 3

C A U	Christian-Albrechts-Universität zu Kiel	Agrar- und Ernährungs- wissenschaftliche Fakultät
------------------	---	--

Declaration of co-authorship

If a dissertation is based on already published or submitted co-authored articles, a declaration from each of the authors regarding the part of the work done by the doctoral candidate must be enclosed when submitting the dissertation.

1. Doctoral candidate

Name: Lea Henneke

2. This co-author declaration applies to the following article:

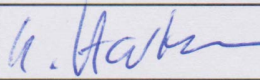
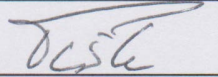
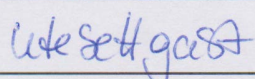
A Dietary Carbohydrate - Gut Parasutterella - Human Fatty Acid Biosynthesis metabolic axis in obesity and type 2 diabetes

The extent of the doctoral candidate's contribution to the article is assessed on the following scale:

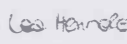
- A. Has contributed to the work (0-33%)
- B. Has made a substantial contribution (34-66%)
- C. Did the majority of the work independently (67-100%)

3. Declaration on the individual phases of the scientific work (A,B,C)	Extent
Concept: Formulation of the basic scientific problem based on theoretical questions which require clarification, including a summary of the general questions which, it is assumed, will be answerable via analyses or concrete experiments/investigations	B
Planning: Planning of experiments/analyses and formulation of investigative methodology, including choice of method and independent methodological development, in such a way that the scientific questions asked can be expected to be answered	B
Execution: Involvement in the analysis or the concrete experiments/investigation	C
Manuscript preparation: Presentation, interpretation and discussion of the results obtained in article form	C

4. Signature of all co-authors

Date	Name	Signature
12.01.2022	Katharina Hartmann	
12.01.2022	Kathrin Türk	
12.01.2022	Ute Settgast	

5. Signature of doctoral candidate

Date	Name	Signature
12.01.2022	Lea Henneke	

Anlage 3

C A U	Christian-Albrechts-Universität zu Kiel	Agrar- und Ernährungs- wissenschaftliche Fakultät
------------------	---	--

Declaration of co-authorship

If a dissertation is based on already published or submitted co-authored articles, a declaration from each of the authors regarding the part of the work done by the doctoral candidate must be enclosed when submitting the dissertation.

1. Doctoral candidate

Name: Lea Henneke

2. This co-author declaration applies to the following article:

A Dietary Carbohydrate - Gut Parasutterella - Human Fatty Acid Biosynthesis metabolic axis in obesity and type 2 diabetes

The extent of the doctoral candidate's contribution to the article is assessed on the following scale:

- A. Has contributed to the work (0-33%)
- B. Has made a substantial contribution (34-66%)
- C. Did the majority of the work independently (67-100%)

3. Declaration on the individual phases of the scientific work (A,B,C)**Extent**

Concept: Formulation of the basic scientific problem based on theoretical questions which require clarification, including a summary of the general questions which, it is assumed, will be answerable via analyses or concrete experiments/investigations

B

Planning: Planning of experiments/analyses and formulation of investigative methodology, including choice of method and independent methodological development, in such a way that the scientific questions asked can be expected to be answered



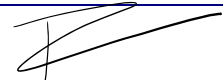
B

Execution: Involvement in the analysis or the concrete experiments/investigation

C

Manuscript preparation: Presentation, interpretation and discussion of the results obtained in article form

C**4. Signature of all co-authors**

Date	Name	Signature
12.01.2022	Carina Knappe	
12.01.2022	Nathalie Rohmann	
12.01.2022	Tim Hollstein	

5. Signature of doctoral candidate

Date	Name	Signature
12.01.2022	Lea Henneke	

Anlage 3

C	A	U	Christian-Albrechts-Universität zu Kiel	Agrar- und Ernährungs- wissenschaftliche Fakultät
----------	----------	----------	---	--

Declaration of co-authorship

If a dissertation is based on already published or submitted co-authored articles, a declaration from each of the authors regarding the part of the work done by the doctoral candidate must be enclosed when submitting the dissertation.

1. Doctoral candidate

Name: Lea Henneke

2. This co-author declaration applies to the following article:

A Dietary Carbohydrate - Gut Parasutterella - Human Fatty Acid Biosynthesis metabolic axis in obesity and type 2 diabetes

The extent of the doctoral candidate's contribution to the article is assessed on the following scale:

- A. Has contributed to the work (0-33%)
- B. Has made a substantial contribution (34-66%)
- C. Did the majority of the work independently (67-100%)

3. Declaration on the individual phases of the scientific work (A,B,C)

Extent

Concept: Formulation of the basic scientific problem based on theoretical questions which require clarification, including a summary of the general questions which, it is assumed, will be answerable via analyses or concrete experiments/investigations

B

Planning: Planning of experiments/analyses and formulation of investigative methodology, including choice of method and independent methodological development, in such a way that the scientific questions asked can be expected to be answered

B

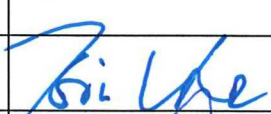

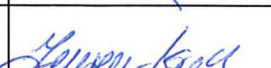
Execution: Involvement in the analysis or the concrete experiments/investigation

C

Manuscript preparation: Presentation, interpretation and discussion of the results obtained in article form

C

4. Signature of all co-authors

Date	Name	Signature
12.01.2022	Karin Schwarz	
12.01.2022	Tobias Demetrowitsch	
12.01.2022	Julia Jensen-Kroll	

5. Signature of doctoral candidate

Date	Name	Signature
12.01.2022	Lea Henneke	

Anlage 3

C A U	Christian-Albrechts-Universität zu Kiel	Agrar- und Ernährungs- wissenschaftliche Fakultät
------------------	---	--

Declaration of co-authorship

If a dissertation is based on already published or submitted co-authored articles, a declaration from each of the authors regarding the part of the work done by the doctoral candidate must be enclosed when submitting the dissertation.

1. Doctoral candidate

Name: Lea Henneke

2. This co-author declaration applies to the following article:

A Dietary Carbohydrate - Gut Parasutterella - Human Fatty Acid Biosynthesis metabolic axis in obesity and type 2 diabetes

The extent of the doctoral candidate's contribution to the article is assessed on the following scale:

- A. Has contributed to the work (0-33%)
- B. Has made a substantial contribution (34-66%)
- C. Did the majority of the work independently (67-100%)

3. Declaration on the individual phases of the scientific work (A,B,C)**Extent**

Concept: Formulation of the basic scientific problem based on theoretical questions which require clarification, including a summary of the general questions which, it is assumed, will be answerable via analyses or concrete experiments/investigations

B

Planning: Planning of experiments/analyses and formulation of investigative methodology, including choice of method and independent methodological development, in such a way that the scientific questions asked can be expected to be answered




B

Execution: Involvement in the analysis or the concrete experiments/investigation

C

Manuscript preparation: Presentation, interpretation and discussion of the results obtained in article form

C**4. Signature of all co-authors**

Date	Name	Signature
12.01.2022	Christoph Kaleta	
12.01.2022	Johannes Zimmermann	
12.01.2022	Corinna Geisler	

5. Signature of doctoral candidate

Date	Name	Signature
12.01.2022	Lea Henneke	

Anlage 3

C A U	Christian-Albrechts-Universität zu Kiel	Agrar- und Ernährungs- wissenschaftliche Fakultät
------------------	---	--

Declaration of co-authorship

If a dissertation is based on already published or submitted co-authored articles, a declaration from each of the authors regarding the part of the work done by the doctoral candidate must be enclosed when submitting the dissertation.

1. Doctoral candidate:

Name: Lea Henneke

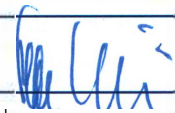


2. This co-author declaration applies to the following article:


A Dietary Carbohydrate - Gut Parasutterella - Human Fatty Acid Biosynthesis metabolic axis in obesity and type 2 diabetes

The extent of the doctoral candidate's contribution to the article is assessed on the following scale:

- A. Has contributed to the work (0-33%)
- B. Has made a substantial contribution (34-66%)
- C. Did the majority of the work independently (67-100%)

3. Declaration on the individual phases of the scientific work (A,B,C)	Extent
Concept: Formulation of the basic scientific problem based on theoretical questions which require clarification, including a summary of the general questions which, it is assumed, will be answerable via analyses or concrete experiments/investigations	B
Planning: Planning of experiments/analyses and formulation of investigative methodology, including choice of method and independent methodological development, in such a way that the scientific questions asked can be expected to be answered	B
Execution: Involvement in the analysis or the concrete experiments/investigation	C
Manuscript preparation: Presentation, interpretation and discussion of the results obtained in article form	C

4. Signature of all co-authors		
Date	Name	Signature
12.01.2022	Stefan Schreiber	
12.01.2022	Daniela Pohlschneider	
12.01.2022	Andre Franke	

5. Signature of doctoral candidate		
Date	Name	Signature
12.01.2022	Lea Henneke	

Anlage 3

C A U	Christian-Albrechts-Universität zu Kiel	Agrar- und Ernährungs- wissenschaftliche Fakultät
------------------	---	--

Declaration of co-authorship

If a dissertation is based on already published or submitted co-authored articles, a declaration from each of the authors regarding the part of the work done by the doctoral candidate must be enclosed when submitting the dissertation.

1. Doctoral candidate

Name: Lea Henneke

2. This co-author declaration applies to the following article:

A Dietary Carbohydrate - Gut Parasutterella - Human Fatty Acid Biosynthesis metabolic axis in obesity and type 2 diabetes

The extent of the doctoral candidate's contribution to the article is assessed on the following scale:

- A. Has contributed to the work (0-33%)
- B. Has made a substantial contribution (34-66%)
- C. Did the majority of the work independently (67-100%)

3. Declaration on the individual phases of the scientific work (A,B,C)
Extent

Concept: Formulation of the basic scientific problem based on theoretical questions which require clarification, including a summary of the general questions which, it is assumed, will be answerable via analyses or concrete experiments/investigations

B

Planning: Planning of experiments/analyses and formulation of investigative methodology, including choice of method and independent methodological development, in such a way that the scientific questions asked can be expected to be answered



B

Execution: Involvement in the analysis or the concrete experiments/investigation

C

Manuscript preparation: Presentation, interpretation and discussion of the results obtained in article form

C
4. Signature of all co-authors

Date	Name	Signature
12.01.2022	John F. Baines	
12.01.2022	Nadia A. Andreani	

5. Signature of doctoral candidate

Date	Name	Signature
12.01.2022	Lea Henneke	

Anlage 3

C A U	Christian-Albrechts-Universität zu Kiel	Agrar- und Ernährungs- wissenschaftliche Fakultät
------------------	---	--

Declaration of co-authorship

If a dissertation is based on already published or submitted co-authored articles, a declaration from each of the authors regarding the part of the work done by the doctoral candidate must be enclosed when submitting the dissertation.

1. Doctoral candidate

Name: Lea Henneke

2. This co-author declaration applies to the following article:

A Dietary Carbohydrate - Gut Parasutterella - Human Fatty Acid Biosynthesis metabolic axis in obesity and type 2 diabetes

The extent of the doctoral candidate's contribution to the article is assessed on the following scale:

- A. Has contributed to the work (0-33%)
- B. Has made a substantial contribution (34-66%)
- C. Did the majority of the work independently (67-100%)

3. Declaration on the individual phases of the scientific work (A,B,C)
Extent

Concept: Formulation of the basic scientific problem based on theoretical questions which require clarification, including a summary of the general questions which, it is assumed, will be answerable via analyses or concrete experiments/investigations

B

Planning: Planning of experiments/analyses and formulation of investigative methodology, including choice of method and independent methodological development, in such a way that the scientific questions asked can be expected to be answered



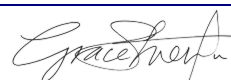
B

Execution: Involvement in the analysis or the concrete experiments/investigation

C

Manuscript preparation: Presentation, interpretation and discussion of the results obtained in article form

C
4. Signature of all co-authors

Date	Name	Signature
12.01.2022	Jane Shearer	
12.01.2022	Shrushti Shah	
12.01.2022	Grace Shen-Tu	

5. Signature of doctoral candidate

Date	Name	Signature
12.01.2022	Lea Henneke	